INFORMATION TO USERS

This manuscript has been reproduced from the microfilm master. UMI films the text directly from the original or copy submitted. Thus, some thesis and dissertation copies are in typewriter face, while others may be from any type of computer printer.

The quality of this reproduction is dependent upon the quality of the copy submitted. Broken or indistinct print, colored or poor quality illustrations and photographs, print bleedthrough, substandard margins, and improper alignment can adversely affect reproduction.

In the unlikely event that the author did not send UMI a complete manuscript and there are missing pages, these will be noted. Also, if unauthorized copyright material had to be removed, a note will indicate the deletion.

Oversize materials (e.g., maps, drawings, charts) are reproduced by sectioning the original, beginning at the upper left-hand corner and continuing from left to right in equal sections with small overlaps.

Photographs included in the original manuscript have been reproduced xerographically in this copy. Higher quality 6" x 9" black and white photographic prints are available for any photographs or illustrations appearing in this copy for an additional charge. Contact UMI directly to order.

ProQuest Information and Learning
300 North Zeeb Road, Ann Arbor, MI 48106-1346 USA
800-521-0600

Université d'Ottawa · University of Ottawa

FOKKER-PLANCK APPROACH TO STOCHASTIC DELAY DIFFERENTIAL EQUATIONS

by
Steve Guillouzic

Thesis submitted to
the Faculty of Graduate and Postdoctoral Studies
in partial fulfilment of the requirements
for the degree of Doctor of Philosophy

Ottawa-Carleton Institute for Physics
University of Ottawa
Ottawa, Canada
December 22, 2000

Abstract

Models written in terms of stochastic delay differential equations (SDDE's) have recently appeared in a number of fields, such as physiology, optics, and climatology. Unfortunately, the development of a Fokker-Planck approach for these equations is being hampered by their non-Markovian nature. In this thesis, an exact Fokker-Planck equation (FPE) is formulated for univariate SDDE's involving Gaussian white noise. Although this FPE is not self-sufficient, it is found to be helpful in at least two different contexts: with a short delay approximation and under an appropriate separation of time scales.

In the short delay approximation, a Taylor expansion is applied to an SDDE with non-delayed diffusion and yields a nondelayed stochastic differential equation. The aforementioned FPE then allows the derivation of an alternate and complementary approximation of the original SDDE. This method is illustrated with linear and logistic SDDE's.

Under the separation of time scales assumption, the FPE of a bistable system is reduced to a form that is uniquely determined by the steady-state probability density when the diffusion term of the SDDE is nondelayed. In the context of an overdamped particle with delayed coupling to a symmetrical and stochastically driven potential, the resulting FPE is used with standard techniques to express the transition rate between wells in terms of the noise amplitude and of the steady-state probability density. The same is also accomplished for the mean first passage time from one point to another. This whole approach is then applied to the case of a quartic potential, for which all realisations eventually stabilise on an oscillatory trajectory with an ever increasing amplitude. Although this latter phenomenon prevents the existence of a steady-state limit, a pseudo-steady-state probability density can be defined and used instead of the non-existent steady-state one when the transition rate to these unbounded oscillatory trajectories is sufficiently small. The transition to this peculiar attractor is investigated in more detail for a family of single-well potentials, and interestingly, the transition rate follows Arrhenius' law when the noise amplitude is small.

Overall, it is found that the Fokker-Planck approach can play a significant role in the analysis of SDDE's.

Résumé

Des équations différentielles stochastiques à délai (EDSD) ont récemment fait leur apparition dans nombre de modèles, notamment en physiologie, en optique et en climatologie. Malheureusement, l'aspect non markovien de ces équations nuit à la mise au point d'une approche de Fokker-Planck pour celles-ci. Une équation de Fokker-Planck (EFP) exacte, quoique non suffisante, est développée ici pour des EDSD univariées impliquant du bruit blanc gaussien. Cette EFP est ensuite utilisée dans le cadre d'une approximation des petits délais et dans celui d'une séparation d'échelles de temps.

Pour de petits délais, un développement de Taylor est utilisé afin de passer d'une EDSD avec un terme de diffusion non retardé à une équation différentielle stochastique sans délai. Une seconde équation approximative est ensuite obtenue à l'aide de l'EFP mentionnée ci-dessus. Cette approche est appliquée à une EDSD linéaire et une EDSD logistique.

Une séparation d'échelles de temps présentée par la suite permet à l'EFP d'un système bistable d'être entièrement déterminée par la densité de probabilité stationnaire lorsque le terme de diffusion de l'EDSD est non retardé. Dans le contexte d'une particule évoluant de façon suramortie dans un potentiel symétrique, retardé et stochastiquement forcé, l'EFP résultante est alors utilisée avec des méthodes connues afin d'exprimer le taux de transition entre les puits et le temps moyen de premier passage d'un point à un autre en fonction de l'amplitude du bruit et de la densité de probabilité stationnaire. Pour le cas particulier du potentiel quartique, la présence de trajectoires oscillatoires non bornées empêche l'existence d'une telle densité de probabilité stationnaire. Il est cependant possible de définir une densité de probabilité pseudo-stationnaire et de l'utiliser à la place de cette dernière lorsque le taux de transition vers les trajectoires non bornées est suffisamment faible. La transition vers cet attracteur inusité est étudiée plus à fond pour une famille de potentiels à un puit. Il est intéressant de noter que, dans ce cas, le taux de transition suit la loi d'Arrhenius lorsque l'amplitude du bruit est suffisamment petite.

Dans l'ensemble, il est clair que l'approche de Fokker-Planck peut jouer un rôle significatif dans l'étude des EDSD.

Acknowledgements

I first want to thank my supervisors, Drs. Ivan L'Heureux and André Longtin, for their advice and support throughout the years. Their confidence in my ability to tackle this subject has been a strong source of motivation.

I also want to thank Drs. Michael C. Mackey and John Milton for sharing their thoughts on this problem, and Dr. Robert Maier for his helpful comments.

I want to address special thanks to all the members of the Physics Department. It has always been a pleasure to spend time and discuss with my fellow colleagues of this worthy institution.

I am also grateful to my friends and relatives for their continuous moral support. Their presence has been a precious asset in this scholarly quest. In addition, I want to thank my brother-in-law Jean-Claude for lending me his computer on several occasions.

Above all, I want to express my deepest thanks to my wife Annie, who encouraged me throughout this whole venture. Her patience and understanding have greatly facilitated my work.

Finally, I want to thank NSERC, IODE, and the University of Ottawa for their financial support.

Contents

List of Figures

List of Tables

Chapter 1

Introduction

Ever since the creation of calculus by Newton and Leibniz in the seventeenth century, differential equations have played a central role in science, notably in physics. Over the years, they have been used both to formulate general principles, such as Newton's second law of dynamics, and to model particular systems. In addition, the past century has seen important developments that have increased even further the modelling power of differential equations. Indeed, new types of differential equation that have been devised over that period can be used in some cases where the traditional ones are inappropriate or yield overly complicated models.

In Brownian motion, for instance, small particles present in water move in a seemingly erratic fashion because of collisions with water molecules. Although this motion could in principle be described using a set of ordinary differential equations, the huge number of water molecules colliding with the particles prevents this method from yielding useful results. On the other hand, the overall contribution of water molecules can be taken into account using a stochastic process built according to their statistical properties. With this latter approach, the evolution of each particle is then modelled by a stochastic differential equation (SDE), which is intrinsically non-deterministic. The theory underlying SDE's is now well established [1, 2], and these differential equations are frequently used to model systems subjected to random fluctuations, also known as noise, whether these fluctuations be of internal or environmental origin. Such a model is often reformulated in terms of the probability density function associated with the dynamical variables of the SDE. This is done by obtaining an evolution equation for the probability density function. For example, the well-known Fokker-Planck equation (FPE) is the evolution equation that arises when an SDE involves Gaussian white noise [1,2]. It is important to note that such an equation allows the determination of more than the probability density itself. Indeed, it can also be used to

characterise rate processes between the various basins of attraction of a deterministically multistable system. This is true whether the SDE is driven by Gaussian white noise [3–5], Ornstein-Uhlenbeck noise [6,7], or dichotomous noise [8–13].

Blood cell regulation is another example where it is advantageous to consider an alternate type of differential equation. In this case, the maturation time of the blood cells, on the order of a few days, induces a significant delay in the feedback loop that regulates their concentration. The variation in the number of blood cells at any given time therefore depends not only on the value of the concentration at that time, but also on its value at some time in the past. This delay can be accounted for by introducing the delayed value of the blood cell concentration in the differential equation that describes the regulation process [14]. If all past values are weighted according to a memory kernel, this results in an integrodifferential equation. However, if only a discrete number of past values are considered, there is no need for an integral, and a delay differential equation (DDE) is obtained [15,16]. Because of the delay, systems described by DDE's, even univariate ones, evolve in an effectively infinite-dimensional phase space. This means that limit cycles and chaotic attractors may be present irrespective of the number of dynamical variables involved. This modelling power, coupled with the omnipresence of delayed feedback in nature, has caused DDE's to be employed in a wide variety of fields in recent decades. For instance, they have been used in modelling optical devices [17–20], population dynamics [21], physiological systems [14,22,23], neural networks [24], economic phenomena [25], chemical kinetics [26], and climate fluctuations [27,28].

Stochastically driven DDE's are called stochastic delay differential equations (SDDE's). Since noise is as ubiquitous as delayed feedback, these equations play an increasingly important role in modelling and are already being used in a number of fields, such as physiology [22,29–31], optics [32,33], and climatology [34]. For instance, in Ref. 34, an SDDE is suggested as a model for the climate fluctuation known as the Southern Oscillation and composed of the El Niño and La Niña phases. In this case, the delayed feedback arises from the coupling between the Pacific ocean and the atmosphere, and the noise represents the overall contribution of varied short term weather fluctuations. In addition, multistability and rate processes in systems exhibiting both random fluctuations and delayed feedback have been the subject of several recent papers, with models ranging from SDDE's [35,36] to stochastic integrate-and-fire models with delayed recurrent loops [37], and from stochastic integrodifferential equations [38–41] to stochastic delayed maps [42]. It is thus essential to develop a good understanding of systems described by SDDE's. Unfortunately, the presence of delayed feedback prevents the evolution equations for the probability density, at least as

formulated for nondelayed SDE's, from being used in the context of SDDE's. Although an approximate FPE has been recently obtained for a particular linear SDDE [43, 44], the derivation of such evolution equations for SDDE's in general remains an open problem.

Correspondingly, this thesis is centred on the Fokker-Planck equation in the context of SDDE's driven by Gaussian white noise. It is organised as follows:

Chapter 2 presents background information relative to both SDE's and DDE's. It also summarises recent results in the field of SDDE's that are relevant for this thesis.

Chapter 3 discusses the applicability of the Fokker-Planck approach for SDDE's. Two different FPE's are presented, in Secs. 3.1 and 3.3.2. The correspondence between Ito and Stratonovich SDDE's is also considered.

Chapter 4 presents a small delay approximation that leads from an SDDE to a nondelayed SDE. When used in conjunction with the FPE presented in Sec. 3.1, this method yields two complementary approximate SDE's.

Chapter 5 considers rate processes in systems that exhibit delayed coupling between an overdamped particle and a stochastically driven potential. In Sec. 5.2, the transition rate to a peculiar attractor consisting of unbounded oscillatory trajectories is investigated for a family of single-well potentials. In Sec. 5.3, rate processes in a symmetric bistable potential are characterised under an appropriate separation of time scales by using the FPE presented in Sec. 3.1 and the steady-state probability density.

Chapter 6 summarises the main conclusions of this thesis and offers some suggestions for future research projects.

Appendix A discusses the numerical methods used for obtaining the results reported in this thesis.

Appendix B lists the publications and the conference presentations that have been based on material presented in this document.

Chapter 2

Background Information

This chapter summarises the key concepts underlying this research project. Section 2.1 first presents an overview of stochastic processes. In particular, it introduces what is known as the Fokker-Planck equation and states its correspondence with stochastic differential equations driven by Gaussian white noise. Section 2.2 then deals with delay differential equations and includes a short review of recent results pertaining to differential equations that are both stochastic and delayed.

2.1 Stochastic Processes

2.1.1 Probability Functions

A *stochastic process* is a collection of random variables parameterised by time [1, 2, 45]. Thus, at any given time, the value assumed by a stochastic process follows a probability distribution instead of being deterministically determined. More precisely, a stochastic process $x(t)$ is defined through an infinite hierarchy [2] composed of the first-order probability distribution function

$$F(x_1, t_1) \equiv \text{probability that } x(t_1) \leq x_1,$$

the second-order probability distribution function

$$F(x_1, t_1; x_2, t_2) \equiv \text{probability that } x(t_1) \leq x_1 \text{ and } x(t_2) \leq x_2,$$

and so on. As illustrated in part (d) of Sec. 2.1.5, the *state space* of a stochastic process, which is the set of values that can be assumed by the state variable x, may be either discrete or continuous. In both cases, probability distribution functions are defined over the whole

real axis. If the state space is discrete, they vary only through discrete jumps at discrete values of the state variable; if it is continuous, they can vary both continuously and through discrete jumps.

A stochastic process defined over a discrete state space may also be characterised using probability functions, such as the first-order probability function

$$P(x_1,t_1) \equiv \lim_{\Delta x_1 \to 0}[F(x_1,t_1) - F(x_1-\Delta x_1,t_1)]$$

and the second-order probability function

$$\begin{aligned} P(x_1,t_1;x_2,t_2) \equiv \lim_{\Delta x_1,\Delta x_2 \to 0}[&F(x_1,t_1;x_2,t_2) + F(x_1-\Delta x_1,t_1;x_2-\Delta x_2,t_2) \\ &- F(x_1-\Delta x_1,t_1;x_2,t_2) - F(x_1,t_1;x_2-\Delta x_2,t_2)]. \end{aligned}$$

Here, $P(x_1,t_1)$ is the probability that $x(t_1) = x_1$, and $P(x_1,t_1;x_2,t_2)$ is the probability that both $x(t_1) = x_1$ and $x(t_2) = x_2$. It is also often useful to consider conditional probability functions, such as

$$P(x_2,t_2|x_1,t_1) \equiv \frac{P(x_1,t_1;x_2,t_2)}{P(x_1,t_1)},$$

which is the probability that $x(t_2) = x_2$ given that $x(t_1) = x_1$.

For stochastic processes defined over a continuous state space, probability distribution functions may increase continuously. Probability functions vanish at the points of state space where this happens, since the probability of being exactly at those points is zero. However, the probability of being in small regions around those points is not zero. This is taken into account by probability density functions, such as the first-order probability density function

$$\begin{aligned} p(x_1,t_1) &\equiv \lim_{\Delta x_1 \to 0} \frac{1}{\Delta x_1}[F(x_1,t_1) - F(x_1-\Delta x_1,t_1)] \\ &= \frac{\partial}{\partial x_1} F(x_1,t_1) \end{aligned} \tag{2.1}$$

and the second-order probability density function

$$\begin{aligned} p(x_1,t_1;x_2,t_2) \equiv \lim_{\Delta x_1,\Delta x_2 \to 0} \frac{1}{\Delta x_1 \Delta x_2}[&F(x_1,t_1;x_2,t_2) + F(x_1-\Delta x_1,t_1;x_2-\Delta x_2,t_2) \\ &- F(x_1-\Delta x_1,t_1;x_2,t_2) - F(x_1,t_1;x_2-\Delta x_2,t_2)] \\ = \frac{\partial^2}{\partial x_1 \partial x_2} F(x_1,t_1;x_2,t_2). \end{aligned} \tag{2.2}$$

For instance, $p(x_1,t_1)dx_1$ is the probability, up to first order in dx_1, that $x(t_1) \in [x_1 - dx_1, x_1]$. Conditional probability density functions are then defined in the same way as conditional probability functions. For example,

$$p(x_2,t_2|x_1,t_1)dx_2 \equiv \frac{p(x_1,t_1;x_2,t_2)}{p(x_1,t_1)}dx_2 \tag{2.3}$$

is the probability, up to first order in dx_2, that $x(t_2) \in [x_2 - dx_2, x_2]$ given that $x(t_1) = x_1$.

When considering a pair of stochastic processes $x(t)$ and $y(t)$, joint probability distribution functions, such as

$$F(x_1,t_1;y_2,t_2) \equiv \text{probability that } x(t_1) \leq x_1 \text{ and } y(t_2) \leq y_2,$$

also need to be considered. These joint distribution functions lead to joint probability functions and joint probability density functions, such as

$$p(x_1,t_1;y_2,t_2) \equiv \lim_{\Delta x_1,\Delta y_2 \to 0} \frac{1}{\Delta x_1 \Delta y_2}[F(x_1,t_1;y_2,t_2) + F(x_1 - \Delta x_1,t_1;y_2 - \Delta y_2,t_2) - F(x_1 - \Delta x_1,t_1;y_2,t_2) - F(x_1,t_1;y_2 - \Delta y_2,t_2)].$$

2.1.2 Realisations and Sample Paths

Each instantiation of a stochastic process is known as a *realisation*, and the set of values assumed by the state variable as a function of time for a given realisation is called a *sample path*. When the state space is discrete, the state variable can vary only through discrete jumps and the sample paths must be either constant or discontinuous. On the other hand, when the state space is continuous, the state variable may be allowed to vary continuously as a function of time and the sample paths may in this case be continuous without being constant.

2.1.3 Ensemble Averages

Ensemble averages $\langle \cdots \rangle$ are defined as averages over realisations and are calculated using probability functions or probability density functions. Over a discrete state space, the ensemble average of the arbitrary univariate function $G(x(t_1))$ is given by

$$\langle G(x(t_1)) \rangle \equiv \sum_{x_1} G(x_1)P(x_1,t_1),$$

and the ensemble average of the arbitrary bivariate function $G(x(t_1), x(t_2))$, by

$$\langle G(x(t_1), x(t_2)) \rangle \equiv \sum_{x_1, x_2} G(x_1, x_2) P(x_1, t_1; x_2, t_2).$$

In the case of a continuous state space, these ensemble averages become

$$\langle G(x(t_1)) \rangle \equiv \int_{-\infty}^{\infty} dx_1 G(x_1) p(x_1, t_1)$$

and

$$\langle G(x(t_1), x(t_2)) \rangle \equiv \int_{-\infty}^{\infty} dx_1 \int_{-\infty}^{\infty} dx_2 G(x_1, x_2) p(x_1, t_1; x_2, t_2).$$

The mean $\mu_x(t_1) \equiv \langle x(t_1) \rangle$ and the autocorrelation function $R_{xx}(t_1, t_2) \equiv \langle x(t_1) x(t_2) \rangle$ are two commonly used ensemble averages. The autocovariance function is also often encountered. It is defined as $C_{xx}(t_1, t_2) \equiv R_{xx}(t_1, t_2) - \mu_x(t_1)\mu_x(t_2)$ and yields the variance $\sigma_x^2(t_1) \equiv \langle x^2(t_1) \rangle - \langle x(t_1) \rangle^2$ when evaluated at $t_2 = t_1$. Another quantity of interest related to these ensemble averages is the correlation coefficient

$$r_{xx}(t_1, t_2) \equiv \frac{R_{xx}(t_1, t_2)}{\sigma_x(t_1)\sigma_x(t_2)}.$$

This function, which can vary between -1 and 1, quantifies the extent to which the state of the process at time t_2 is a linear function of its state at time t_1. If $r_{xx}(t_1, t_2) = \pm 1$, the state of the process at times t_1 and t_2 can be expressed as linear functions of one another. On the other hand, if $r_{xx}(t_1, t_2) = 0$, there is no linear relation between the state of the process at these two times, which means either that the states are not related or that the relation between them has no linear component.

Using joint probability functions and joint probability density functions, ensemble averages involving two stochastic processes, such as

$$\langle G(x(t_1), y(t_2)) \rangle \equiv \int_{-\infty}^{\infty} dx_1 \int_{-\infty}^{\infty} dy_2 G(x_1, x_2) p(x_1, t_1; y_2, t_2),$$

may also be calculated. These averages lead, for instance, to the cross-correlation function $R_{xy}(t_1, t_2) \equiv \langle x(t_1) y(t_2) \rangle$.

Furthermore, ensemble averages can also be defined using conditional probability functions and conditional probability density functions. For instance, over a continuous state

space,

$$\langle G(x(t_2))|x_1,t_1\rangle \equiv \int_{-\infty}^{\infty} dx_2 G(x_2) p(x_2,t_2|x_1,t_1)$$

and

$$\langle G(x(t_2),x(t_3))|x_1,t_1\rangle \equiv \int_{-\infty}^{\infty} dx_2 \int_{-\infty}^{\infty} dx_3 G(x_2,x_3) p(x_2,t_2;x_3,t_3|x_1,t_1).$$

This leads to the conditional mean $\langle x(t_2)|x_1,t_1\rangle$, the conditional autocorrelation function $\langle x(t_2)x(t_3)|x_1,t_1\rangle$, etc.

2.1.4 Stationary Processes

A *stationary* process is one for which all statistical properties are invariant with respect to the time of measurement [1, 2, 45]. In other words, a stationary process is one for which all probability distribution functions, or equivalently all probability functions or probability density functions, are invariant to time shifts. In particular, in the case of a process defined over a continuous state space, this means that

$$\begin{aligned} p(x_1,t_1) &= p(x_1,t_1+\Delta t) \\ &\equiv p^s(x_1) \end{aligned}$$

and

$$\begin{aligned} p(x_1,t_1;x_2,t_2) &= p(x_1,t_1+\Delta t;x_2,t_2+\Delta t) \\ &\equiv p^s(x_1;x_2,t_2-t_1) \end{aligned}$$

for all values of Δt. Since $p^s(x_1)$ and $p^s(x_1;x_2,t_2-t_1)$ are time-shift invariant, they are called *steady-state* probability density functions. Stationary processes also possess time-shift invariant conditional probability density functions, since these are defined as ratios of non-conditional probability density functions. The same holds for conditional probability functions.

Steady-state ensemble averages, which are denoted by $\langle\cdots\rangle_s$, are defined using the formulas presented in Sec. 2.1.3, but with respect to steady-state probability functions and steady-state probability density functions. Whereas the mean $\mu(t_1)$ and the variance $\sigma_x^2(t_1)$ are time-dependent, the steady-state mean and the steady-state variance are time-independent and are thus denoted as $\mu_x \equiv \langle x\rangle_s$ and $\sigma_x^2 \equiv \langle x^2\rangle_s - \langle x\rangle_s^2$. Similarly, the steady-state autocorrelation function $R_{xx}(t_2-t_1) \equiv \langle x(t_1)x(t_2)\rangle_s$, cross-correlation function $R_{xy}(t_2-t_1) \equiv \langle x(t_1)y(t_2)\rangle_s$, autocovariance function $C_{xx}(t_2-t_1) \equiv R_{xx}(t_2-t_1) - \mu_x^2$, and

correlation coefficient

$$r_{xx}(t_2 - t_1) \equiv \frac{R_{xx}(t_2 - t_1)}{\sigma_x^2} \tag{2.4}$$

only depend on the time difference $\Delta t \equiv t_2 - t_1$. The correlation time, which can be defined as [1, 46]

$$\tau_{\text{cor}} \equiv \int_0^\infty r_{xx}(t)dt,$$

is the time scale over which $r_{xx}(\Delta t)$ relaxes. This quantity characterises the memory of the process, since the steady-state correlation coefficient $r_{xx}(\Delta t)$ approaches zero for $\Delta t \gg \tau_{\text{cor}}$.

A process for which $\langle x(t_1) \rangle$ is independent of t_1 and $\langle x(t_1)x(t_2) \rangle$ depends only on $t_2 - t_1$ is said to be wide-sense stationary. Clearly, all stationary processes are wide-sense stationary, but the converse is not true. The Wiener-Khinchin theorem [1] states that for a wide-sense stationary process, the power spectrum, defined in general as

$$S_{xx}(\omega) \equiv \lim_{T \to \infty} \frac{1}{T} \left| \int_0^T e^{-i\omega t} x(t)dt \right|^2,$$

is given by

$$S_{xx}(\omega) = \int_{-\infty}^\infty e^{-i\omega t} R_{xx}(t)dt.$$

Defining the Fourier transform $S(\omega)$ of a function $R(t)$ as

$$\begin{aligned} S(\omega) &= \mathcal{F}\{R(t)\} \\ &\equiv \int_{-\infty}^\infty e^{-i\omega t} R(t)dt, \end{aligned} \tag{2.5}$$

the inverse Fourier transform of $S(\omega)$ is then given by

$$\begin{aligned} R(t) &= \mathcal{F}^{-1}\{S(\omega)\} \\ &\equiv \frac{1}{2\pi} \int_{-\infty}^\infty e^{i\omega t} S(\omega)d\omega \end{aligned} \tag{2.6}$$

and the power spectrum is seen to be the Fourier transform of the autocorrelation function. Similarly, two stochastic processes are said to be jointly wide-sense stationary if each is wide-sense stationary and if, in addition, their cross-correlation function is also time-shift invariant. The cross-spectrum $S_{xy}(\omega)$ of such two processes is calculated as the Fourier transform of their cross-correlation function.

2.1.5 Markov Processes

a) Chapman-Kolmogorov Equation

A stochastic process defined over a continuous state space is said to be Markovian if the equality

$$p(x_2', t_2'; x_2'', t_2''; \cdots | x_1', t_1'; x_1'', t_1''; \cdots) = p(x_2', t_2'; x_2'', t_2''; \cdots | x_1, t_1), \tag{2.7}$$

where $t_1 \equiv \max(t_1', t_1'', \cdots)$ and $t_1 < \min(t_2', t_2'', \cdots)$, holds for all its conditional probability density functions [1]. In other words, once the state $x(t)$ of a Markov process is known at time $t = t_1$, specifying $x(t)$ for $t < t_1$ does not improve the predictability of $x(t)$ for $t > t_1$.

For any stochastic process, the probability of going from an initial state $x_1(t_1)$ to a final state $x_3(t_3)$ through a completely unspecified path can be expressed in terms of the probability of going from $x_1(t_1)$ to $x_3(t_3)$ through an intermediate state $x_2(t_2)$. This is done by summing over all the values that the intermediate state variable x_2 can assume. In the case of a continuous state space, this is written as

$$p(x_3, t_3 | x_1, t_1) = \int dx_2 p(x_3, t_3 | x_2, t_2; x_1, t_1) p(x_2, t_2 | x_1, t_1), \tag{2.8}$$

where $t_1 < t_2 < t_3$. For a Markov process, Eq. (2.8) reduces to the Chapman-Kolmogorov equation

$$p(x_3, t_3 | x_1, t_1) = \int dx_2 p(x_3, t_3 | x_2, t_2) p(x_2, t_2 | x_1, t_1), \tag{2.9}$$

since the evolution from $x_1(t_1)$ to $x_2(t_2)$ and the evolution from $x_2(t_2)$ to $x_3(t_3)$ are statistically independent. The differential Chapman-Kolmogorov equation [1]

$$\begin{aligned} &\frac{\partial}{\partial t_3} p(x_3, t_3 | x_1, t_1) \\ &\quad = -\frac{\partial}{\partial x_3}[A(x_3, t_3) p(x_3, t_3 | x_1, t_1)] + \frac{1}{2}\frac{\partial^2}{\partial x_3^2}[B(x_3, t_3) p(x_3, t_3 | x_1, t_1)] \\ &\qquad + \int dx_2 [w(x_3 | x_2, t_3) p(x_2, t_3 | x_1, t_1) - w(x_2 | x_3, t_3) p(x_3, t_3 | x_1, t_1)], \end{aligned} \tag{2.10}$$

can be obtained from Eq. (2.9) if, for all $\epsilon > 0$,

$$\lim_{\Delta t \to 0} \frac{1}{\Delta t} p(x_2, t_1 + \Delta t | x_1, t_1) \equiv w(x_2 | x_1, t_1) \tag{2.11}$$

converges uniformly in x_1, t_1, and x_2 for $|x_2 - x_1| \geq \epsilon$, while

$$\lim_{\Delta t \to 0} \frac{1}{\Delta t} \int_{x_1-\epsilon}^{x_1+\epsilon} dx_2 (x_2 - x_1) p(x_2, t_1 + \Delta t | x_1, t_1) \equiv A(x_1, t_1) + \mathcal{O}(\epsilon) \tag{2.12}$$

and

$$\lim_{\Delta t \to 0} \frac{1}{\Delta t} \int_{x_1-\epsilon}^{x_1+\epsilon} dx_2 (x_2 - x_1)^2 p(x_2, t_1 + \Delta t | x_1, t_1) \equiv B(x_1, t_1) + \mathcal{O}(\epsilon) \tag{2.13}$$

converge uniformly in x_2, t_2, and ϵ. The functions $w(x_2|x_1, t_1)$, $A(x_1, t_1)$, and $B(x_1, t_1)$ correspond to three different types of physical phenomenon. The distribution of discontinuous jumps is given by $w(x_1|x_2, t_2)$, while $A(x_1, t_1)$ and $B(x_1, t_1)$ respectively describe the deterministic drift and the diffusion. Equation (2.9) can also lead to the *backward* differential Chapman-Kolmogorov equation [1]

$$\begin{aligned} &\frac{\partial}{\partial t_1} p(x_3, t_3 | x_1, t_1) \\ &\quad = - A(x_1, t_1) \frac{\partial}{\partial x_1} p(x_3, t_3 | x_1, t_1) - \frac{1}{2} B(x_1, t_1) \frac{\partial^2}{\partial x_1^2} p(x_3, t_3 | x_1, t_1) \\ &\qquad + \int dx_2 w(x_2 | x_1, t_1) [p(x_3, t_3 | x_1, t_1) - p(x_3, t_3 | x_2, t_1)]. \end{aligned} \tag{2.14}$$

The fundamental difference between Eqs. (2.10) and (2.14) lies in the respective roles of t_1 and t_3. In Eq. (2.10), t_1 is kept fixed and t_3 is allowed to increase from t_1 to ∞, subject to the initial condition

$$p(x_3, t_1 | x_1, t_1) = \delta(x_3 - x_1). \tag{2.15}$$

This equation, in which $\delta(x)$ represents the Dirac delta function, simply states that $x(t)$ cannot assume two different values at the same time. In Eq. (2.14), on the other hand,

$$p(x_3, t_3 | x_1, t_3) = \delta(x_3 - x_1), \tag{2.16}$$

is considered to be a final condition and t_1 varies between $-\infty$ and t_3, which is held fixed. Both equations are nevertheless considered to be equivalent, since they lead to the same solutions for $p(x_3, t_3|x_1, t_1)$ [1].

In the case of a stochastic process defined over a discrete state space, the Markov assumption reads

$$P(x_2', t_2'; x_2'', t_2''; \cdots | x_1', t_1'; x_1'', t_1''; \cdots) = P(x_2', t_2'; x_2'', t_2''; \cdots | x_1, t_1) \tag{2.17}$$

and the Chapman-Kolmogorov equation becomes

$$P(x_3,t_3|x_1,t_1) = \sum_{x_2} P(x_3,t_3|x_2,t_2)P(x_2,t_2|x_1,t_1). \tag{2.18}$$

For such a process, the differential Chapman-Kolmogorov equation simplifies to the so-called Master equation [1]

$$\frac{\partial}{\partial t_3}P(x_3,t_3|x_1,t_1) = \sum_{x_2}[w(x_3|x_2,t_3)P(x_2,t_3|x_1,t_1) - w(x_2|x_3,t_3)P(x_3,t_3|x_1,t_1)], \tag{2.19}$$

since there can be no drift or diffusion. Similarly, the backward differential Chapman-Kolmogorov equation reduces to the backward Master equation [1]

$$\frac{\partial}{\partial t_1}P(x_3,t_3|x_1,t_1) = \sum_{x_2} w(x_2|x_1,t_1)[P(x_3,t_3|x_1,t_1) - P(x_3,t_3|x_2,t_1)]. \tag{2.20}$$

In Eqs. (2.19) and (2.20), $w(x_2|x_1,t_1)$ is now defined as

$$w(x_2|x_1,t_1) \equiv \lim_{\Delta t\to 0}\frac{1}{\Delta t}P(x_2,t_1+\Delta t|x_1,t_1), \tag{2.21}$$

but still characterises the distribution of jump processes.

b) Homogeneous Markov Processes

A Markov process is called *time homogeneous* when its conditional probability density $p(x_2,t_2|x_1,t_1)$ is time-shift invariant [1,2]. This invariance implies that $A(x_1,t_1)$, $B(x_1,t_1)$, and $w(x_2|x_1,t_1)$ are independent of time, as seen from Eqs. (2.11) to (2.13). It is important to note that a time homogeneous process need not be stationary, even though a stationary process is necessarily time homogeneous. However, several homogeneous processes tend to a stationary limit as they evolve.

c) Types of Markov Process

Not all Markov processes defined over a continuous state space are such that $A(x_1,t_1)$, $B(x_1,t_1)$, and $w(x_2|x_1,t_1)$ are non-zero. Setting some of these quantities to zero leads to particular types of Markov process.

Deterministic Processes For a deterministic system, there are no discontinuous jumps and no diffusion. Thus, $w(x_2|x_1,t_1) = B(x_1,t_1) = 0$, and Eq. (2.10) reduces to the Liouville

equation

$$\frac{\partial}{\partial t_2}p(x_2,t_2|x_1,t_1) = -\frac{\partial}{\partial x_2}[A(x_2,t_2)p(x_2,t_2|x_1,t_1)].$$

This corresponds to a system whose evolution is given by [1]

$$\frac{d}{dt}x(t) = A\big(x(t),t\big),$$

thus illustrating that $A(x_1,t_1)$ corresponds to the drift.

Diffusion Processes If only $w(x_1|x_2,t_2)$ is zero, Eq. (2.10) yields a diffusion process with drift and reduces to the well-known Fokker-Planck equation (FPE) [1]

$$\frac{\partial}{\partial t_2}p(x_2,t_2|x_1,t_1) = -\frac{\partial}{\partial x_2}J(x_2,t_2|x_1,t_1), \tag{2.22}$$

where

$$J(x_2,t_2|x_1,t_1) \equiv A(x_2,t_2)p(x_2,t_2|x_1,t_1) - \frac{1}{2}\frac{\partial}{\partial x_2}[B(x_2,t_2)p(x_2,t_2|x_1,t_1)]$$

is a probability current density. Diffusion processes have continuous, but nowhere differentiable, sample paths. For a time homogeneous process, both $A(x_1,t_1) \equiv A(x_1)$ and $B(x_1,t_1) \equiv B(x_1)$ are time independent, as seen in part (b). Assuming the existence of the steady-state limits

$$p^s(x_2) \equiv \lim_{(t_2-t_1)\to\infty} p(x_2,t_2|x_1,t_1)$$

and

$$J^s(x_2) \equiv \lim_{(t_2-t_1)\to\infty} J(x_2,t_2|x_1,t_1),$$

Eq. (2.22) leads to

$$\frac{d}{dx_2}J^s(x_2) = 0. \tag{2.23}$$

The steady-state probability current density $J^s(x_1)$ is thus equal to a constant determined by the boundary conditions [1].

A boundary where the probability current density is set to zero and where the probability density is left unspecified is called *reflecting*. When both boundaries are of this type, Eq. (2.23) leads to the so-called potential solution

$$p^s(x_2) = \frac{N}{B(x_2)}\exp\left(\int_c^{x_2} dx_2'\frac{A(x_2')}{B(x_2')}\right), \tag{2.24}$$

where N is a normalisation constant and c is arbitrary. However, if the probability density at one of the boundaries is set to zero and the probability current density at that point is left unspecified, the said boundary is then *absorbing* and there can be no steady-state probability density. Indeed, absorbing boundaries act as drains for the probability density and cause $p(x_2, t_2|x_1, t_1)$ to identically approach zero as $t_2 - t_1 \to \infty$. The choice of the names *reflecting* and *absorbing* for these two types of boundary condition is best understood by considering an example where the state variable $x(t)$ represents the position of a particle. In such a case, reflecting and absorbing boundaries respectively correspond to points where the particle is reflected and absorbed.

For a diffusion process, the backward Chapman-Kolmogorov equation [Eq. (2.14)] leads to the backward FPE [1]

$$\frac{\partial}{\partial t_1} p(x_2, t_2|x_1, t_1) = -A(x_1, t_1)\frac{\partial}{\partial x_1} p(x_2, t_2|x_1, t_1) - \frac{1}{2} B(x_1, t_1)\frac{\partial^2}{\partial x_1^2} p(x_2, t_2|x_1, t_1). \quad (2.25)$$

When working with this equation, the conditions used for obtaining the various types of boundary differ slightly from those presented in the previous paragraph. This results from the fact that x_2 and t_2 are the variables considered to be fixed in Eq. (2.25), while this role is played by x_1 and t_1 in Eq. (2.22). In the context of the backward FPE, reflecting and absorbing boundaries are obtained by respectively setting $\partial p(x_2, t_2|x_1, t_1)/\partial x_1$ and $p(x_2, t_2|x_1, t_1)$ to zero.

Jump Processes Setting $A(x_1, t_1) = B(x_1, t_1) = 0$ in Eq. (2.10) leads to

$$\frac{\partial}{\partial t_3} p(x_3, t_3|x_1, t_1) = \int dx_2 [w(x_3|x_2, t_3)p(x_2, t_3|x_1, t_1) - w(x_2|x_3, t_3)p(x_3, t_3|x_1, t_1)],$$

which is another form of the Master equation [1]. This equation describes a jump process over a continuous state space, whereas Eq. (2.19) is concerned with jump processes defined over a discrete state space. All jump processes, whether defined over a continuous or a discrete state space, exhibit sample paths that are composed of constant sections interspersed with discrete jumps.

d) Examples of Markov Processes

Ornstein-Uhlenbeck Process The Ornstein-Uhlenbeck process $\zeta(t)$ is a time homogeneous diffusion process for which $A(\zeta_1) = -k\zeta_1$ and $B(\zeta_1) = D$, where k and D are positive coefficients. The evolution of its conditional probability density function is thus given by

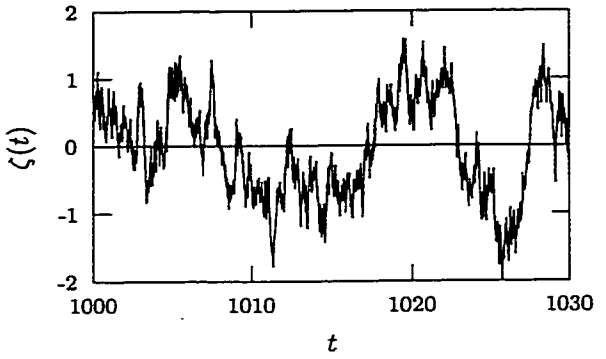

Figure 2.1: Steady-state realisation of the Ornstein-Uhlenbeck process with $k = D = 1$

the FPE

$$\frac{\partial}{\partial t_2} p(\zeta_2, t_2|\zeta_1, t_1) = k\frac{\partial}{\partial \zeta_2}[\zeta_2 p(\zeta_2, t_2|\zeta_1, t_1)] + \frac{1}{2}D\frac{\partial^2}{\partial \zeta_2^2} p(\zeta_2, t_2|\zeta_1, t_1).$$

Choosing the whole real axis as the domain and specifying reflecting boundary conditions, this equation yields a Gaussian univariate conditional probability density $p(\zeta_2, t_2|\zeta_1, t_1)$ [1] with average

$$\langle \zeta(t_2)|\zeta_1, t_1\rangle = \zeta_1 e^{-k(t_2-t_1)} \tag{2.26}$$

and variance

$$\langle \zeta^2(t_2)|\zeta_1, t_1\rangle - \langle \zeta(t_2)|\zeta_1, t_1\rangle^2 = \frac{D}{2k}\left(1 - e^{-2k(t_2-t_1)}\right). \tag{2.27}$$

The steady-state limit of $p(\zeta_2, t_2|\zeta_1, t_1)$ is obtained by letting $(t_2 - t_1) \to \infty$ in Eqs. (2.26) and (2.27). This leads to

$$p^s(\zeta_2) = \sqrt{\frac{k}{\pi D}} \exp\left(\frac{-k\zeta_2^2}{D}\right).$$

The bivariate steady-state probability density $p^s(\zeta_1; \zeta_2, t_2 - t_1)$ is then given by

$$p^s(\zeta_1; \zeta_2, t_2 - t_1) = p(\zeta_2, t_2|\zeta_1, t_1)p^s(\zeta_1),$$

from which the steady-state autocorrelation function is calculated to be

$$\langle \zeta_1(t_1)\zeta_2(t_2)\rangle_s = \frac{D}{2k} e^{-k(t_2-t_1)},$$

and the correlation time, $\tau_{\text{cor}} = 1/k$. Figure 2.1 shows a realisation of the Ornstein-Uhlenbeck process.

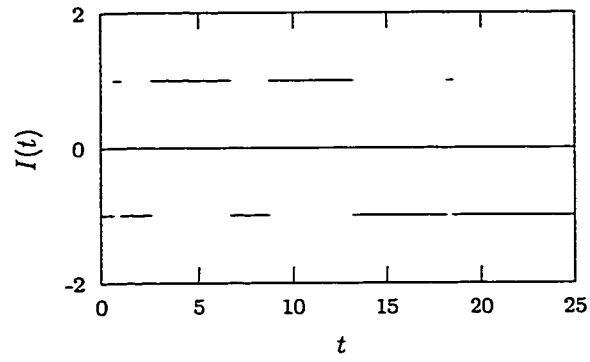

Figure 2.2: Steady-state realisation of the symmetric dichotomous process with $\Delta = \gamma = 1$

Symmetric Dichotomous Process Dichotomous processes are time homogeneous jump processes that are defined over a discrete state space composed of only two values. One such process is the symmetric dichotomous process $I(t)$, for which the two states $\pm\Delta$ are equiprobable. This process is characterised by the transition rate matrix [2]

$$\begin{aligned}\mathbf{w}(t_1) &\equiv \begin{pmatrix} w(-\Delta|-\Delta,t_1) & w(-\Delta|\Delta,t_1) \\ w(\Delta|-\Delta,t_1) & w(\Delta|\Delta,t_1) \end{pmatrix} \\ &= \begin{pmatrix} -\gamma/2 & \gamma/2 \\ \gamma/2 & -\gamma/2 \end{pmatrix},\end{aligned}$$

where γ is a positive coefficient, and the evolution of the probability vector

$$\mathbf{P}(t_2|I_1,t_1) \equiv \begin{pmatrix} P(-\Delta,t_2|I_1,t_1) \\ P(\Delta,t_2|I_1,t_1) \end{pmatrix}$$

is thus given by the Master equation

$$\frac{\partial}{\partial t_2}\mathbf{P}(t_2|I_1,t_1) = \mathbf{w}(t_2)\mathbf{P}(t_2|I_1,t_1).$$

Using the normalisation condition

$$P(-\Delta,t_2|I_1,t_1) + P(\Delta,t_2|I_1,t_1) = 1,$$

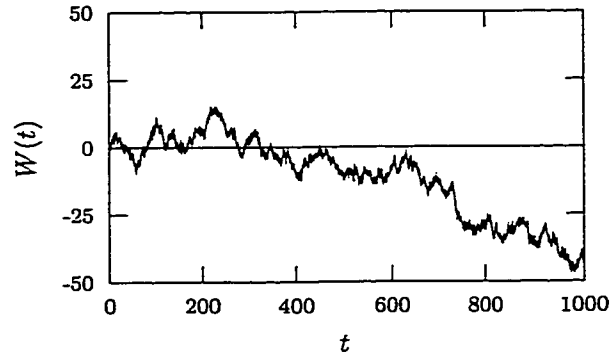

Figure 2.3: Realisation of the Wiener process

this equation is easily solved to yield the steady-state probability vector

$$\mathbf{P}^s \equiv \lim_{t_2 \to \infty} \mathbf{P}(t_2|I_1, t_1) = \begin{pmatrix} 1/2 \\ 1/2 \end{pmatrix}.$$

Furthermore, the steady-state mean of the symmetric dichotomous noise is zero, its steady-state autocorrelation function is given by

$$\langle I_1(t_1) I_2(t_2) \rangle_s = \Delta^2 e^{-\gamma(t_2 - t_1)},$$

and $\tau_{\text{cor}} = 1/\gamma$. A realisation of the symmetric dichotomous process is presented in Fig. 2.2. The results presented in this section are easily generalised to the case, called asymmetric, where the two states $\pm\Delta$ are not equiprobable [2].

Wiener Process The Wiener process $W(t)$ is a diffusion process with a null drift coefficient $A(W_1, t_1)$ and a unit diffusion coefficient $B(W_1, t_1)$. It is thus characterised by the FPE

$$\frac{\partial}{\partial t_2} p(W_2, t_2|W_1, t_1) = \frac{1}{2} \frac{\partial^2}{\partial W_2^2} p(W_2, t_1|W_1, t_1).$$

Solving this equation over the whole real axis yields the Gaussian conditional probability density function [1]

$$p(W_2, t_2|W_1, t_1) = \frac{1}{\sqrt{2\pi(t_2 - t_1)}} \exp\left(\frac{-(W_2 - W_1)^2}{2(t_2 - t_1)}\right), \tag{2.28}$$

whose mean and variance are $\langle W(t_2)|W_1,t_1\rangle = W_1$ and $\langle (W(t_2)-W_1)^2|W_1,t_1\rangle = t_2 - t_1$. Since this conditional probability density is time-shift invariant, the Wiener process is time homogeneous. However, its variance increases indefinitely with time. Thus, the Wiener process does not possess a stationary limit. Furthermore, since $W(t)$ is a diffusion process, its sample paths are continuous, but not differentiable. Figure 2.3 presents a realisation of the Wiener process.

Gaussian White Noise Gaussian white noise $\xi(t)$ is, as its name implies, a Gaussian distributed stochastic process. It is defined [1] through its mean

$$\langle \xi(t) \rangle = 0 \tag{2.29}$$

and its correlation function

$$\langle \xi(t_1)\xi(t_2) \rangle = \delta(t_1 - t_2), \tag{2.30}$$

where $\delta(t)$ is the Dirac delta function. Using Eqs. (2.29) and (2.30), the correlation time of $\xi(t)$ is calculated to be zero and the integral of $\xi(t)$ is formally found to be the Wiener process $W(t)$. Since no stochastic process found in nature has a zero correlation time and since the sample paths of the Wiener process are not differentiable, Gaussian white noise is clearly a mathematical artefact. However, it is useful when modelling a fluctuating input with a correlation time much smaller than all the other relevant time scales of the driven system.

2.1.6 Stochastic Differential Equations

Differential equations driven by stochastic processes are called stochastic differential equations (SDE's). Since the driving stochastic process usually appears linearly, the equation

$$\frac{d}{dt}x(t) = f\big(x(t)\big) + \sigma g\big(x(t)\big)\eta(t) \tag{2.31}$$

can be seen as the archetypal SDE. In this equation, $f(x)$ and $g(x)$ represent known functions and $\eta(t)$ is an arbitrary stochastic process. Stochastic differential equations are classified according to the definition of the function $g(x)$. If $g(x)$ is independent of x, the SDE is said to be driven by *additive noise*. Otherwise, the noise is said to be *multiplicative*.

In most cases, SDE's are interpreted using the usual rules of calculus. However, Gaussian white noise $\xi(t)$ cannot be integrated in the Riemann sense, since it is the derivative of the

non-differentiable Wiener process $W(t)$. Because of this, $\xi(t)$ can only appear in integral equations. Thus, the differential equation

$$\frac{d}{dt}x(t) = f\big(x(t)\big) + \sigma g\big(x(t)\big)\xi(t), \tag{2.32}$$

where σ scales the noise amplitude, must be interpreted as representing the integral equation

$$x(t_b) = x(t_a) + \int_{t_a}^{t_b} f\big(x(t)\big)dt + \sigma \int_{t_a}^{t_b} g\big(x(t)\big)dW(t). \tag{2.33}$$

In this equation, the first integral is the well-known Riemann integral, the second one is a Riemann-Stieltjes integral, and t_a and t_b are respectively the starting and ending integration times. In addition, $dW(t)$ is the differential of the Wiener process and thus represents $\xi(t)dt$.

The Riemann integral of a function $G(t)$ over the interval $[t_a, t_b]$ is defined as the limit

$$\int_{t_a}^{t_b} G(t)dt \equiv \lim_{n\to\infty} \sum_{i=1}^{n} G(t_i')(t_i - t_{i-1}), \tag{2.34}$$

where $t_a = t_0 < t_1 < .. < t_{n-1} < t_n = t_b$ and $t_i' \in [t_{i-1}, t_i]$. On the other hand, the corresponding Riemann-Stieltjes integral with respect to a given function $H(t)$ is defined as the limit

$$\int_{t_a}^{t_b} G(t)dH(t) \equiv \lim_{n\to\infty} \sum_{i=1}^{n} G(t_i')[H(t_i) - H(t_{i-1})]. \tag{2.35}$$

The Riemann integral is thus a Riemann-Stieltjes integral with respect to $H(t) = t$.

If the function $H(t)$ is a stochastic process, the limit in Eq. (2.35) is understood to be in the *mean square* [1]. This is written as

$$\int_{t_a}^{t_b} G(t)dH(t) \equiv \underset{n\to\infty}{\text{ms-lim}} \sum_{i=1}^{n} G(t_i')[H(t_i) - H(t_{i-1})] \tag{2.36}$$

and means that

$$\left\langle \left(\int_{t_a}^{t_b} G(t)dH(t) - \lim_{n\to\infty} \sum_{i=1}^{n} G(t_i')[H(t_i) - H(t_{i-1})] \right)^2 \right\rangle = 0,$$

where the average is performed over realisations (see Sec. 2.1.3). Furthermore, if $H(t) = W(t)$, as in Eq. (2.33), the result of the limiting process in Eq. (2.36) depends on the exact

choice of t_i''s. If $t_i' = t_{i-1}$, the Ito integral

$$\mathcal{I}\int_{t_a}^{t_b} G(t)dW(t) \equiv \underset{n\to\infty}{\text{ms-lim}} \sum_{i=1}^{n} G(t_{i-1})[W(t_i) - W(t_{i-1})] \tag{2.37}$$

is obtained. The identities [1]

$$\begin{aligned}\mathcal{I}\int_{t_a}^{t_b} G(t)[dW(t)]^2 &\equiv \underset{n\to\infty}{\text{ms-lim}} \sum_{i=1}^{n} G(t_{i-1})[W(t_i) - W(t_{i-1})]^2 \\ &= \int_{t_a}^{t_b} G(t)dt\end{aligned} \tag{2.38}$$

and

$$\begin{aligned}\mathcal{I}\int_{t_a}^{t_b} G(t)[dW(t)]^m[dt]^n &\equiv \underset{n\to\infty}{\text{ms-lim}} \sum_{i=1}^{n} G(t_{i-1})[W(t_i) - W(t_{i-1})]^m(t_i - t_{i-1})^n \\ &= 0,\end{aligned} \tag{2.39}$$

where $m, n \in N$ and $m + 2n > 2$, are two properties of Ito integrals that are frequently used when studying SDE's. They are usually summarised by stating that $dW(t)$ is an infinitesimal quantity of order $1/2$. Another important feature of Ito integrals, which follows from the independence of Wiener increments, is that [1]

$$\begin{aligned}&\mathcal{I}\int_{t_a}^{t_b} G(t)dW(t-\tau)dW(t) \\ &\qquad \equiv \underset{n\to\infty}{\text{ms-lim}} \sum_{i=1}^{n} G(t_{i-1})[W(t_i) - W(t_{i-1})][W(t_i - \tau) - W(t_{i-1} - \tau)] \\ &\qquad = 0.\end{aligned} \tag{2.40}$$

This is true unless $\tau = 0$, in which case Eq. (2.38) is recovered.

The Stratonovich integral is an another type of stochastic integral that is useful in the context of SDE's. It is defined as [1]

$$\mathcal{S}\int_{t_a}^{t_b} G(x(t), t)dW(t) \equiv \underset{n\to\infty}{\text{ms-lim}} \sum_{i=1}^{n} G\left(\frac{x(t_{i-1}) + x(t_i)}{2}, t_{i-1}\right)[W(t_i) - W(t_{i-1})] \tag{2.41}$$

for a given function $G(x_o, t_o)$ and a stochastic process $x(t)$. There is no general relation between the Ito and Stratonovich integrals of arbitrary functions.

Since SDE's driven by Gaussian white noise, like Eq. (2.32), are defined in terms of integral equations, Ito and Stratonovich integrals lead to two different types of SDE. If the Riemann-Stieltjes integral in Eq. (2.33) is interpreted as an Ito integral, Eq. (2.32) is called an Ito SDE. If it is interpreted as a Stratonovich integral, then Eq. (2.32) is a Stratonovich SDE. In order to differentiate between the two, Ito SDE's will be written as

$$dx(t) = f\big(x(t)\big)dt + \sigma g\big(x(t)\big)dW(t), \tag{2.42}$$

and Stratonovich SDE's, as

$$dx(t) = f\big(x(t)\big)dt + \sigma g\big(x(t)\big) \circ dW(t). \tag{2.43}$$

In these two equations, the differential of the Wiener process is used instead of $\xi(t)$ to acknowledge that they must be interpreted in terms of integral equations.

Even though there is no general formula relating the Ito and Stratonovich integrals of arbitrary functions, there is a simple relation between Ito and Stratonovich SDE's. Indeed, the Stratonovich SDE (2.43) is equivalent to the Ito SDE [1]

$$dx(t) = \left[f(x_o) + \frac{\sigma^2}{2} g(x_o)\frac{d}{dx_o}g(x_o)\right]_{x_o=x(t)} dt + \sigma g\big(x(t)\big)dW(t). \tag{2.44}$$

Considering that Ito SDE's are more mathematically tractable than Stratonovich SDE's, Eq. (2.44) simplifies the analysis of the latter. This is extremely important, since the zero correlation time limit of real stochastic processes leads to Stratonovich SDE's. A relation similar to Eq (2.44) is derived in Sec 3.2 for stochastic delay differential equations.

The rules used to perform a change of variable in an SDE driven by Gaussian white noise depend on whether Ito or Stratonovich calculus is used. For an arbitrary function $G(x)$ and a process $x(t)$ given by the Ito SDE (2.42), it can be shown that [1]

$$\begin{aligned} dG\big(x(t)\big) = &\left[f(x_o)\frac{d}{dx_o}G(x_o) + \frac{\sigma^2}{2}g^2(x_o)\frac{d^2}{dx_o^2}G(x_o)\right]_{x_o=x(t)} dt \\ &+ \left[\sigma g(x_o)\frac{d}{dx_o}G(x_o)\right]_{x_o=x(t)} dW(t). \end{aligned} \tag{2.45}$$

This equation is known as Ito's formula. Using Eq. (2.45) and the relation between Ito and Stratonovich SDE's, the corresponding formula for a process $x(t)$ described by the

Stratonovich SDE (2.43) is found to be

$$dG(x(t)) = \left[\frac{d}{dx_o}G(x_o)\right]_{x_o=x(t)} [f(x(t))dt + \sigma g(x(t)) \circ dW(t)]. \tag{2.46}$$

Thus, changes of variables involving Stratonovich SDE's follow the usual rules of calculus, which is not the case for Ito SDE's.

The stochastic input of SDE's implies that their output is also stochastic. Thus, SDE's give rise to new stochastic processes. It can be shown that the evolution of the conditional probability density $p(x_2, t_2|x_1, t_1)$ associated with the stochastic process arising from Eq. (2.42) is given by the FPE [1]

$$\frac{\partial}{\partial t_2}p(x_2, t_2|x_1, t_1) = -\frac{\partial}{\partial x_2}[f(x_2, t_2)p(x_2, t_2|x_1, t_1)] + \frac{\sigma^2}{2}\frac{\partial^2}{\partial x_2^2}[g^2(x_2, t_2)p(x_2, t_2|x_1, t_1)]. \tag{2.47}$$

Thus, an SDE driven by Gaussian white noise describes a diffusion process with drift, the drift and diffusion originating respectively from the deterministic and stochastic terms of the SDE. Conversely, a diffusion process can, under appropriate assumptions [47], be expressed in terms of an SDE. For example, the Orsntein-Ulhenbeck process presented in Sec. 2.1.5 can be written as

$$d\zeta(t) = -k\zeta(t)dt + \sqrt{D}dW(t).$$

A Fokker-Planck like equation for the conditional probability density of processes described by SDDE's is derived in Chap. 3.

2.1.7 Example: Logistic Equation

The logistic, or Verhulst, equation [2]

$$\frac{d}{dt}x = \alpha x - \beta x^2, \tag{2.48}$$

where α and β are positive coefficients and x is confined to the positive x-axis, was originally developed in the field of population dynamics. It was used to model population growth in an environment where resources are limited. In this context, α represents the Malthusian growth rate and β scales the environmental constraints. Applying Gaussian white noise to parameter α and using Stratonovich calculus leads to the SDE

$$dx = (\alpha x - \beta x^2)dt + \sigma x \circ dW, \tag{2.49}$$

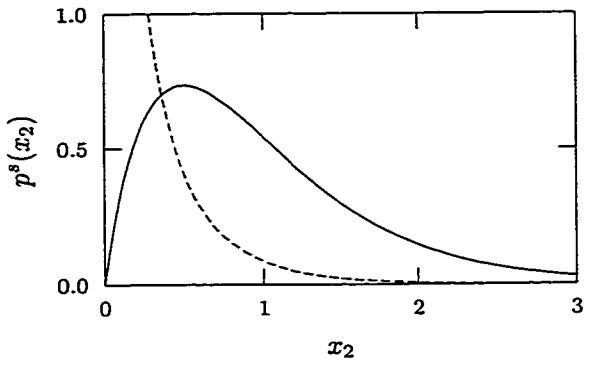

Figure 2.4: Steady-state probability density [Eq. (2.51)] for the nondelayed logistic SDE (2.49) with $\beta = \sigma^2 = 1$ (see App. A.1). The dashed line corresponds to $\alpha = 0.1$, and the solid line, to $\alpha = 1$.

where σ scales the noise amplitude. The equivalent Ito SDE is

$$dx = \left[\left(\alpha + \frac{\sigma^2}{2}\right) x - \beta x^2\right] dt + \sigma x dW,$$

and the corresponding FPE,

$$\frac{\partial}{\partial t_2} p(x_2, t_2|x_1, t_1) = -\frac{\partial}{\partial x_2}\left\{\left[\left(\alpha + \frac{\sigma^2}{2}\right) x_2 - \beta x_2^2\right] p(x_2, t_2|x_1, t_1)\right\} + \frac{\sigma^2}{2}\frac{\partial^2}{\partial x_2^2}[x_2^2 p(x_2, t_2|x_1, t_1)]. \tag{2.50}$$

For this FPE, the boundaries at the origin and positive infinity are both natural for $\alpha > 0$ [2]. In other words, they are both naturally reflecting, and boundary conditions need not be externally imposed [1]. In this regime, Eq. (2.50) leads to the steady-state probability density

$$p^s(x_2) = N x_2^{2\alpha/\sigma^2 - 1} e^{-2\beta x_2/\sigma^2}, \tag{2.51}$$

where N is a normalisation constant. As illustrated in Fig. 2.4, the shape of $p^s(x_2)$ depends on the relation between α and σ^2. If $0 < \alpha < \sigma^2/2$, $p^s(x_2)$ diverges at the origin and decreases monotonically as x_2 increases. On the other hand, if $\alpha > \sigma^2/2$, $p^s(x_2)$ is then zero at the origin and reaches a maximum at $x_2 = (\alpha - \sigma^2/2)/\beta$.

2.2 Delay Differential Equations

2.2.1 Deterministic DDE's

The variables and derivatives appearing in a differential equation are usually evaluated at the same point in time. For instance, in the ordinary differential equation (ODE)

$$\frac{d}{dt}x = x,$$

both x and dx/dt are implicitly assumed to be evaluated at time t, and this equation can thus be written as

$$\frac{d}{dt}x(t) = x(t).$$

In general, however, the quantities appearing in a differential equation may be evaluated at different times. When this is the case, the differential equation is said to have *deviating arguments* and is called a *functional differential equation* [15, 16]. In such an equation, a given dynamical variable or derivative may even be evaluated at more than one instant. For example, in the equation

$$\frac{d}{dt}x(t) = \alpha x(t-\tau) + \beta x(t),$$

x is evaluated at times t and $t-\tau$, and its first derivative dx/dt is evaluated at time t. While the delay τ is constant in this particular example, deviations may in general be time or state dependent.

Functional differential equations are classified in three categories: delay, advanced, and neutral [15]. They are called *delay differential equations* (DDE's) when

1. all the terms involving the highest order derivative of the state variable are evaluated at the same time, and

2. the highest order derivative is never evaluated at earlier times than the state variable and its lower order derivatives.

Equations for which item 1 holds and for which the word *earlier* is replaced with *later* in item 2 are called *advanced differential equations.* All other equations with deviating arguments are qualified as *neutral.*

This thesis concentrates on constant delay DDE's of the form

$$\frac{d}{dt}x(t) = f\big(x(t), x(t-\tau)\big), \tag{2.52}$$

where $f(x_o, x_\tau)$ is a given function. In this equation, the retarded variable $x(t-\tau)$ represents delayed feedback. Because of this retarded variable, a complete knowledge of $x(t)$ over one delay τ is needed to uniquely specify the state of the system. In particular, integration forward in time for $t > t'$ requires an initial function $\{x'(t)|t \in [t'-\tau, t']\}$. This also implies that systems described by DDE's effectively evolve in an infinite-dimensional phase space, thus allowing the existence of a large variety of attractors even in univariate DDE's. For example, depending on the value of the delay, the DDE

$$\frac{d}{dt}x(t) = x(t-\tau) - x^3(t-\tau),$$

which is studied in more detail in Sec. 5.3.4, exhibits fixed points, limit cycles, and aperiodic behaviour.

2.2.2 Stochastic DDE's

The expression *stochastic delay differential equations* (SDDE's) refers to stochastically driven DDE's. As mentioned at the end of Sec. 2.2.1, systems described by DDE's, and therefore by SDDE's, evolve in a phase space that effectively contains an infinite number of degrees of freedom. For instance, in the case of the SDDE

$$dx(t) = f\big(x(t), x(t-\tau)\big)dt + g\big(x(t)\big)dW(t), \tag{2.53}$$

uniquely specifying the state of the system requires the knowledge of $x(t)$ at all t's within a period of time equal to the delay τ. Even though an evolution equation for a probability density defined over such an infinite-dimensional domain may be formally written (see Sec. 3.3.2), it does not seem to be exactly solvable in general.

Most of the research on SDDE's has been concerned either with the existence and the properties of its solutions [16, 48–52] or the existence, uniqueness, and smoothness of the probability densities [53]. In order to study the evolution of the probability densities, Losson and Mackey [54] developed, through a discretisation procedure, an approximation scheme for DDE's and SDDE's in terms of coupled map lattices. This approach allows techniques developed for coupled map lattices to be used in the context of SDDE's, such as the numerical computation of evolving probability densities. However, they did not obtain analytical expressions for the probability densities. In fact, to our knowledge, no general method for obtaining exact analytical expressions of the probability densities has ever been devised for nonlinear SDDE's.

On the other hand, a variety of techniques can be used to solve linear SDDE's for their

probability densities. For example, Küchler and Mensch [55] expressed the sample paths of the process described by the linear SDDE

$$dx(t) = [\alpha x(t) + \beta x(t-\tau)]dt + \sigma dW(t), \tag{2.54}$$

with $\sigma = 1$, in terms of those of the Wiener process $W(t)$. They used this expression to determine the range of parameter values for which a stationary solution exists, to show that the steady-state probability density $p^s(x)$ is a zero mean Gaussian, and to calculate the covariance function of the process. Since a Gaussian is uniquely specified by its mean and variance, they effectively determined the steady-state probability density.

Furthermore, Mackey and Nechaeva [56] analytically studied the stability of $\langle x(t_1)\rangle$ and $\langle x(t_1)x(t_2)\rangle$ for systems described by Eq. (2.54) and by

$$dx(t) = [\alpha x(t) + \beta x(t-\tau)]dt + \sigma x(t) dW(t). \tag{2.55}$$

They also considered cases where these equations are driven by Ornstein-Uhlenbeck noise instead of Gaussian white noise. Subsequently, Hunter and Milton [57] noted that the assumption $\langle x(t)^2\rangle_s = \langle x(t)x(t-\tau)\rangle_s$ used in [56] to obtain a characteristic equation for $\langle x(t_1)x(t_2)\rangle$ in the case of Eq. (2.54) is inappropriate. However, Hunter and Milton stressed that this problem does not intervene in the characterisation of $\langle x(t_1)\rangle$ and in the analysis of Eq. (2.55).

In addition, Hunter and Milton [58] obtained the power spectrum of the state variable for a system whose evolution is given by

$$dx(t) = [\alpha x(t) + \beta x(t-\tau)]dt + \eta(t)dt, \tag{2.56}$$

where $\eta(t)$ is an arbitrary stochastic process, using Laplace transforms and the linearity of the differential equation. An approach similar to theirs but formulated in terms of Fourier transforms is presented in Sec. 2.2.3.

On a different note, Ohira [43,44] obtained an approximate FPE for the delayed Langevin equation

$$dx(t) = -\alpha x(t-\tau)dt + \sigma dW(t), \tag{2.57}$$

with $\sigma = 1$, in the limit where $\alpha \ll 1$. This was done by using a correspondence with a discrete time random walk for which the transition probabilities at a given time depend on the state of the system at a previous time [59]. Such an FPE is very interesting, since it allows the determination of both the steady-state limit and the time evolution of the

probability density. Unfortunately, the approach used by Ohira is specific to the linear SDDE (2.57). Chapter 3 explores the possibility of obtaining a Fokker-Planck equation for a general nonlinear SDDE.

2.2.3 Example: Delayed Linear Equation

The delayed linear equation

$$\frac{d}{dt}x(t) = -\alpha x(t-\tau), \tag{2.58}$$

which was studied by Wright [60] and in which α and τ are positive coefficients, regularly appears when linearising nonlinear DDE's around fixed points. It is thus useful to perform its stability analysis. Its complex eigenvalues $\lambda = \mu + i\omega$, around its only fixed point $x(t) = 0$, are obtained by substituting the trial solution $x(t) = Ae^{\lambda t}$. This results in the characteristic equation

$$\lambda + \alpha e^{-\lambda\tau} = 0, \tag{2.59}$$

which is equivalent to the pair of real equations

$$\mu + \alpha e^{-\mu\tau}\cos(\omega\tau) = 0 \tag{2.60a}$$

$$\omega - \alpha e^{-\mu\tau}\sin(\omega\tau) = 0. \tag{2.60b}$$

The number of roots of Eq. (2.59) depends on the value of the delay τ. When the delay is zero, it has only one root, which is real and is given by $\lambda = -\alpha$. On the other hand, when the delay is non-zero, it has an infinite number of roots, all of which must be determined numerically. Despite this fact, some properties of these roots can still be studied analytically. For instance, since Eqs. (2.60a) and (2.60b) are left unmodified by the transformation $\omega \to -\omega$, all eigenvalues with non-zero imaginary parts must come in complex conjugate pairs. Furthermore, by setting $\omega = 0$ in Eqs. (2.60a) and (2.60b), it is found that two of the roots are real when $0 < \alpha\tau < 1/e$ and that there is no real root when $\alpha\tau > 1/e$. Numerically, it is found that all roots have real parts that are more negative than $-\alpha$ when $0 < \alpha\tau < 1/e$. As $\alpha\tau$ approaches zero, one of the real roots converges to $-\alpha$, the real parts of all the other roots diverge to $-\infty$, and the imaginary parts of the complex roots diverge to $\pm\infty$. If $\alpha\tau$ increases, the two real roots merge and become a complex conjugate pair as $\alpha\tau$ goes through $1/e$. This pair crosses the imaginary axis when $\alpha\tau = \pi/2$, as can be seen by setting $\mu = 0$ in Eqs. (2.60a) and (2.60b).

The behaviour of the roots of Eq. (2.59) is illustrated in Fig. 2.5. In this figure, the eigenvalues have been determined using iterative techniques with appropriate initial conditions.

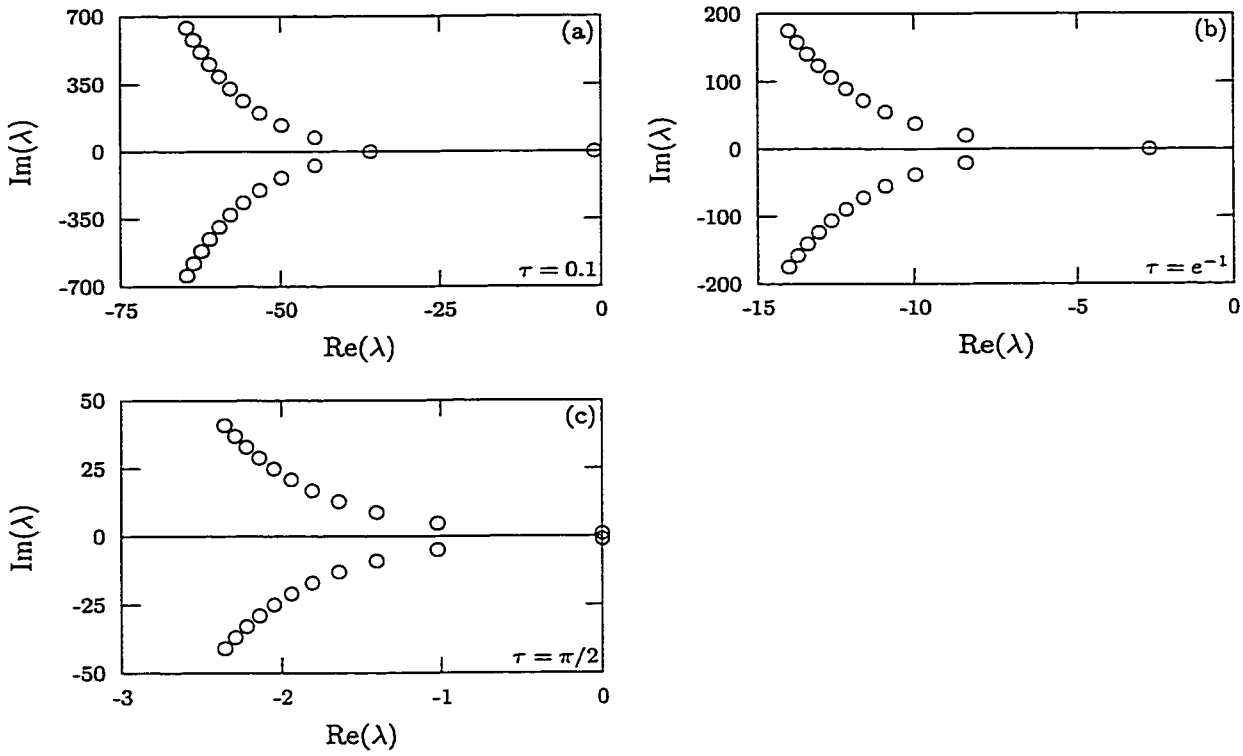

Figure 2.5: Eigenvalues of the linear DDE (2.58) for $\alpha = 1$ (see App. A.1) and various values of the delay. Only the eleven pairs of eigenvalues with the least negative real parts are presented. They have been numerically determined using iterative techniques, as discussed in Sec. 2.2.3. On graph (b), two eigenvalues are merged on the real axis. On graph (c), two pure imaginary eigenvalues are located near the origin.

Parametric plots of Eqs. (2.60a) and (2.60b) have led to the conclusion that

$$\omega = \pm\frac{\pi}{\tau}\left(2n + \frac{1}{2}\right) \tag{2.61}$$

and

$$\mu = \frac{1}{\tau}\ln\left(\frac{\alpha}{|\omega|}\right), \tag{2.62}$$

where $n \in N_o$, constitute suitable initial conditions for the determination of the complex roots ($n = 0$ is applicable only for $\alpha\tau > 1/e$). The origin was used for the least negative real root, and trial and error was used for the other one.

This eigenvalue analysis shows that initial conditions decay monotonically to zero when $\tau = 0$, since the single eigenvalue is real and negative. For constant initial conditions, the

same also holds when $0 < \alpha\tau < 1/e$, since the eigenvalue with the least negative real part has no imaginary part. When $1/e < \alpha\tau < \pi/2$, constant initial conditions lead to damped oscillations, since all the eigenvalues have negative real parts and non-zero imaginary parts. Finally, constant initial conditions lead to diverging oscillations when $\alpha\tau > \pi/2$, because some of the eigenvalues have positive real parts.

Subjecting Eq. (2.58) to an arbitrary zero-mean and wide-sense stationary stochastic process $\eta(t)$ leads to the delayed linear Langevin equation

$$\frac{d}{dt}x(t) = -\alpha x(t-\tau) + \eta(t), \tag{2.63}$$

which is the simplest of all linear SDDE's and will act as a reference point for the discussion presented in this thesis. The linearity of this equation greatly facilitates the determination of the steady-state probability density $p^s(x)$. Indeed, once the initial condition of $x(t)$ has decayed, Eq. (2.63) is a linear time-invariant transformation. Because of this, and since $\eta(t)$ is wide-sense stationary, $\eta(t)$ and $x(t)$ are jointly wide-sense stationary. In other words, their means, autocorrelation functions, and cross-correlation function are all time-shift invariant. In the particular case where $\eta(t)$ is Gaussian distributed, it also implies that $x(t)$ is itself Gaussian distributed and that the steady-state probability density $p^s(x)$ is thus uniquely determined by its mean and variance.

Calculating the ensemble average of Eq. (2.63) leads to an evolution equation for the mean $\langle x(t)\rangle$. Indeed, since $\langle \eta(t)\rangle = 0$,

$$\frac{d}{dt}\langle x(t)\rangle = -\alpha\langle x(t-\tau)\rangle.$$

The stability analysis carried out for Eq. (2.58) also applies to this one. In particular, $\langle x(t)\rangle = 0$ is the only fixed point and is stable when $\alpha\tau < \pi/2$. The steady-state probability density thus has a zero mean.

Evaluating Eq. (2.63) at $t = t_1$, multiplying it by $x(t_2)$, and calculating the ensemble average of the product leads to

$$\frac{\partial}{\partial t_1}\langle x(t_1)x(t_2)\rangle = -\alpha\langle x(t_1-\tau)x(t_2)\rangle + \langle \eta(t_1)x(t_2)\rangle. \tag{2.64}$$

Similarly,

$$\frac{\partial}{\partial t_2}\langle \eta(t_1)x(t_2)\rangle = -\alpha\langle \eta(t_1)x(t_2-\tau)\rangle + \langle \eta(t_1)\eta(t_2)\rangle. \tag{2.65}$$

As mentioned above, once $x(t)$ has reached steady-state, $\eta(t)$ and $x(t)$ are jointly wide-sense

stationary and all their correlation functions are time-shift invariant. Thus, at steady-state, Eqs. (2.64) and (2.65) lead to

$$\frac{d}{dt}R_{xx}(t) = \alpha R_{xx}(t+\tau) - R_{\eta x}(t)$$

and

$$\frac{d}{dt}R_{\eta x}(t) = -\alpha R_{\eta x}(t-\tau) + R_{\eta\eta}(t),$$

where $t \equiv t_2 - t_1$. Taking the Fourier transform [see Eq. (2.5)] of these equations yields

$$i\omega S_{xx}(\omega) = \alpha e^{i\omega\tau} S_{xx}(\omega) - S_{\eta x}(\omega)$$

and

$$i\omega S_{\eta x}(\omega) = -\alpha e^{-i\omega\tau} S_{\eta x}(\omega) + S_{\eta\eta}(\omega),$$

from which

$$S_{xx}(\omega) = \frac{S_{\eta\eta}(\omega)}{\alpha^2 + \omega^2 - 2\alpha\omega\sin(\omega\tau)}. \tag{2.66}$$

This expression is compatible with the one obtained by Hunter and Milton [58] for a process described by Eq. (2.56). The variance of the process $x(t)$ can be obtained from the spectrum $S_{xx}(\omega)$ through

$$\begin{aligned}\sigma_x^2 &= R_{xx}(0) \\ &= \frac{1}{2\pi}\int_{-\infty}^{\infty} \frac{S_{\eta\eta}(\omega)}{\alpha^2 + \omega^2 - 2\alpha\omega\sin(\omega\tau)} d\omega,\end{aligned}$$

which completely determines the steady-state probability density $p^s(x)$ in cases where it is a Gaussian.

The spectrum of the Gaussian white noise $\sigma\xi(t)$ is found to be $S_{\xi\xi}(\omega) = \sigma^2$ using Eq. (2.30). Thus, if $\eta(t)$ is considered to be this type of process, Eq. (2.57) is recovered and

$$\sigma_x^2 = \frac{\sigma^2}{2\pi}\int_{-\infty}^{\infty} \frac{1}{\alpha^2 + \omega^2 - 2\alpha\omega\sin(\omega\tau)} d\omega. \tag{2.67}$$

Numerical integration shows that this expression is equivalent, for $0 \leq \alpha\tau < \pi/2$, to

$$\sigma_x^2 = \frac{\sigma^2}{2\alpha}\left[\frac{1+\sin(\alpha\tau)}{\cos(\alpha\tau)}\right], \tag{2.68}$$

which is a special case of a formula obtained by Küchler and Mensch [55] for a system described by Eq. (2.54).

Chapter 3

Fokker-Planck Approach to SDDE's

The central result of this thesis, a Fokker-Planck equation for Ito SDDE's, is derived in Sec. 3.1. A correspondence between Ito and Stratonovich SDDE's is then established in Sec. 3.2, thus allowing the FPE obtained in the first section to be used with both types of SDDE. After this, Sec. 3.3 presents two alternate representations for SDDE's and shows that they yield yet another Fokker-Planck equation. Finally, these methods are applied to a linear and a logistic SDDE in Sec. 3.4.

3.1 Ito SDDE's

Characterising a stochastic process involves calculating its probability density functions. In the case of nondelayed SDE's, presented in Sec. 2.1.6, the first-order probability density function can be determined through the FPE [Eq. (2.47)]. In this section, the technique used to obtain an FPE from a nondelayed SDE is applied to a general SDDE and is seen to yield an integrodifferential equation involving the second-order probability density function [see Eq. (2.2)]. Although the resulting equation is not self-sufficient, it is far from being useless. Indeed, it is found to be helpful when used in association with either the small delay approximation of Chap. 4 or the separation of time scales assumption of Sec. 5.3. Moreover, it also leads to a better understanding of the problems involved in obtaining evolution equations for the probability density functions of delayed systems.

In general, the drift and diffusion terms of an SDDE may both involve delayed feedback.

Consequently, this section considers the Ito SDDE

$$dx(t) = f\big(x(t), x(t-\tau)\big)dt + \sigma g\big(x(t), x(t-\tau)\big)dW(t), \tag{3.1}$$

where $f(x_o, x_\tau)$ and $g(x_o, x_\tau)$ are given functions. In addition, the initial condition is set to $\{x(t) = x'(t) | t \in [t'-\tau, t']\}$, where $x'(t)$ is another given function, and the state variable x is confined to the range $[a, b]$. The first step in obtaining the evolution equation for the first-order probability density function associated with Eq. (3.1) is to derive the change of variable equation for an arbitrary C^2 function $G(x_o)$ defined on $[a, b]$. A Taylor expansion of $G\big(x(t) + dx(t)\big)$ in powers of $dx(t)$ in the differential

$$dG\big(x(t)\big) \equiv G\big(x(t) + dx(t)\big) - G\big(x(t)\big) \tag{3.2}$$

leads to

$$dG\big(x(t)\big) = \left[\frac{d}{dx_o}G(x_o)\right]_{x_o=x(t)} dx(t) + \frac{1}{2}\left[\frac{d^2}{dx_o^2}G(x_o)\right]_{x_o=x(t)} [dx(t)]^2 + \cdots . \tag{3.3}$$

Using the identity $[dW(t)]^2 = dt$ [see Eq. (2.38)] and keeping terms up to first-order in dt, Eqs. (3.1) and (3.3) yield Ito's formula [16,48]

$$\begin{aligned} dG\big(x(t)\big) = &\left[f\big(x_o, x(t-\tau)\big)\frac{d}{dx_o}G(x_o) + \frac{\sigma^2}{2}g^2\big(x_o, x(t-\tau)\big)\frac{d^2}{dx_o^2}G(x_o)\right]_{x_o=x(t)} dt \\ &+ \left[\sigma g\big(x_o, x(t-\tau)\big)\frac{d}{dx_o}G(x_o)\right]_{x_o=x(t)} dW(t). \end{aligned} \tag{3.4}$$

This change of variable equation has the same form as for nondelayed SDE's [see Eq. (2.45)].

In Eq. (3.4), $dW(t)$ is independent of $x(t)$ and $x(t-\tau)$, and its average is zero. Thus, the ensemble average of Eq. (3.4) can be written as

$$\begin{aligned} &\big\langle dG\big(x(t)\big) \big| x', t' \big\rangle \\ &\quad = \int_a^b dx_o \int_a^b dx_\tau p(x_o, t; x_\tau, t-\tau | x', t') \\ &\qquad\qquad \times \left(f(x_o, x_\tau)\frac{d}{dx_o}G(x_o) + \frac{\sigma^2}{2}g^2(x_o, x_\tau)\frac{d^2}{dx_o^2}G(x_o)\right) dt, \end{aligned} \tag{3.5}$$

where x' and t' represent the initial condition $\{x(t) = x'(t) | t \in [t'-\tau, t']\}$. Under the

assumption that

$$\lim_{x_o \to a} G(x_o) = \lim_{x_o \to b} G(x_o) = 0$$

and

$$\lim_{x_o \to a} \frac{d}{dx_o} G(x_o) = \lim_{x_o \to b} \frac{d}{dx_o} G(x_o) = 0,$$

integrating the right-hand side of Eq. (3.5) by parts with respect to x_o yields

$$\begin{aligned} &\langle dG(x(t)) | x', t' \rangle \\ &\quad = \int_a^b dx_o G(x_o) \int_a^b dx_\tau \Big(- \frac{\partial}{\partial x_o} [f(x_o, x_\tau) p(x_o, t; x_\tau, t - \tau | x', t')] \\ &\qquad + \frac{\sigma^2}{2} \frac{\partial^2}{\partial x_o^2} [g^2(x_o, x_\tau) p(x_o, t; x_\tau, t - \tau | x', t')] \Big) dt. \end{aligned} \tag{3.6}$$

From Eq. (3.2), the ensemble average of the differential $dG(x(t))$ can also be written as

$$\begin{aligned} \langle dG(x(t)) | x', t' \rangle = \int_a^b dx_o G(x_o) \int_a^b dx_\tau [&p(x_o, t + dt; x_\tau, t + dt - \tau | x', t') \\ &- p(x_o, t; x_\tau, t - \tau | x', t')] \end{aligned} \tag{3.7}$$

Equating the last two equations and dividing by dt results in

$$\begin{aligned} &\int_a^b dx_o G(x_o) \int_a^b dx_\tau \frac{\partial}{\partial t} p(x_o, t; x_\tau, t - \tau | x', t') \\ &\quad = \int_a^b dx_o G(x_o) \int_a^b dx_\tau \Big(- \frac{\partial}{\partial x_o} [f(x_o, x_\tau) p(x_o, t; x_\tau, t - \tau | x', t')] \\ &\qquad + \frac{\sigma^2}{2} \frac{\partial^2}{\partial x_o^2} [g^2(x_o, x_\tau) p(x_o, t; x_\tau, t - \tau | x', t')] \Big). \end{aligned} \tag{3.8}$$

Since $G(x_o)$ is arbitrary, Eq. (3.8) leads to

$$\begin{aligned} \int_a^b dx_\tau \frac{\partial}{\partial t} p(x_o, t; x_\tau, t - \tau | x', t') = \int_a^b dx_\tau \Big(&- \frac{\partial}{\partial x_o} [f(x_o, x_\tau) p(x_o, t; x_\tau, t - \tau | x', t')] \\ &+ \frac{\sigma^2}{2} \frac{\partial^2}{\partial x_o^2} [g^2(x_o, x_\tau) p(x_o, t; x_\tau, t - \tau | x', t')] \Big). \end{aligned}$$

Inverting the order in which the integral and the derivatives are performed and defining

$$p(x_o, t_o | x', t') \equiv \int_a^b dx_\tau p(x_o, t_o; x_\tau, t_\tau | x', t') \tag{3.9}$$

and

$$p(x_\tau, t_\tau | x_o, t_o; x', t') \equiv \frac{p(x_o, t_o; x_\tau, t_\tau | x', t')}{p(x_o, t_o | x', t')}, \tag{3.10}$$

this equation becomes

$$\frac{\partial}{\partial t} p(x_o, t | x', t') = -\frac{\partial}{\partial x_o}\left(p(x_o, t | x', t') \int_a^b dx_\tau f(x_o, x_\tau) p(x_\tau, t-\tau | x_o, t; x', t') \right) + \frac{\sigma^2}{2} \frac{\partial^2}{\partial x_o^2}\left(p(x_o, t | x', t') \int_a^b dx_\tau g^2(x_o, x_\tau) p(x_\tau, t-\tau | x_o, t; x', t') \right). \tag{3.11}$$

This integrodifferential equation describes the evolution of the conditional probability density $p(x_o, t|x', t')$ and thus corresponds to the FPE of nondelayed SDE's [Eq. (2.47)]. Unfortunately, it is an integrodifferential equation and the function $p(x_\tau, t-\tau|x_o, t; x', t')$ appearing on its right-hand side implies that it is not self-sufficient. The appearance of this conditional probability density in Eq. (3.11) follows from the presence of $x(t-\tau)$ in the differential $dG\big(x(t)\big)$. If an arbitrary bivariate function $G(x_o, x_\tau)$ was used instead of $G(x_o)$, the integral over x_τ in Eq. (3.8) could be removed in the same way as the one over x_o. However, since the differential $dG\big((x(t), x(t-\tau)\big)$ involves the delayed variable $x(t-2\tau)$, the third order probability density $p(x_o, t; x_\tau, t-\tau; x_{2\tau}, t-2\tau | x', t')$ would now appear in Eq. (3.8). Conditional averages would therefore still be present in Eq. (3.11), which would now describe the evolution of the bivariate probability density $p(x_o, t; x_\tau, t-\tau | x', t')$. Repetitively increasing the number of independent variables of the function G would thus lead to an infinite hierarchy of integrodifferential equations that are not self-sufficient. This seems to indicate that no finite-order probability density could be determined independently from higher-order ones. This would certainly make sense, since all systems described by SDDE's effectively evolve in an infinite-dimensional phase space. Even though none of the FPE's arising from this approach is self-sufficient, an appropriate closure scheme, where the probability density of a given order is expressed a priori in terms of lower order ones, may yield a valid approximate FPE.

Equation (3.11) can be written in a more compact notation by using the ensemble averages

$$\bar{f}(x_o, t_o | x', t') \equiv \int_a^b dx_\tau f(x_o, x_\tau) p(x_\tau, t_o - \tau | x_o, t_o; x', t') \tag{3.12}$$

and

$$\bar{g^2}(x_o, t_o|x', t') \equiv \int_a^b dx_\tau g^2(x_o, x_\tau) p(x_\tau, t - \tau|x_o, t_o; x', t'). \tag{3.13}$$

From Eq. (3.1), $\bar{f}(x_o, t_o|x', t')$ is seen to be the average of $dx(t)/dt$ at time $t = t_o$ given that $x(t_o) = x_o$ and can thus be called a conditional average drift (CAD). Using $\bar{f}(x_o, t_o|x', t')$ and $\bar{g^2}(x_o, t_o|x', t')$, Eq. (3.11) becomes

$$\frac{\partial}{\partial t} p(x_o, t|x', t') = -\frac{\partial}{\partial x_o}[\bar{f}(x_o, t|x', t') p(x_o, t|x', t')] + \frac{\sigma^2}{2} \frac{\partial^2}{\partial x_o^2}[\bar{g^2}(x_o, t|x', t') p(x_o, t|x', t')]. \tag{3.14}$$

This equation has the same form as the FPE (2.47), which is associated with nondelayed SDE's. Furthermore, Eq. (3.14) simplifies to Eq. (2.47) as the delay vanishes. Indeed, $p(x_o, t_o|x_\tau, t_o - \tau; x', t')$ approaches the Dirac delta function $\delta(x_o - x_\tau)$ in such a limit, thus leading to $\bar{f}(x_o, t_o|x', t') = f(x_o, x_o)$ and $\bar{g^2}(x_o, t_o|x', t') = g^2(x_o, x_o)$. Equation (3.14) is a novel result and is one of the central contributions of this thesis.

Even though the integrodifferential nature of the evolution equation for the probability density is not apparent when written as in Eq. (3.14), it is still present. Indeed, the functions $\bar{f}(x_o, t_o|x', t')$ and $\bar{g^2}(x_o, t_o|x', t')$ appearing in this equation are given by Eqs. (3.12) and (3.13). However, Eq. (3.14) can still be quite useful in certain circumstances. For instance, it is interesting to note that the nondelayed SDE

$$dx(t) = \bar{f}(x(t), t|x', t')dt + \sigma \sqrt{\bar{g^2}(x(t), t|x', t')} dW(t), \tag{3.15}$$

would also lead to the FPE (3.14). Thus, if a given SDDE possesses well-defined conditional averages $\bar{f}(x_o, t_o|x', t')$ and $\bar{g^2}(x_o, t_o|x', t')$, there is a nondelayed SDE that exhibits exactly the same probability density as the SDDE. In addition, two particular applications of the FPE (3.14) are presented in Chap. 4 and in Sec. 5.3 in association with appropriate approximation schemes.

Assuming the existence of the steady-state probability density

$$p^s(x_o) \equiv \lim_{t \to \infty} p(x_o, t|x', t')$$

and of the steady-state averages

$$\bar{f}^s(x_o) \equiv \lim_{t_o \to \infty} \bar{f}(x_o, t_o|x', t') \tag{3.16}$$

and

$$\bar{g^2}^s(x_o) \equiv \lim_{t_o \to \infty} \bar{g^2}(x_o, t_o | x', t'), \tag{3.17}$$

reflecting boundary conditions lead from Eq. (3.14) to the so-called potential solution,

$$p^s(x_o) = \frac{N}{\bar{g^2}^s(x_o)} \exp\left(\frac{2}{\sigma^2} \int_c^{x_o} dx'_o \frac{\bar{f}^s(x'_o)}{\bar{g^2}^s(x'_o)} \right). \tag{3.18}$$

In this equation, c is an arbitrary point located within the support of $p^s(x_o)$. This support is the set of x's over which $p^s(x_o)$ is non-zero, and it is necessarily contained within the range $[a, b]$ of the dynamical variable x. On the other hand, the constant N appearing in Eq. (3.18) is determined from the normalisation condition

$$\int_a^b dx_o p^s(x_o) = 1$$

and implicitly depends on τ and c.

Systems where the diffusion term is not retarded are of particular interest, since the steady-state CAD is in such cases uniquely determined by the steady-state probability density. Once $g\big(x(t), x(t-\tau)\big)$ is replaced by $g\big(x(t)\big)$ in Eq. (3.1), the conditional average diffusion becomes $\bar{g^2}(x_o, t_o | x', t') = g^2(x_o)$. Inverting Eq. (3.18) then yields

$$\bar{f}^s(x_o) = \frac{\sigma^2}{2} g^2(x_o) \frac{d}{dx_o} \ln p^s(x_o) + \sigma^2 g(x_o) \frac{d}{dx_o} g(x_o), \tag{3.19}$$

which plays an important role in Chap. 4 and in Sec. 5.3.

3.2 Stratonovich SDDE's

As mentioned in Sec. 2.1.6, a Stratonovich SDE can be converted to an equivalent Ito SDE and vice versa. In this section, it is shown that the same can be done for SDDE's, and expressions relating the drift and diffusion terms of equivalent Ito and Stratonovich SDDE's are derived. Given that $x(t)$ is a solution of the Stratonovich SDDE

$$dx(t) = f_S\big(x(t), x(t-\tau)\big)dt + \sigma g_S\big(x(t), x(t-\tau)\big) \circ dW(t), \tag{3.20}$$

where $f_S(x_o, x_\tau)$ and $g_S(x_o, x_\tau)$ are known functions, the goal is to determine functions $f_I(x_o, x_\tau)$ and $g_I(x_o, x_\tau)$ such that $x(t)$ is also a solution of the Ito SDDE

$$dx(t) = f_I\big(x(t), x(t-\tau)\big)dt + \sigma g_I\big(x(t), x(t-\tau)\big)dW(t). \tag{3.21}$$

In order to do so, the implicit Stratonovich integral in Eq. (3.20) must be expressed in terms of Riemann and Ito integrals.

The Stratonovich integral of the diffusion term in Eq. (3.20) can be defined as (see Sec. 2.1.6)

$$\begin{aligned}
&\mathcal{S}\int_{t_a}^{t_b} \sigma g_S\big(x(t), x(t-\tau)\big)dW(t) \\
&\quad \equiv \underset{n\to\infty}{\text{ms-lim}} \sum_{i=1}^{n} \sigma g_S\left(\frac{x(t_{i-1}) + x(t_i)}{2}, \frac{x(t_{i-1}-\tau) + x(t_i-\tau)}{2}\right) \\
&\qquad\qquad \times [W(t_i) - W(t_{i-1})] \\
&\quad = \underset{n\to\infty}{\text{ms-lim}} \sum_{i=1}^{n} \sigma g_S\left(x(t_{i-1}) + \frac{1}{2}dx(t_{i-1}), x(t_{i-1}-\tau) + \frac{1}{2}dx(t_{i-1}-\tau)\right) \\
&\qquad\qquad \times [W(t_i) - W(t_{i-1})],
\end{aligned} \tag{3.22}$$

where $dx(t)$ is given either by Eq. (3.20) or Eq. (3.21). Expanding Eq. (3.22) in powers of dt and $dW(t)$ using Eq. (3.21), while keeping terms only up to first order in dt [see Eq. (2.39)], leads to

$$\begin{aligned}
&\mathcal{S}\int_{t_a}^{t_b} \sigma g_S\big(x(t), x(t-\tau)\big)dW(t) \\
&\quad = \underset{n\to\infty}{\text{ms-lim}} \sum_{i=1}^{n} \sigma g_S\big(x(t_{i-1}), x(t_{i-1}-\tau)\big)[W(t_i) - W(t_{i-1})] \\
&\qquad + \frac{\sigma^2}{2} \underset{n\to\infty}{\text{ms-lim}} \sum_{i=1}^{n} \left[\frac{\partial}{\partial x_o} g_S\big(x_o, x(t_{i-1}-\tau)\big)\right]_{x_o = x(t_{i-1})} \\
&\qquad\qquad \times g_I\big(x(t_{i-1}), x(t_{i-1}-\tau)\big)[W(t_i) - W(t_{i-1})]^2 \\
&\qquad + \frac{\sigma^2}{2} \underset{n\to\infty}{\text{ms-lim}} \sum_{i=1}^{n} \left[\frac{\partial}{\partial x_\tau} g_S\big(x(t_{i-1}), x_\tau\big)\right]_{x_\tau = x(t_{i-1}-\tau)} \\
&\qquad\qquad \times g_I\big(x(t_{i-1}-\tau), x(t_{i-1}-2\tau)\big) \\
&\qquad\qquad \times [W(t_i-\tau) - W(t_{i-1}-\tau)][W(t_i) - W(t_{i-1})].
\end{aligned} \tag{3.23}$$

On the right-hand side of this equation, the first term is the definition of the Ito integral

[see Eq. (2.37)]. The second and third terms respectively come from the averages $\big(x(t_{i-1})+x(t_i)\big)/2$ and $\big(x(t_{i-1}-\tau)+x(t_i-\tau)\big)/2$ appearing in Eq. (3.22). Using Eqs. (2.38) and (2.40), the second term is seen to yield a normal Riemann integral and the third term is found to be zero. Thus, Eq. (3.23) becomes

$$\begin{aligned}\mathcal{S}\int_{t_a}^{t_b}&\sigma g_S\big(x(t),x(t-\tau)\big)dW(t)\\ &=\mathcal{I}\int_{t_a}^{t_b}\sigma g_S\big(x(t),x(t-\tau)\big)dW(t)\\ &\quad+\frac{\sigma^2}{2}\int_{t_a}^{t_b}\left[g_I\big(x_o,x(t-\tau)\big)\frac{\partial}{\partial x_o}g_S\big(x_o,x(t-\tau)\big)\right]_{x_o=x(t)}dt.\end{aligned}\tag{3.24}$$

Using Eq. (3.24), the Stratonovich SDDE (3.20) leads to the Ito SDDE

$$\begin{aligned}dx(t)=&\left[f_S\big(x_o,x(t-\tau)\big)+\frac{\sigma^2}{2}g_I\big(x_o,x(t-\tau)\big)\frac{\partial}{\partial x_o}g_S\big(x_o,x(t-\tau)\big)\right]_{x_o=x(t)}dt\\ &+\sigma g_S\big(x(t),x(t-\tau)\big)dW(t).\end{aligned}$$

Comparing this equation with Eq. (3.21) yields

$$f_I(x_o,x_\tau)=f_S(x_o,x_\tau)+\frac{\sigma^2}{2}g_S(x_o,x_\tau)\frac{\partial}{\partial x_o}g_S(x_o,x_\tau)\tag{3.25}$$

and

$$g_I(x_o,x_\tau)=g_S(x_o,x_\tau),\tag{3.26}$$

which relate Ito and Stratonovich SDDE's. Once a Stratonovich SDDE has been converted into an equivalent Ito SDDE, it can be solved using the tools developed for the latter.

As seen is Sec. 2.1.6, the usual rules of calculus apply to changes of variables involving nondelayed Stratonovich SDE's. The same also holds for Stratonovich SDDE's and can be verified as follows. The Stratonovich SDDE (3.20) is equivalent to the Ito SDDE

$$\begin{aligned}dx(t)=&\left[f_S\big(x_o,x(t-\tau)\big)+\frac{\sigma^2}{2}g_S\big(x_o,x(t-\tau)\big)\frac{\partial}{\partial x_o}g_S\big(x_o,x(t-\tau)\big)\right]_{x_o=x(t)}dt\\ &+\sigma g_S\big(x(t),x(t-\tau)\big)dW(t),\end{aligned}\tag{3.27}$$

and applying Ito's rule for SDDE's [Eq. (3.4)] on $G\big(x(t)\big)$, where $G(x_o)$ is an invertible C^2

function and $x(t)$ is given by Eq. (3.27), leads to

$$\begin{aligned} dG(x(t)) = \Bigg[& f_S(x_o, x(t-\tau)) \frac{d}{dx_o} G(x_o) \\ & + \frac{\sigma^2}{2} g_S(x_o, x(t-\tau)) \left(\frac{\partial}{\partial x_o} g_S(x_o, x(t-\tau)) \right) \frac{d}{dx_o} G(x_o) \\ & + \frac{\sigma^2}{2} g_S^2(x_o, x(t-\tau)) \frac{d^2}{dx_o^2} G(x_o) \Bigg]_{x_o = x(t)} dt \\ & + \left[\sigma g_S(x_o, x(t-\tau)) \frac{d}{dx_o} G(x_o) \right]_{x_o = x(t)} dW(t). \end{aligned} \tag{3.28}$$

This equation can also be written in terms of the new state variable $y(t) \equiv G(x(t))$. Defining $\hat{f}_S(y_o, y_\tau) \equiv f_S(H(y_o), H(y_\tau))$ and $\hat{g}_S(y_o, y_\tau) \equiv g_S(H(y_o), H(y_\tau))$, where $H(y_o)$ is the inverse of $G(x_o)$, Eq. (3.28) can be written as

$$\begin{aligned} dy(t) = \Bigg[& \hat{f}_S(y_o, y(t-\tau)) \left(\frac{d}{dy_o} H(y_o) \right)^{-1} \\ & + \frac{\sigma^2}{2} \hat{g}_S(y_o, y(t-\tau)) \left(\frac{\partial}{\partial y_o} \hat{g}_S(y_o, y(t-\tau)) \right) \left(\frac{d}{dy_o} H(y_o) \right)^{-2} \\ & - \frac{\sigma^2}{2} \hat{g}_S^2(y_o, y(t-\tau)) \left(\frac{d}{dy_o} H(y_o) \right)^{-3} \frac{d^2}{dy_o^2} H(y_o) \Bigg]_{y_o = y(t)} dt \\ & + \left[\sigma \hat{g}_S(y_o, y(t-\tau)) \left(\frac{d}{dy_o} H(y_o) \right)^{-1} \right]_{y_o = y(t)} dW(t), \end{aligned} \tag{3.29}$$

since

$$\begin{aligned} \frac{d}{dx_o} G(x_o) &= \left(\frac{d}{dy_o} H(y_o) \right)^{-1} \Bigg|_{y_o = G(x_o)}, \\ \frac{d^2}{dx_o^2} G(x_o) &= - \left(\frac{d}{dy_o} H(y_o) \right)^{-3} \frac{d^2}{dy_o^2} H(y_o) \Bigg|_{y_o = G(x_o)}, \end{aligned}$$

and

$$\frac{\partial}{\partial x_o} g_S(x_o, x_\tau) = \left(\frac{d}{dy_o} H(y_o) \right)^{-1} \frac{\partial}{\partial y_o} \hat{g}_S(y_o, y_\tau) \Bigg|_{y_o = G(x_o), y_\tau = G(x_\tau)}.$$

Finally, converting Eq. (3.29) back to Stratonovich calculus yields

$$dy(t) = \left[\left(\frac{d}{dy_o}H(y_o)\right)^{-1}\right]_{y_o=y(t)} \left[\hat{f}_S\big(y(t), y(t-\tau)\big)dt + \sigma\hat{g}_S\big(y(t), y(t-\tau)\big) \circ dW(t)\right],$$

which is equivalent to

$$dG\big(x(t)\big) = \left[\frac{d}{dx_o}G(x_o)\right]_{x_o=x(t)} \left[f_S\big(x(t), x(t-\tau)\big)dt + \sigma g_S\big(x(t), x(t-\tau)\big) \circ dW(t)\right]. \quad (3.30)$$

This equation is the change of variable formula for Stratonovich SDDE's. Similarly to the nondelayed case, it corresponds to the usual rules of calculus.

3.3 Alternate Representations of SDDE's

3.3.1 Sets of Non-Delayed Differential Equations

As stated in Chap. 2, systems described by delay differential equations, whether deterministic or stochastic, effectively evolve in an infinite-dimensional phase space. This can be illustrated using a procedure that was suggested by Banks for deterministic DDE's [61]. Generalising this approach to stochastic systems, the SDDE

$$\frac{d}{dt}x(t) = f\big(x(t), x(t-\tau)\big) + g\big(x(t), x(t-\tau)\big)\eta(t), \quad (3.31)$$

where $\eta(t)$ is an arbitrary stochastic process, can be converted to a set of nondelayed equations consisting of an SDE and an infinite number of linear ODE's.

Using the $n+1$ variables $\{x_i | i \in N_o, i \leq n\}$ defined by

$$x_i(t) \equiv x\left(t - \frac{i\tau}{n}\right),$$

Eq. (3.31) can be written as

$$\frac{d}{dt}x_0(t) = f\big(x_0(t), x_n(t)\big) + g\big(x_0(t), x_n(t)\big)\eta(t).$$

Furthermore, the x_i's are related by

$$x_{i-1}(t) = x_i\left(t + \frac{\tau}{n}\right),$$

where $1 \leq i \leq n$, and a Taylor expansion of this equation to $O(\tau^2/n^2)$ leads to the approximate ODE

$$\frac{d}{dt}x_i(t) \simeq \frac{n}{\tau}[x_{i-1}(t) - x_i(t)].$$

Thus, the set of $n+1$ equations

$$\frac{d}{dt}x_i(t) = \begin{cases} f\big(x_0(t), x_n(t)\big) + g\big(x_0(t), x_n(t)\big)\eta(t) & \text{for } i = 0 \\ \frac{n}{\tau}[x_{i-1}(t) - x_i(t)] & \text{for } 1 \leq i \leq n \end{cases} \tag{3.32}$$

approximates the SDDE (3.31) with $x_0(t) \equiv x(t)$. This approximation improves as n increases, and SDDE's are thus equivalent to infinite sets of nondelayed differential equations.

3.3.2 Integrodifferential Equations

In an SDDE, such as Eq. (3.31), memory effects are introduced solely through the value of the state variable at discrete times in the past. In general, however, all the past values of the state variable may be important. When this is the case, an integrodifferential equation, such as

$$\begin{aligned} \frac{d}{dt}x_o(t) &= f\big(x_o(t), x_\tau(t)\big) + g\big(x_o(t), x_\tau(t)\big)\eta(t) \\ x_\tau(t) &= \int_{-\infty}^{t} K(t-t')x_o(t')dt', \end{aligned} \tag{3.33}$$

needs to be considered. In Eq. (3.33), $K(t)$ is called the *memory kernel* and weights the contribution of past values of the state variable. For instance, choosing $K(t) = \delta(t-\tau)$ and setting $x_o(t) \equiv x(t)$ leads to Eq. (3.31).

The gamma distribution function

$$G_\alpha^n(t) = \begin{cases} \frac{\alpha^{n+1}}{n!}t^n e^{-\alpha t} & \text{for } t \geq 0 \\ 0 & \text{for } t < 0, \end{cases}$$

where α is a positive real number and n is a non-negative integer, is a particularly interesting kernel. Indeed, if n and α are increased to infinity in such a way that n/α is constant, $K(t) \equiv G_\alpha^{n-1}(t)$ approaches $\delta(t-n/\alpha)$ and can therefore be used to study the discrete delay limit of integrodifferential equations. In particular, if the $n+1$ variables $\{x_i | i \in N_o, i \leq n\}$

are defined as

$$x_i(t) \equiv \begin{cases} x(t) & \text{for } i = 0 \\ \int_{-\infty}^{t} G_\alpha^{i-1}(t-t')x(t')dt' & \text{for } i > 0, \end{cases}$$

the set of equations (3.32) is recovered with $\tau \equiv n/\alpha$ [62].

If $\eta(t)$ represents Gaussian white noise, then $\eta(t)dt = \sigma dW(t)$ and the set of equations (3.32) becomes

$$dx_i(t) = \begin{cases} f\big(x_0(t), x_n(t)\big)dt + \sigma g\big(x_0(t), x_n(t)\big)dW(t) & \text{for } i = 0 \\ \frac{n}{\tau}[x_{i-1}(t) - x_i(t)]dt & \text{for } 1 \leq i \leq n. \end{cases} \tag{3.34}$$

The method used to obtain an FPE from a univariate SDE subjected to Gaussian white noise, mentioned in Sec. 2.1.6, can also be applied to multivariate SDE's [1]. Defining $\vec{x}$ as representing all the x_i's and specifying $\vec{x}(t') = \vec{x}'$ as the initial condition, this method leads from the set of equations (3.34) to

$$\begin{aligned} \frac{\partial}{\partial t}p(\vec{x}, t|\vec{x}', t') = &- \frac{\partial}{\partial x_0}[f(x_0, x_n)p(\vec{x}, t|\vec{x}', t')] - \frac{n}{\tau}\sum_{i=1}^{n}\frac{\partial}{\partial x_i}[(x_{i-1} - x_i)p(\vec{x}, t|\vec{x}', t')] \\ &+ \frac{\sigma^2}{2}\frac{\partial^2}{\partial x_0^2}[g^2(x_0, x_n)p(\vec{x}, t|\vec{x}', t')]. \end{aligned} \tag{3.35}$$

Unlike Eq. (3.14), this FPE does not require the prior determination of averages like $\bar{f}(x, t|x', t')$ or $\bar{g^2}(x, t|x', t')$. In cases where the $n \to \infty$ limit of this equation is well-defined, it can thus be used as an arbitrarily precise FPE for the SDDE (3.31) with Gaussian white noise. Unfortunately, although an analytical expression for the steady-state probability density can be obtained from Eq. (3.35) when $f(x_0, x_n)$ is linear and $g(x_0, x_n)$ is constant [63], we are not aware of any such result for the general case.

The "infinite-order" probability density obtained by taking the $n \to \infty$ limit of Eq. (3.35) must be contrasted with the one arising from the infinite hierarchy of FPE's discussed in Sec. 3.1. In that section, the "infinite-order" probability density is a function of the present and past values of the state variable at intervals of one delay. Here, it considers the value of the state variable at all times within one delay. These two probability densities are thus very different from one another.

3.4 Examples

3.4.1 Delayed Linear Equation

a) Fokker-Planck Equation

The delayed linear equation (2.57) can be used to illustrate the formalism presented in Sec. 3.1. Küchler and Mensch [55] have shown for Eq. (2.54), of which Eq. (2.57) is a special case, that the steady-state probability density functions of all orders are Gaussian. In particular, this implies that the second order steady-state probability density of the state variable x in Eq. (2.57) is given by

$$p^s(x_o, t_o; x_\tau, t_o - \tau) = \frac{1}{2\pi\sigma_x^2\sqrt{1 - r_{xx}^2(\tau)}} \exp\left(-\frac{x_o^2 - 2r_{xx}(\tau)x_o x_\tau + x_\tau^2}{2\sigma_x^2[1 - r_{xx}^2(\tau)]}\right), \tag{3.36}$$

where σ_x^2 is the steady-state variance and $r_{xx}(t)$ is the steady-state correlation coefficient function [see Eq. (2.4)]. The initial condition is omitted in Eq. (3.36) because its influence disappears at steady-state. By integrating Eq. (3.36) over x_τ, the first-order steady-state probability density is found to be

$$p^s(x_o) = \frac{1}{\sqrt{2\pi\sigma_x^2}} \exp\left(-\frac{x_o^2}{2\sigma_x^2}\right). \tag{3.37}$$

The steady-state CAD, defined in Sec. 3.1, can then be expressed as

$$\bar{f}^s(x_o) = -\alpha r_{xx}(\tau)x_o, \tag{3.38}$$

which leads to

$$p^s(x_o) = \sqrt{\frac{\alpha r_{xx}(\tau)}{\pi\sigma^2}} \exp\left(-\frac{\alpha r_{xx}(\tau)x_o^2}{\sigma^2}\right) \tag{3.39}$$

using Eq. (3.18). Comparing Eqs. (3.37) and (3.39) leads to the relation

$$\sigma_x^2 = \frac{\sigma^2}{2\alpha r_{xx}(\tau)} \tag{3.40}$$

between the variance and the correlation coefficient function. Using an expression of the steady-state covariance function obtained by Küchler and Mensch [55], the variance and the correlation coefficient function are found to be given, respectively, by Eq. (2.68) and by

$$r_{xx}(\tau) = \frac{\cos(\alpha\tau)}{1 + \sin(\alpha\tau)}. \tag{3.41}$$

Using these expressions, the equality (3.40), which arises from the Fokker–Planck approach presented in Sec. 3.1, is seen to be fulfilled.

Equation (3.40) shows that the variance diverges when $r_{xx}(\tau) = 0$, that is, when there is no correlation between $x(t)$ and $x(t-\tau)$. This can be explained by the fact that the steady-state CAD, given by Eq. (3.38), is then identically zero. Indeed, Eq. (3.15) implies that the steady-state FPE associated with the delayed linear equation (2.57) approaches the FPE of the Wiener process as $\bar{f}^s(x_o)$ becomes zero. It is thus normal for σ_x^2 to diverge when $r_{xx}(\tau) = 0$. Furthermore, it is interesting to note from Eq. (3.41) that $r_{xx}(\tau)$ becomes zero at $\alpha\tau = \pi/2$. As seen in Sec. 2.2.3, this is the value of $\alpha\tau$ at which the system becomes deterministically unstable. Thus, the divergence of the variance and the disappearance of correlation between $x(t)$ and $x(t-\tau)$ are related to the instability of the underlying deterministic system.

b) Set of Non-Delayed Differential Equations

Applying the formalism of Sec. 3.3 to the delayed linear Langevin equation (2.63) leads to

$$\frac{d}{dt}x_i(t) = \begin{cases} -\alpha x_n(t) + \eta(t) & \text{for } i = 0 \\ \frac{n}{\tau}[x_{i-1}(t) - x_i(t)] & \text{for } 1 \leq i \leq n. \end{cases} \tag{3.42}$$

The analysis performed in Sec. 2.2.3 for Eq. (2.63) can be applied almost verbatim to the set of Eqs. (3.42). In particular, these equations constitute a linear time-invariant transformation once the initial condition has decayed. In this limit, the $x_i(t)$'s are therefore jointly wide-sense stationary, since $\eta(t)$ is itself wide-sense stationary. If, in addition, $\eta(t)$ is Gaussian distributed, the $x_i(t)$'s are then jointly Gaussian and their joint probability density is thus solely determined by their average and correlation functions.

As is the case for $\langle x(t)\rangle$ in Sec. 2.2.3, the origin is the only fixed point for the $\langle x_i(t)\rangle$'s. Deriving evolution equations for the steady-state correlation functions in the same way as in Sec. 2.2.3 leads to

$$\frac{d}{dt}R_{x_ix_j}(t) = \begin{cases} \alpha R_{x_nx_j}(t) - R_{\eta x_j}(t) & \text{for } i = 0 \\ -\frac{n}{\tau}[R_{x_{i-1}x_j}(t) - R_{x_ix_j}(t)] & \text{for } 1 \leq i \leq n \end{cases}$$

and

$$\frac{d}{dt}R_{\eta x_i}(t) = \begin{cases} -\alpha R_{\eta x_n}(t) + R_{\eta\eta}(t) & \text{for } i = 0 \\ \frac{n}{\tau}[R_{\eta x_{i-1}}(t) - R_{\eta x_i}(t)] & \text{for } 1 \leq i \leq n, \end{cases}$$

where $j \in N_o$ and $j \leq n$. Fourier transforms of these equations then yield

$$i\omega S_{x_i x_j}(\omega) = \begin{cases} \alpha S_{x_n x_j}(\omega) - S_{\eta x_j}(\omega) & \text{for } i = 0 \\ -\frac{n}{\tau}[S_{x_{i-1} x_j}(\omega) - S_{x_i x_j}(\omega)] & \text{for } 1 \leq i \leq n \end{cases}$$

and

$$i\omega S_{\eta x_i}(\omega) = \begin{cases} -\alpha S_{\eta x_n}(\omega) + S_{\eta\eta}(\omega) & \text{for } i = 0 \\ \frac{n}{\tau}[S_{\eta x_{i-1}}(\omega) - S_{\eta x_i}(\omega)] & \text{for } 1 \leq i \leq n, \end{cases}$$

from which

$$S_{x_0 x_0}(\omega) = \frac{S_{\eta\eta}(\omega)}{\alpha^2 \left[1 + \left(\frac{\omega\tau}{n}\right)^2\right]^{-n} + \omega^2 + i\omega\alpha \left[\left(1 - \frac{i\omega\tau}{n}\right)^{-n} - \left(1 + \frac{i\omega\tau}{n}\right)^{-n}\right]}$$

and

$$S_{x_i x_i}(\omega) = \left[1 + \left(\frac{\omega\tau}{n}\right)^2\right]^{-i} S_{x_0 x_0}(\omega)$$

are obtained through simple algebraic manipulations. It is interesting to note that

$$\lim_{n \to \infty} S_{x_i x_i}(\omega) = S_{x_0 x_0}(\omega)$$

for all values of i between 0 and n. Thus, all the $x_i(t)$'s exhibit the same spectra in the $n \to \infty$ limit. Furthermore,

$$\lim_{n \to \infty} S_{x_0 x_0}(\omega) = \frac{S_{\eta\eta}(\omega)}{\alpha^2 + \omega^2 - 2\alpha\omega \sin(\omega\tau)},$$

and Eq. (2.66) is recovered for all $x_i(t)$'s. This result supports the validity of Eq. (3.42) as an approximation of Eq. (2.63).

3.4.2 Delayed Logistic Equation

Since the diffusion term in Eq. (2.57) is state independent, the second term on the right-hand side of Eq. (3.25) is zero and Stratonovich calculus is equivalent to Ito calculus. Another system is therefore required in order to illustrate the difference between Ito and Stratonovich SDDE's. The DDE [64]

$$\frac{d}{dt}x(t) = [\alpha - \beta x(t - \tau)]x(t) \tag{3.43}$$

is a delayed version of the logistic equation [Eq. (2.48)] and is an appropriate starting point for such a system. In the context of population dynamics, it corresponds to cases where the reaction of the population to environmental constraints is delayed. When $x(t)$ approaches zero in Eq. (3.43), its time derivative also approaches zero unless $x(t-\tau)$ diverges. Therefore, non-pathological positive initial conditions lead to solutions that are bounded from below by the origin, as appropriate for population dynamics.

Equation (3.43) has two fixed points, $x_1 \equiv 0$ and $x_2 \equiv \alpha/\beta$. The first one is always unstable, while the stability of the second one depends on the value of $\alpha\tau$. Indeed, linearising Eq. (3.43) around x_2 leads to

$$\frac{d}{dt}y(t) = -\alpha y(t-\tau),$$

where $y(t) \equiv x(t) - \alpha/\beta$. Equation (2.58) is thus recovered, and the stability analysis performed for this delayed linear equation in Sec. 2.2.3 also applies to the fixed point x_2 of Eq. (3.43).

If Gaussian white noise $\sigma\xi(t)$ is added to parameter α in Eq. (3.43), it leads to an SDDE with a nondelayed diffusion term. This equation is considered in Sec. 4.2.2. On the other hand, if $\sigma\xi(t)$ is applied to parameter β, the diffusion term is delayed. Depending on whether Ito or Stratonovich calculus is used, either

$$dx(t) = [\alpha - \beta x(t-\tau)]x(t)dt + \sigma x(t)x(t-\tau)dW(t) \tag{3.44}$$

or

$$dx(t) = [\alpha - \beta x(t-\tau)]x(t)dt + \sigma x(t)x(t-\tau) \circ dW(t), \tag{3.45}$$

is obtained. Equation (3.45) can be converted to its equivalent Ito SDDE

$$dx(t) = \left[\alpha - \beta x(t-\tau) + \frac{\sigma^2}{2}x^2(t-\tau)\right] x(t)dt + \sigma x(t)x(t-\tau)dW(t), \tag{3.46}$$

using Eqs. (3.25) and (3.26). The presence of $x^2(t-\tau)x(t)$ in the drift term causes the system described by Eq. (3.46), and thus by Eq. (3.45), to be unstable even when $\tau = 0$, since the drift term is positive for large enough values of $x(t-\tau)$. Even then, a pseudo-steady-state limit can still be studied when σ^2 is sufficiently small.

The (pseudo-)steady-state probability density is shown in Fig. 3.1. All the results were obtained from numerical simulations using the techniques presented in App. A. Similarly to the linear case presented in part (a) of Sec. 3.4.1, Eq. (3.18) is seen to yield the cor-

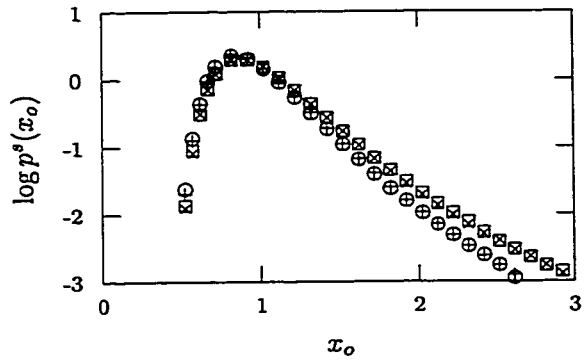

Figure 3.1: (Pseudo-)steady-state probability density for the logistic SDDE with delayed diffusion, $\alpha = \beta = 1$ (see App. A.1), and $\tau = \sigma^2 = 0.1$. The circles and the plus signs result from integrating Eq. (3.44) using the Euler scheme. For the circles, $p^s(x_o)$ has been determined directly from the sample paths, and for the plus signs, through Eq. (3.18). The squares and the x's have been obtained directly from sample paths for, respectively, Eq. (3.46) integrated with the Euler scheme and Eq. (3.45) integrated with the midpoint scheme.

rect steady-state probability density for Eq. (3.44). Furthermore, the same pseudo-steady-state probability density was obtained by integrating Eq. (3.46) with the Euler scheme and Eq. (3.45) with the midpoint scheme. Since the midpoint scheme mimics the definition of the Stratonovich integral, this indicates that Eq. (3.46) is indeed the appropriate Ito SDDE corresponding to the Stratonovich SDDE (3.45). This also supports the validity of Eqs. (3.25) and (3.26).

Chapter 4

Small Delay Expansion

An exact Fokker-Planck equation [Eq. (3.14)] was derived in Sec. 3.1 for the probability density $p(x_o, t|x', t')$ corresponding to the SDDE (3.1). Unfortunately, the FPE (3.14) is not self-sufficient, and an alternate means of obtaining an FPE is thus desirable. Section 4.1 presents a small delay approximation that leads to an approximate FPE in cases where only the drift term of the SDDE is delayed. This method is applied to the delayed linear equation (2.57) in Sec. 4.2.1, and a delayed logistic equation in Sec. 4.2.2.

4.1 Formalism

In order to introduce the small delay expansion, it is appropriate to consider the Stratonovich SDDE

$$dx(t) = f\big(x(t), x(t-\tau)\big)dt + \sigma g\big(x(t)\big) \circ dW(t), \tag{4.1}$$

which has a nondelayed diffusion term, with the state variable x confined to $[a, b]$. Performing an $O(\tau^2)$ Taylor expansion around $\tau = 0$ on the function $f\big(x(t), x(t-\tau)\big)$ yields

$$\begin{aligned} &f\big(x(t), x(t-\tau)\big)dt \\ &\quad \simeq f\big(x(t), x(t)\big)dt - \tau \left[\frac{\partial}{\partial x_\tau} f\big(x(t), x_\tau\big)\right]_{x_\tau = x(t)} dx(t) \\ &\quad \simeq f\big(x(t), x(t)\big)dt - \tau \left[\frac{\partial}{\partial x_\tau} f\big(x(t), x_\tau\big)\right]_{x_\tau = x(t)} \big[f\big(x(t), x(t)\big)dt + \sigma g\big(x(t)\big) \circ dW(t)\big]. \end{aligned}$$

Using this result, the SDDE (4.1) can be approximated by the nondelayed SDE

$$dx(t) = f_a\big(x(t)\big)dt + \sigma g_a\big(x(t)\big) \circ dW(t), \tag{4.2}$$

where the subscript a stands for *approximate*, and where

$$f_a(x_o) \equiv f(x_o, x_o) \left[1 - \tau \frac{\partial}{\partial x_\tau} f(x_o, x_\tau)\right]_{x_\tau = x_o}$$

and

$$g_a(x_o) \equiv g(x_o) \left[1 - \tau \frac{\partial}{\partial x_\tau} f(x_o, x_\tau)\right]_{x_\tau = x_o}.$$

This approximation is expected to be valid for sufficiently small delays, as Eqs. (4.1) and (4.2) yield the same nondelayed SDE in the vanishing delay limit. It is interesting to note that, although the diffusion term of the SDDE (4.1) is nondelayed, the delay explicitly appears in the function $g_a(x_o)$. This illustrates the fact that the drift and diffusion terms of an SDDE like Eq. (4.1) are effectively coupled by the delay.

Using Eq. (2.44), the Stratonovich SDE (4.2) is found to be equivalent to the Ito SDE

$$dx(t) = \left[f_a(x_o) + \frac{\sigma^2}{2} g_a(x_o) \frac{d}{dx_o} g_a(x_o)\right]_{x_o = x(t)} dt + \sigma g_a\big(x(t)\big) dW(t). \tag{4.3}$$

As mentioned in Sec. 2.1.6, the first-order probability density associated with the state variable of a univariate Ito SDE evolves according to the FPE (2.47). In the case of Eq. (4.3), this FPE is written as

$$\begin{aligned} \frac{\partial}{\partial t} p_a(x_o, t|x', t') = &- \frac{\partial}{\partial x_o} \left[\left(f_a(x_o) + \frac{\sigma^2}{2} g_a(x_o) \frac{d}{dx_o} g_a(x_o)\right) p_a(x_o, t|x', t')\right] \\ &+ \frac{\sigma^2}{2} \frac{\partial^2}{\partial x_o^2} [g_a^2(x_o) p_a(x_o, t|x', t')], \end{aligned} \tag{4.4}$$

where $p_a(x_o, t_o|x', t')$ is the conditional probability density associated with variable x in Eq. (4.3). Assuming the existence of the steady-state limit

$$p_a^s(x_o) \equiv \lim_{t_o \to \infty} p_a(x_o, t_o|x', t')$$

and specifying reflecting boundary conditions leads to the so-called potential solution

$$p_a^s(x_o) = \frac{N_a}{g_a^2(x_o)} \exp\left(\frac{2}{\sigma^2} \int_c^{x_o} dx_o' \frac{f_a(x_o') + \frac{\sigma^2}{2} g_a(x_o') \frac{d}{dx_o'} g_a(x_o')}{g_a^2(x_o')}\right) \tag{4.5}$$

in the same way as in Sec. 3.1. In Eq. (4.5), N_a is the normalisation constant and c is located

within the support of $p_a^s(x_o)$, which may differ from the support of the exact probability density $p^s(x_o)$. Since $f_a(x_o)$ and $g_a(x_o)$ approach $f(x_o, x_o)$ and $g(x_o)$ in the zero delay limit, Eq. (4.5) yields the exact steady-state probability density for Eq. (4.1) when the delay is zero.

Substituting Eq. (4.5) in Eq. (3.19) allows the determination of the approximate expression

$$\bar{f}_a^s(x_o) = \frac{f(x_o, x_o) + \tau \frac{\sigma^2}{2} g^2(x_o) \frac{d}{dx_o} \left[\frac{\partial}{\partial x_\tau} f(x_o, x_\tau) \right]_{x_\tau = x_o}}{1 - \tau \left[\frac{\partial}{\partial x_\tau} f(x_o, x_\tau) \right]_{x_\tau = x_o}} + \frac{\sigma^2}{2} g(x_o) \frac{d}{dx_o} g(x_o) \tag{4.6}$$

for the steady-state CAD $\bar{f}^s(x_o)$ of the SDDE (4.1). It must be noted that the second term on the right-hand side of this equation arises because Eq. (4.1) is a Stratonovich SDDE. When used in conjunction with Eq. (3.15), this expression for the CAD leads to the equation

$$dx(t) = \bar{f}_a^s\big(x(t)\big)dt + \sigma g\big(x(t)\big)dW(t), \tag{4.7}$$

which is another approximate nondelayed Ito SDE for the SDDE (4.1). Because of the way $\bar{f}_a^s(x_o)$ is defined, the state variable x possesses the same steady-state probability density $p_a^s(x_o)$ whether Eq. (4.3) or (4.7) is considered. Furthermore, both approximate SDE's are equivalent in the zero delay limit. However, they differ in the way the delay-induced coupling between the drift and diffusion terms of the SDDE (4.1) is taken into account. In Eq. (4.3), the coupling appears in the diffusion term, whereas in Eq. (4.7), it appears in the drift term. Indeed, the diffusion function of Eq. (4.7) is identical to the one of the SDDE (4.1), whereas the diffusion function of Eq. (4.3) has been modified by the Taylor expansion. In addition, the CAD's of these two SDE's also differ, since the CAD of a nondelayed Ito SDE is simply equal to its drift function. Both $f_a(x_o) + (\sigma^2/2) g_a(x_o) dg_a(x_o)/dx_o$ and $\bar{f}_a^s(x_o)$ are compared with numerical simulation results in Sec. 4.2.

It must be stressed that the $O(\tau^2)$ Taylor expansion has been performed only on the SDDE (4.1) and was not repeated in subsequent steps of the calculation. In particular, $p_a^s(x_o)$ and $\bar{f}_a^s(x_o)$ have clearly not been expanded to $O(\tau^2)$, since the delay τ appears nonlinearly in them. Even though expansions of these functions to $O(\tau^2)$ should not alter their quantitative accuracy within their convergence radii, they may induce qualitative modifications outside this range. As illustrated with the delayed logistic example in Sec. 4.2.2, the unexpanded expressions of $p_a^s(x_o)$ and $\bar{f}_a^s(x_o)$ may be significantly more accurate than the expanded ones. Because of this, systematic expansions of $p_a^s(x_o)$ and $\bar{f}_a^s(x_o)$ should be considered on a case by case basis.

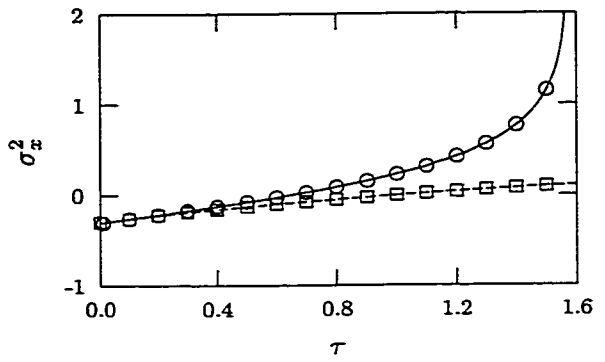

Figure 4.1: Steady-state variance for the linear SDDE (2.57) with $\alpha = 1$ (see App. A.1). The circles and the squares were obtained through simulations of, respectively, Eq. (2.57) and the approximate SDE (4.10). On the other hand, the two lines represent analytical expressions for the variance. The continuous lines stands for Eq. (2.68), and the dashed line, for Eq. (4.12).

4.2 Examples

4.2.1 Delayed Linear Equation

Applying the formalism presented in Sec. 4.1 to the delayed linear equation (2.57), for which Ito calculus is equivalent to Stratonovich calculus, leads to

$$f_a(x_o) = -\alpha(1 + \alpha\tau)x_o \tag{4.8}$$

and

$$g_a(x_o) = 1 + \alpha\tau. \tag{4.9}$$

Equation (2.57) can thus be approximated to $O(\tau^2)$ by the nondelayed SDE

$$dx(t) = -\alpha(1 + \alpha\tau)x(t)dt + (1 + \alpha\tau)\sigma dW(t). \tag{4.10}$$

This equation yields the Gaussian steady-state probability density

$$p_a^s(x_o) = N_a \exp\left(\frac{-\alpha x_o^2}{\sigma^2(1 + \alpha\tau)}\right), \tag{4.11}$$

where N_a is the normalisation constant. The variance of this zero-mean probability density is easily found to be

$$\sigma_x^2 = \frac{\sigma^2}{2\alpha}(1 + \alpha\tau). \tag{4.12}$$

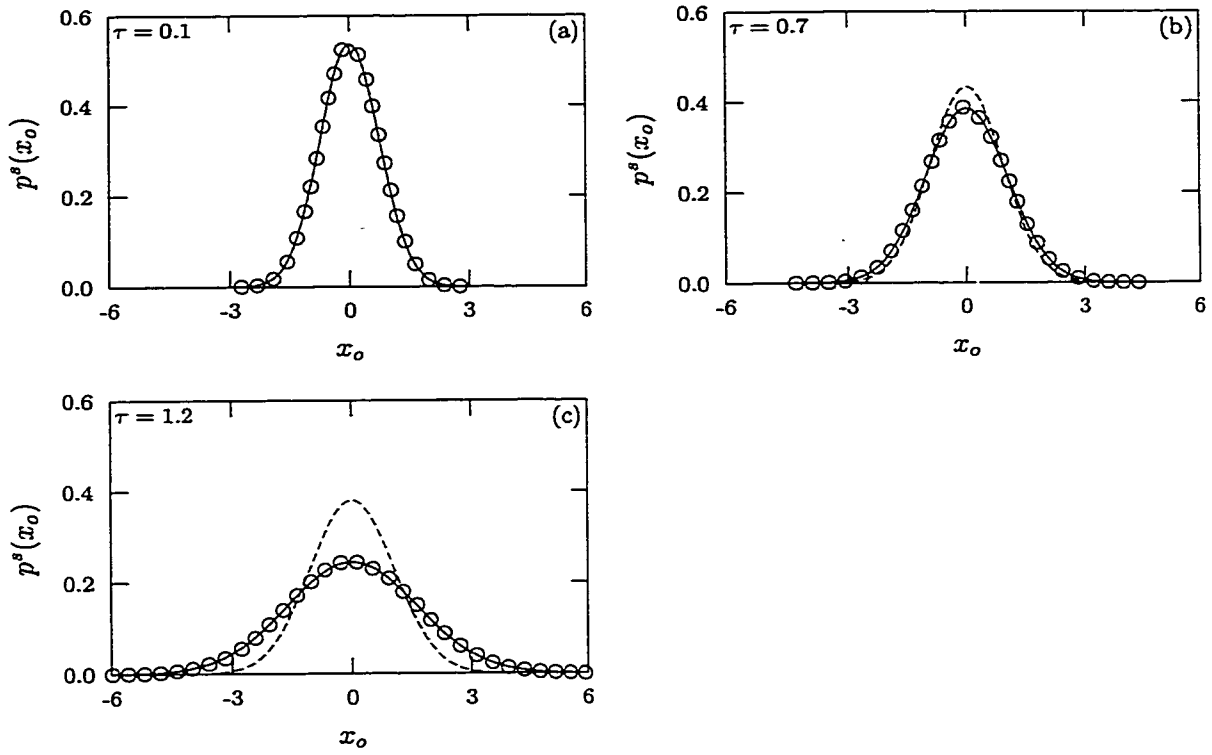

Figure 4.2: Steady-state probability density for the linear SDDE (2.57) with $\alpha = 1$ (see App. A.1) and the indicated values of the delay. The circles represent simulation results, and the continuous and dashed lines are zero-mean Gaussians with variances given by, respectively, Eqs. (2.68) and (4.12). In graph (a), the two lines are practically indistinguishable.

Equation (4.12) can also be obtained by performing a Taylor expansion on either Eq. (2.67) or (2.68), both of which are exact expressions for the steady-state variance of variable x in the SDDE (2.57).

As shown in Figs. 4.1 and 4.2, the results of the small delay expansion agree very well with the exact results when the delay is small. At $\tau = 0.1$, the two steady-state probability densities cannot be easily distinguished from one another. Even at $\tau = 0.7$, where there is a 20% difference between the variances, the two steady-state probability densities still look very similar. However, at $\tau = 1.2$, the variance is significantly underestimated and the probability densities are now quite different. Overall, the $O(\tau^2)$ Taylor expansion seems to yield valid probability densities up to approximately $\tau = 0.7$, which constitutes a reasonably large range of delays.

As seen in Sec. 2.2.3, the eigenvalue of the DDE (2.58) with the least negative real part initially becomes more negative as the delay increases from zero. This behaviour seems to be in contradiction with Fig. 4.1, where the steady-state variance is seen to increase with

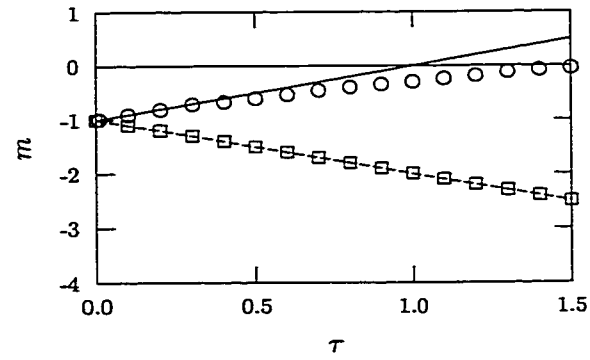

Figure 4.3: Slope m of the steady-state CAD for the linear SDDE (2.57) with $\alpha = 1$ (see App. A.1). The circles and the squares represent simulation results for, respectively, Eq. (2.57) and the approximate SDE (4.10). The continuous and dashed lines stand for the slope of, respectively, the steady-state CAD $\bar{f}_a^s(x_o)$ [Eq. (4.13)] and the approximate drift $f_a(x_o)$ [Eq. (4.8)].

the delay. This apparent paradox stems from the fact that the drift and diffusion terms of the SDDE are effectively coupled through the delay, as shown by the presence of τ in the diffusion term of Eq. (4.10). Thus, as τ increases, Eq. (2.57) initially becomes deterministically more stable, but at the same time, more sensitive to noise. In this particular case, the net result of these two opposing effects is an increase in the variance of x.

The steady-state CAD $f^s(x_o)$ can be approximated using Eq. (4.6). Performing an $O(\tau^2)$ Taylor expansion on the result leads to

$$\bar{f}_a^s(x_o) = -\alpha(1 - \alpha\tau)x_o, \tag{4.13}$$

from which the approximate nondelayed SDE

$$dx(t) = -\alpha(1 - \alpha\tau)x(t)dt + \sigma dW(t) \tag{4.14}$$

is obtained. It is interesting to compare the deterministic eigenvalues of Eq. (2.57) with those of Eqs. (4.10) and (4.14). The eigenvalues of Eq. (2.58), which is the deterministic part of Eq. (2.57), were studied in Sec. 2.2.3. As seen in that section, the eigenvalue with the least negative real part initially becomes more negative as the delay increases from zero. The deterministic eigenvalue of Eq. (4.10), which is $-\alpha(1 + \alpha\tau)$, captures this initial behaviour and becomes more negative as τ increases. However, exactly the opposite happens to the deterministic eigenvalue of Eq. (4.14). Indeed, it is equal to $-\alpha(1 - \alpha\tau)$, which becomes less negative as τ increases. The reason for this disagreement is that the diffusion term of Eq. (4.14) is, by construction, identical to the one of Eq. (2.57) and is thus independent

of τ. Since the variance of x increases with τ, regardless of whether Eq. (4.10) or (4.14) is considered, the deterministic eigenvalue of Eq. (4.14) must decrease as τ increases. Still, the two approximate SDE's are valid approximations of the SDDE (2.57). As stated in Sec. 4.1 for the general case, they simply compensate differently for the coupling between the drift and diffusion terms of the SDDE (2.57). Figure 4.3 illustrates this difference by showing the CAD's of the two approximate SDE's with numerical results obtained from simulating Eqs. (2.57) and (4.10). Since Eq. (4.14) is designed to have the same CAD as Eq. (2.57), it is a better approximation than Eq. (4.10) in cases where this quantity must be considered.

4.2.2 Delayed Logistic Equation

The small delay expansion, as formulated in Sec. 4.1, cannot be applied to the logistic SDDE of Sec. 3.4.2, since its diffusion term is delayed. A logistic SDDE with nondelayed diffusion can however be obtained if Gaussian white noise is added to parameter α instead of β in Eq. (3.43). If Stratonovich calculus is used, this leads to

$$dx(t) = [\alpha - \beta x(t-\tau)]x(t)dt + \sigma x(t) \circ dW(t), \tag{4.15}$$

which is equivalent to the Ito SDDE

$$dx(t) = \left[\alpha + \frac{\sigma^2}{2} - \beta x(t-\tau)\right] x(t)dt + \sigma x(t)dW(t). \tag{4.16}$$

The stability analysis performed for the DDE (3.43) also applies to the deterministic part of the SDDE (4.16),

$$\frac{d}{dt}x(t) = \left[\alpha + \frac{\sigma^2}{2} - \beta x(t-\tau)\right] x(t), \tag{4.17}$$

if α is replaced by $\alpha + \sigma^2/2$ in the results of Sec. 3.4.2. The extra $\sigma^2/2$ obviously arises because Stratonovich calculus is used for the diffusion term of the SDDE (4.15). Equations (4.15) and (4.16) correspond to systems with random fluctuations on the relative growth rate of the population. Similarly to the DDE on which they are based, these SDDE's possess trajectories that are bounded by the origin when positive initial conditions are considered.

Performing the small delay expansion on Eq. (4.15) yields the drift function $f_a(x_o) = (1 + \beta\tau x_o)(\alpha - \beta x_o)x_o$, the diffusion function $g_a(x_o) = (1 + \beta\tau x_o)x_o$, and the differential equation

$$dx(t) = [1 + \beta\tau x(t)]\,[\alpha - \beta x(t)]\,x(t)dt + \sigma[1 + \beta\tau x(t)]x(t) \circ dW(t). \tag{4.18}$$

This nondelayed Stratonovich SDE is equivalent to the Ito SDE

$$dx(t) = [1 + \beta\tau x(t)] \left[\alpha + \frac{\sigma^2}{2} - \beta(1 - \tau\sigma^2)x(t)\right] x(t)dt + \sigma[1 + \beta\tau x(t)]x(t)dW(t), \quad (4.19)$$

and the steady-state probability density associated with these two SDE's is

$$p_a^s(x_o) = \frac{N_a x_o^{2\alpha/\sigma^2 - 1}}{(1 + \beta\tau x_o)^{2(\tau^{-1} + \alpha)/\sigma^2 + 1}}, \quad (4.20)$$

where N_a is the normalisation constant. The moments of this probability density are given by

$$\langle x^n \rangle_s = \frac{\Gamma(2\alpha/\sigma^2 + n)\Gamma(2/\tau\sigma^2 - n + 1)}{(\beta\tau)^n \Gamma(2\alpha/\sigma^2)\Gamma(2/\tau\sigma^2 + 1)}, \quad (4.21)$$

where $\Gamma(x)$ is the gamma function. This equation is valid when the arguments of the gamma functions are positive, which is the case when $n < 1 + 2/\tau\sigma^2$. Using Eq. (4.21), the steady-state mean is found to be

$$\mu_x = \frac{\alpha}{\beta}, \quad (4.22)$$

and the steady-state variance,

$$\sigma_x^2 = \frac{\alpha\sigma^2(1 + \alpha\tau)}{\beta^2(2 - \tau\sigma^2)}. \quad (4.23)$$

Equations (4.22) and (4.23) are compared with numerical simulation results in Fig. 4.4. For $\tau = 0.1$, these expressions for the mean and the variance are seen to be accurate for all values of σ^2 between 0.0 and 2.0. In addition, Fig. 4.5 shows that the agreement between the approximate steady-state probability density and the simulation results remains excellent even at $\tau = 0.1$ and $\sigma^2 = 2.0$. This is true even though the origin, which is a local minimum at small noise amplitudes, becomes the global maximum of the probability density at some value of σ^2 between 1.0 and 2.0 for $\tau = 0.1$. Such a modification in the extrema of the probability density is what Horsthemke and Lefever call a noise-induced transition [2]. This transition in the type of extremum at the origin is also exhibited by the nondelayed case of the logistic equation presented in Sec. 2.1.7. Thus, $p_a^s(x_o)$ simply inherits from Eq. (2.51), which is its $\tau = 0$ limit, its capability to appropriately describe the steady-state probability density at all noise amplitudes when the delay is small.

Figures 4.4 and 4.5 also include results for $\sigma^2 = 0.1$ and various values of τ. As the delay increases, the shape of the steady-state probability density obtained through simulations of the SDDE (4.16) undergoes qualitative modifications. Around $\tau = 1.4$, its slope at the origin changes from 0 to infinity, and for τ larger than approximately 1.7, $p^s(x_o)$ itself

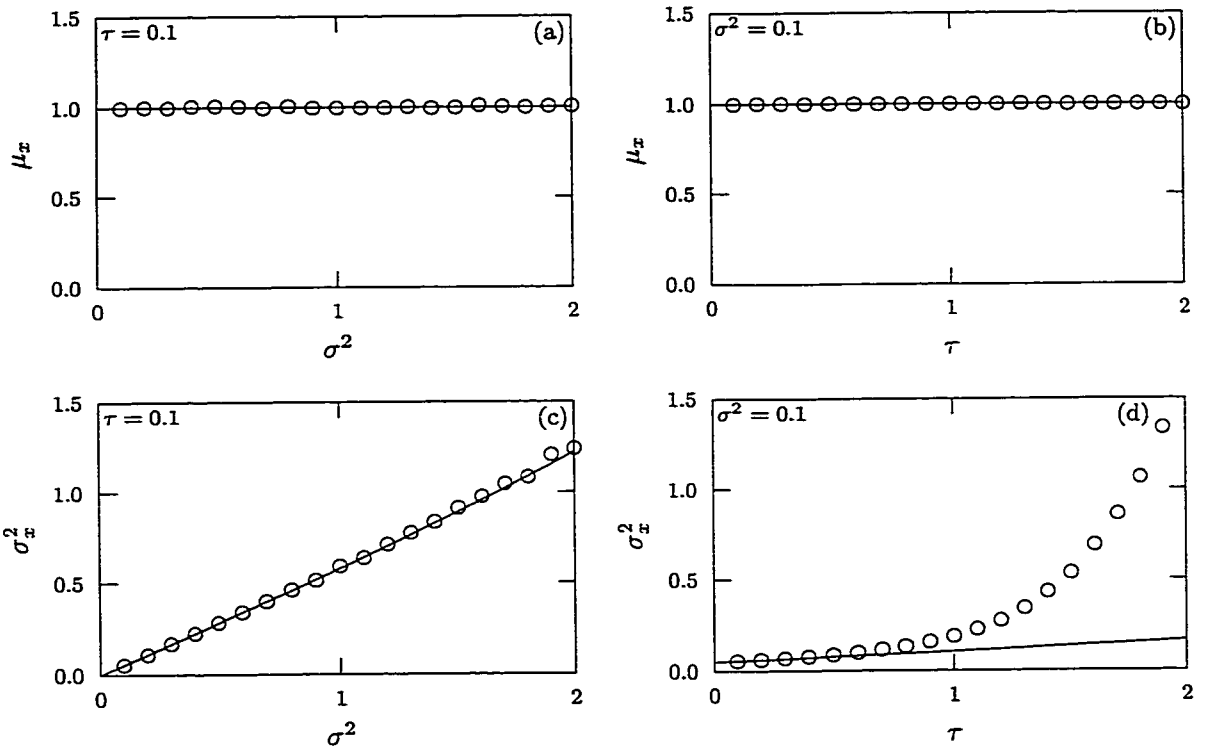

Figure 4.4: Steady-state mean and variance for the logistic SDDE with nondelayed diffusion and $\alpha = \beta = 1$ (see App. A.1). The circles represent simulation results for the logistic SDDE (4.16). In (a) and (b), the continuous line is given by Eq. (4.22), and in (c) and (d), by Eq. (4.23).

diverges at $x_o = 0$. Since Eq. (4.20) results from a small delay expansion, it does not predict this change of behaviour. Still, it is qualitatively accurate up to about $\tau = 0.9$, as illustrated in Fig. 4.5. Furthermore, Eq. (4.22) accurately predicts the value of the mean for all delays between 0.0 and 2.0. For the variance, Eq. (4.23) is reasonably accurate for delays smaller than approximately 0.6. Indeed, at that value of τ, there is roughly a 20% difference between the value of the variance predicted by Eq. (4.23) and the one observed through simulations of the SDDE (4.16).

The steady-state CAD $\bar{f}^s(x_o)$ of the Stratonovich SDDE (4.15), and thus of the Ito SDDE (4.16), can be approximated using Eq. (4.6). This yields

$$\bar{f}_a^s(x_o) = \frac{x_o}{1 + \beta\tau x_o}\left(\alpha + \frac{\sigma^2}{2} - \beta x_o\right), \tag{4.24}$$

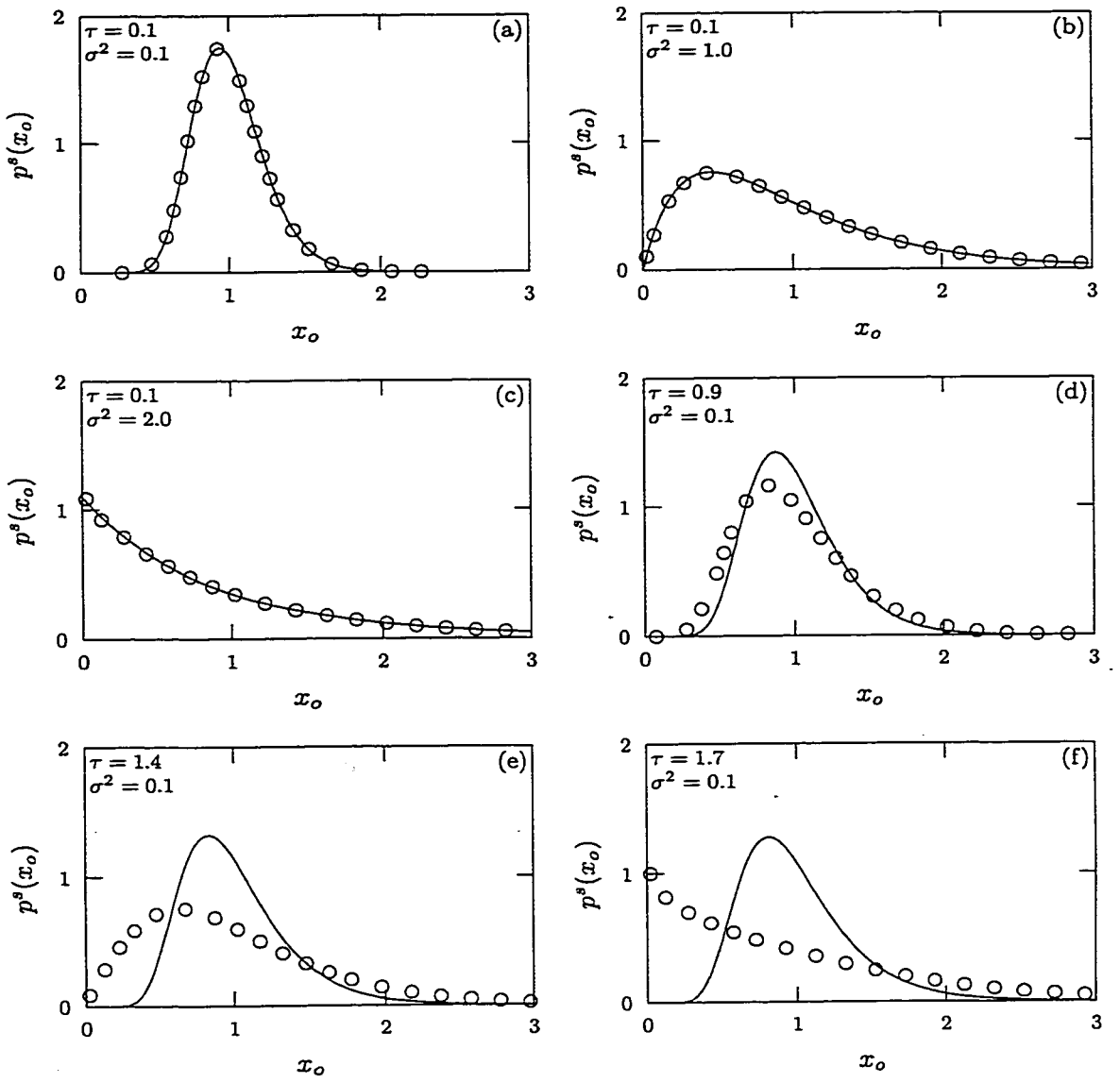

Figure 4.5: Steady-state probability density for the logistic SDDE with nondelayed diffusion, $\alpha = \beta = 1$ (see App. A.1), and various combinations of τ and σ^2. The circles represent simulation results for the SDDE (4.16), and the continuous line stands for the approximate probability density given by Eq. (4.20).

from which the approximate Ito SDE

$$dx(t) = \frac{x(t)}{1+\beta\tau x(t)}\left(\alpha + \frac{\sigma^2}{2} - \beta x(t)\right)dt + \sigma x(t)dW(t) \tag{4.25}$$

is obtained. Performing an $O(\tau^2)$ expansion on Eq. (4.24) leads to

$$\bar{f}_a^s(x_o) = x_o(1-\beta\tau x_o)\left(\alpha + \frac{\sigma^2}{2} - \beta x_o\right). \tag{4.26}$$

Equations (4.24) and (4.26) have a similar accuracy for $x_o \ll 1/\beta\tau$, but their $x_o \to \infty$ limits differ dramatically. Indeed, $\bar{f}_a^s(x_o)$ approaches $-\infty$ in Eq. (4.24), and $+\infty$ in Eq. (4.26). Because of this, an approximate nondelayed SDE built from Eq. (4.26) would need an externally imposed boundary condition in order to prevent divergence of the sample paths, while Eq. (4.25) does not require one. Since such a boundary condition is not necessary in the case of the original SDDE (4.16), Eq. (4.24) seems more faithful to this SDDE than Eq. (4.26). As shown by this example, Taylor expansions on results that follow from the integration of an expanded SDDE must be performed with great care. Even if a Taylor expansion has been applied to the original SDDE, subsequent expansions should be postponed until the end of the calculation in order to allow a better analysis of their repercussions.

The delay-induced coupling between the drift and diffusion terms of Eq. (4.16) can be investigated by looking at the drift terms of Eqs. (4.19) and (4.25), similarly to what was done in Sec. 4.2.1 for the delayed linear equation. The differential equation

$$\begin{aligned}\frac{d}{dt}x(t) &= \left[f_a(x_o) + \frac{\sigma^2}{2}g_a(x_o)\frac{d}{dx_o}g_a(x_o)\right]_{x_o=x(t)} \\ &= [1+\beta\tau x(t)]\left[\alpha + \frac{\sigma^2}{2} - \beta(1-\tau\sigma^2)x(t)\right]x(t)\end{aligned} \tag{4.27}$$

has three fixed points: $x_1 = 0$, $x_2 = (\alpha + \sigma^2/2)/[\beta(1-\tau\sigma^2)]$, and $x_3 = -1/\beta\tau$. Since the origin is repelling, as in Eq. (4.17), $x(t)$ remains positive at all times and the fixed point x_3 is never approached. Linearising Eq. (4.27) around the remaining fixed point, x_2, yields the negative eigenvalue $-(\alpha+\sigma^2/2)[1+(\alpha-\sigma^2/2)\tau]/(1-\tau\sigma^2)$. As the delay increases from zero, this eigenvalue initially becomes more negative and the fixed point x_2 becomes more stable, similarly to the corresponding fixed point of Eq. (4.17). However, the delay-induced coupling between the drift and diffusion terms effectively increases the sensitivity to noise for Eq. (4.16), as shown by the way the delay τ appears in $g_a(x_o)$. As mentioned earlier in this chapter, $\bar{f}_a^s(x_o)$ incorporates these two contributions and can therefore be used to

study the net effect of increasing the delay. The differential equation

$$\begin{aligned}\frac{d}{dt}x(t) &= \bar{f}_a^s(x(t)) \\ &= \frac{x(t)}{1+\beta\tau x(t)}\left(\alpha + \frac{\sigma^2}{2} - \beta x(t)\right),\end{aligned} \tag{4.28}$$

like Eq. (4.17), has only two fixed points. The first one is $x_1 = 0$ and is always unstable. Linearising Eq. (4.28) around the second one, $x_2 = (\alpha + \sigma^2/2)/\beta$, leads to the negative eigenvalue $-(\alpha + \sigma^2/2)/[1 + (\alpha + \sigma^2/2)\tau]$. As the delay increases, this eigenvalue becomes less negative. This shows that the delay-induced coupling between the drift and diffusion terms reduces the stability of Eq. (4.16) when the delay increases from zero, despite the increased stability due to the drift term.

The steady-state CAD of Eq. (4.16), determined using numerical simulations, is compared with the drift functions of Eqs. (4.19) and (4.25) in Fig. 4.6. The approximate steady-state CAD $\bar{f}_a^s(x_o)$ is seen to be accurate for roughly the same range of delays as $p_a^s(x_o)$, which seems normal since they are related by Eq. (3.19). In addition, the difference in behaviour between $f_a(x_o) + (\sigma^2/2)g_a(x_o)dg_a(x_o)/dx_o$ and $\bar{f}_a^s(x_o)$ appears again very clearly in Fig. 4.6. The larger the delay, the faster $f_a(x_o) + (\sigma^2/2)g_a(x_o)dg_a(x_o)/dx_o$ decreases at large values of x_o, whereas exactly the opposite happens for $\bar{f}_a^s(x_o)$. This once more illustrates the fact that the system becomes more sensitive to noise as the delay increases.

Overall, the small delay expansion presented in Sec. 4.1 yields good results for the delayed logistic equation (4.15) when the delay is small. This is true even when σ^2 is so large that it induces a qualitative change in the shape of the steady-state probability density. Furthermore, as the delay increases with $\sigma^2 = 0.1$, results remain quantitatively accurate up to about $\tau = 0.6$, which is far from being negligible.

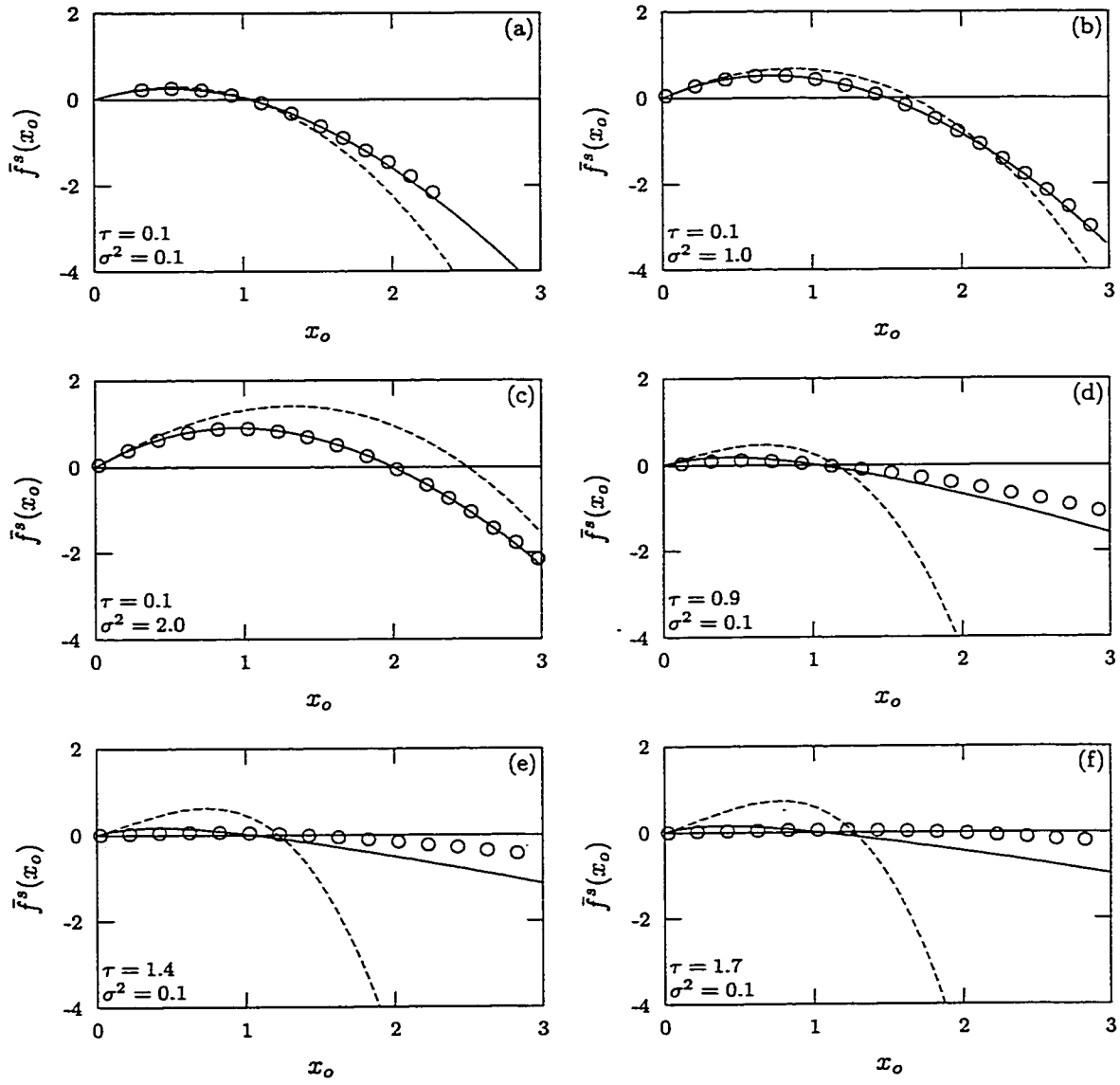

Figure 4.6: Steady-state CAD for the logistic SDDE with nondelayed diffusion, $\alpha = \beta = 1$ (see App. A.1), and the same combinations of τ and σ^2 as in Fig. 4.5. The circles represent simulation results for the SDDE (4.16). The continuous line stands for the approximate steady-state CAD $\bar{f}^s_a(x_o)$ given by Eq. (4.24), and the dashed line, for the drift function $f_a(x_o) + (\sigma^2/2) g_a(x_o) dg_a(x_o)/dx_o$ of the approximate SDE (4.19).

Chapter 5

Noise-Induced Rate Processes

This chapter considers multistability and noise-induced rate processes in the context of SDDE's driven by additive noise. Section 5.1 shows that such SDDE's can arise, for instance, when the coupling between an overdamped particle and a stochastically driven potential is delayed. As discussed in Sec. 5.2, a large class of these SDDE's are inherently unstable, but exhibit metastability under appropriate conditions. Section 5.3 then presents a separation of time scales assumption that can be used to study noise-induced rate processes between coexisting metastable states. This approach is applied, in Sec. 5.3.4, to a particle evolving in a quartic potential.

5.1 Potentials

The motion of a particle of mass m in a potential $U(x)$ is described, when the velocity is small, by the second order differential equation

$$m\frac{d^2}{dt^2}x(t) = -\left.\frac{d}{dx_o}U(x_o)\right|_{x_o=x(t)} - \nu\frac{d}{dt}x(t), \tag{5.1}$$

where x is the position of the particle and ν is the damping coefficient. A delayed coupling between the particle and the potential can be introduced in Eq. (5.1) by evaluating $dU(x_o)/dx_o$ at $x_o = x(t-\tau)$ instead of $x_o = x(t)$, thus leading to

$$m\frac{d^2}{dt^2}x(t) = -\left.\frac{d}{dx_o}U(x_o)\right|_{x_o=x(t-\tau)} - \nu\frac{d}{dt}x(t). \tag{5.2}$$

If the ratio ν/m is such that $|\nu dx(t)/dt| \gg |md^2x(t)/dt^2|$ at all times, the inertial term of Eq. (5.2) can be neglected and the particle is said to be *overdamped*. When this condition is verified, the first order differential equation

$$\frac{d}{dt}x(t) = -\frac{1}{\nu}\frac{d}{dx_o}U(x_o)\Big|_{x_o=x(t-\tau)} \tag{5.3}$$

straightforwardly follows from Eq. (5.2). In Eq. (5.3), the damping coefficient ν only acts as a scaling parameter for the potential $U(x)$. Accordingly, Eq. (5.3) is often written as

$$\frac{d}{dt}x(t) = -\frac{d}{dx_o}\hat{U}(x_o)\Big|_{x_o=x(t-\tau)}, \tag{5.4}$$

where

$$\hat{U}(x_o) \equiv \frac{1}{\nu}U(x_o) \tag{5.5}$$

is a scaled potential.

If $d\hat{U}(x_o)/dx_o$ is a stochastic process, Eq. (5.4) becomes an SDDE. This is the case, for instance, when

$$\hat{U}(x_o) \equiv V(x_o) - \sigma x_o \xi(t), \tag{5.6}$$

where $V(x_o)$ is a given scaled potential and σ scales the amplitude of the Gaussian white noise $\xi(t)$. The scaled potential $V(x_o)$ is assumed to be such that the range of $x(t)$ is $(-\infty, +\infty)$. Using this definition for $\hat{U}(x_o)$, Eq. (5.4) becomes

$$dx(t) = f\big(x(t-\tau)\big)dt + \sigma dW(t), \tag{5.7}$$

where

$$f(x_o) \equiv -\frac{d}{dx_o}V(x_o). \tag{5.8}$$

It is important to note that Eq. (5.7) is driven by additive instead of multiplicative noise. This leads to more tractable calculations and, in particular, allows the use of a method developed by Wu and Kapral [4] in order to calculate the phenomenological transition rate between the two wells of a symmetrical double-well potential. Their approach is presented in Sec. 5.3.2.

5.2 Metastability

5.2.1 Unbounded Oscillatory Solutions

While investigating noise-induced rate processes between the wells of the quartic potential presented in Sec. 5.3.4, a very important attribute of Eq. (5.7) was uncovered: unbounded oscillatory solutions. These solutions play an essential role in the long time evolution of an overdamped particle with delayed coupling to a stochastically driven potential. They must therefore be considered in some detail before proceeding with the analysis of noise-induced rate processes in these systems.

For a large class of potentials $V(x_o)$, all particles evolving according to Eq. (5.7) eventually start to oscillate with an amplitude that increases indefinitely with time. This behaviour arises because of the existence of unbounded solutions for the DDE

$$\frac{d}{dt}x(t) = f\big(x(t-\tau)\big), \tag{5.9}$$

which is the deterministic part of Eq. (5.7). For instance, integrating Eq. (5.9) over one delay yields

$$\frac{x(t'+\tau)}{x(t')} = 1 + \frac{f(x')}{x'}\tau \tag{5.10}$$

when the constant initial condition $\{x(t) = x' | t \in [t'-\tau, t']\}$ is considered. If

$$\lim_{x_o \to -\infty} \frac{f(x_o)}{x_o} = -\infty \tag{5.11}$$

and

$$\lim_{x_o \to \infty} \frac{f(x_o)}{x_o} = -\infty, \tag{5.12}$$

then the outer sides of $V(x_o)$ are steeper than those of any harmonic potential. In this case, all values of $|x'|$ larger than some threshold lead to $-x(t'+\tau)/x(t') \gg 1$. In turn, if $|x(t'+\tau)|$ is sufficiently large, then $-x(t'+2\tau)/x(t'+\tau) \gg 1$, and so on. Thus, when Eqs. (5.11) and (5.12) are satisfied, the DDE (5.9) exhibits unbounded oscillatory solutions for large initial conditions. It must be noted that this conclusion applies to all initial conditions, and not only to those that are constant.

The presence of these unbounded solutions is very important when the particle evolves according to Eq. (5.7). Since Gaussian white noise can make the particle reach arbitrarily large values of x, it is guaranteed to eventually exhibit unbounded oscillatory behaviour. Once this happens, the deterministic term of Eq. (5.7) rapidly dominates over the stochastic

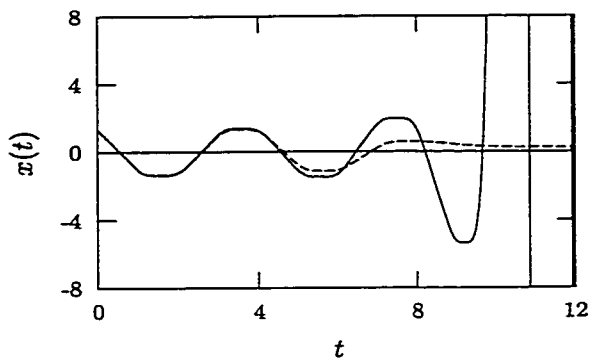

Figure 5.1: Deterministic evolution in the single-well potential [Eq. (5.14)] with $n = 3$, $\alpha = \tau = 1$ (see App. A.1), and two closeby constant initial conditions. When the particle starts from $x = 1.328$, it oscillates for a while and then slowly relaxes to $x = 0$ (dashed line). On the other hand, an initial condition of $x = 1.332$ leads to an oscillation amplitude that increases indefinitely with time (solid line).

one, and the probability of escape from the unbounded trajectory becomes negligible. The system can therefore be seen, on a coarse-grained level, as being composed of two states. On one hand, the unbounded oscillatory trajectories constitute an extremely stable class of attractors and act as a globally stable state. On the other hand, the basins of attraction of all the usual attractors, such as fixed points and limit cycles, make up a metastable suprastate that is characterised by an overall mean residence time called τ_{meta}. In the end, all realisations relax to unbounded oscillatory trajectories. Because of this, the probability density $p(x_o, t_o|x', t')$ continually widens and flattens over time, and $x(t)$ thus possesses no steady-state limit. If τ_{meta}^{-1} is sufficiently small, however, some pseudo-steady-state limit may be considered in order to study transitions within the metastable suprastate. In this limit, steady-state quantities are replaced by pseudo-steady-state ones, such as the probability density $p^m(x_o)$ and the CAD $\bar{f}^m(x_o)$. Here, the superscript m stands for *metastable* and denotes pseudo-steady-state quantities.

5.2.2 Example: Single-Well Potential

In order to clearly illustrate the transition to unbounded oscillatory trajectories, it is desirable to avoid the complications that could arise from coexisting attractors in the metastable suprastate. In this context, the single-well potential

$$V(x_o) = \frac{\alpha}{n+1}|x_o|^{n+1}, \tag{5.13}$$

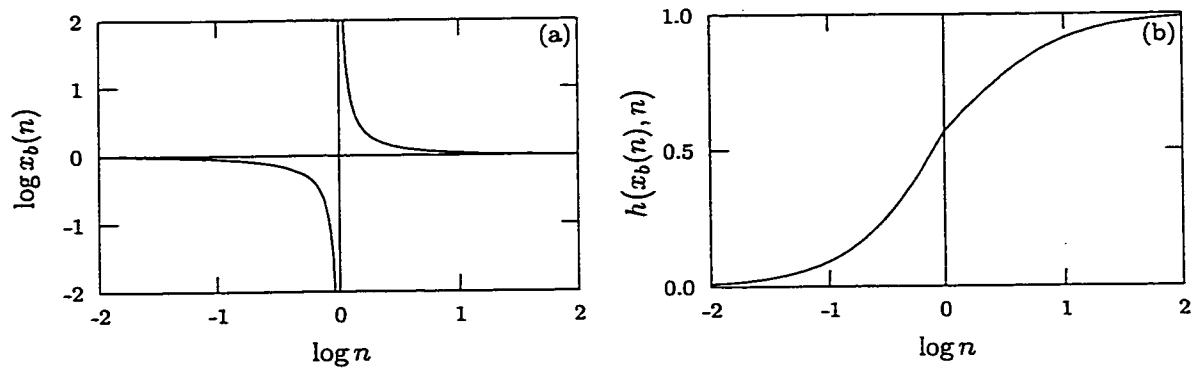

Figure 5.2: Boundedness of the deterministic trajectories in the single-well potential for $\alpha = \tau = 1$ (see App. A.1). (a) For $0 < n < 1$, $x_b(n)$ is the amplitude of the limit cycle; for $n > 1$, it is the threshold above which constant initial conditions lead to unbounded oscillatory trajectories. It was determined through successive numerical integrations of the DDE (5.14). (b) The function $h(x_b(n), n)$ characterises where the particle is located after starting from a constant initial condition of $x_b(n)$ and evolving for one delay [see Eq. (5.15)].

where $n > 0$, is a particularly appropriate choice. With this potential, Eqs. (5.8) and (5.9) lead to the DDE

$$\frac{d}{dt}x(t) = -\alpha \operatorname{sign}\big(x(t-\tau)\big)|x(t-\tau)|^n, \tag{5.14}$$

which reduces to Eq. (2.58) when $n = 1$. For that value of n, the particle relaxes to the origin when $\alpha\tau < \pi/2$ and, as long as $x' \neq 0$, oscillates with an ever increasing amplitude when $\alpha\tau > \pi/2$ (see Sec. 2.2.3). For $n \neq 1$, its asymptotic behaviour has been studied using numerical simulations with the constant initial condition $\{x(t) = x' | t \in [t' - \tau, t']\}$. When $0 < n < 1$, the particle always approaches a bounded limit cycle unless $x' = 0$. On the other hand, when $n > 1$, the particle exhibits unbounded oscillatory trajectories if $|x'|$ is larger than some threshold and relaxes to zero otherwise (see Fig. 5.1). The function

$$x_b(n) \equiv \begin{cases} \text{amplitude of the limit cycle} & \text{for } 0 < n < 1 \\ \text{threshold of } x' \text{ above which unbounded solutions are obtained} & \text{for } n > 1, \end{cases}$$

where the subscript b stands for *boundary*, is plotted in Fig. 5.2(a) for $\alpha = \tau = 1$. For this set of parameter values, the initial condition threshold for unbounded oscillatory trajectories increases from 1 to ∞ as n approaches 1 from above. Then, as n decreases from 1 to 0, the amplitude of the limit cycle increases from 0 to 1.

Although not readily apparent from its definition or from Fig. 5.2(a), there is a close relation between $x_b(n)$ for $0 < n < 1$ and $x_b(n)$ for $n > 1$. Indeed, the quantity $h(x_b(n), n)$,

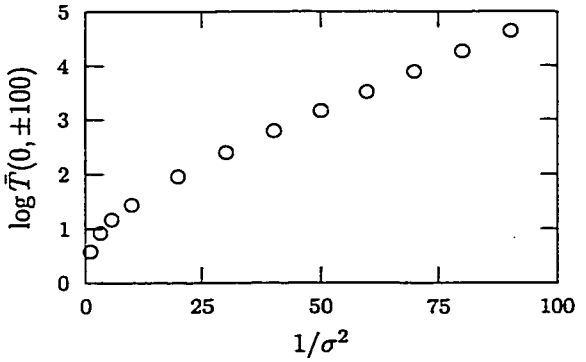

Figure 5.3: Mean first passage time $\bar{T}(0, \pm 100)$ in the single-well potential with delayed coupling, $n = 10$, and $\alpha = \tau = 1$ (see App. A.1). It was determined using numerical simulations of the SDDE (5.17).

where

$$h(x', n) \equiv -\frac{x(t' + \tau)}{x(t')} = \alpha\tau |x'|^{n-1} - 1 \tag{5.15}$$

is obtained using Eq. (5.10), is continuous across $n = 1$ [see Fig. 5.2(b)]. This suggests that the dynamics that yields the limit cycle when $n < 1$ is the same one that induces the unbounded oscillatory trajectories when $n > 1$. The slight discontinuity in the slope of $h\big(x_b(n), n\big)$ at $n = 1$ is probably due to the fact that $x_b(n)$ represents different quantities for $n < 1$ and $n > 1$.

It is interesting to note that the $n = 1$ limit of $h\big(x_b(n), n\big)$ can be determined analytically by considering

$$x_b(n) = \left(\frac{h\big(x_b(n), n\big) + 1}{\alpha\tau} \right)^{\frac{1}{n-1}}, \tag{5.16}$$

which follows from inverting Eq. (5.15). As mentioned earlier in this section, all constant initial conditions relax to $x = 0$ when $n = 1$ and $\alpha\tau < \pi/2$. This indicates that $x_b(1)$ is effectively infinite for these values of $\alpha\tau$. On the other hand, $x_b(1)$ must be zero when $\alpha\tau > \pi/2$, since all constant initial conditions except $x' = 0$ result in unbounded oscillatory trajectories. In order for Eq. (5.16) to yield these two limits for $x_b(n)$ as n approaches 1 from above, $h\big(x_b(1), 1\big)$ must be equal to $\pi/2 - 1$. This is indeed the $n = 1$ limit exhibited by $h\big(x_b(n), n\big)$ in Fig. 5.2(b).

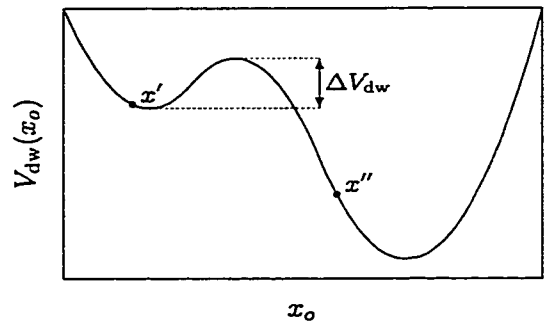

Figure 5.4: A particle that evolves according to the nondelayed SDE $dx(t) = f_{\rm dw}(x(t))dt + \sigma dW(t)$, where $f_{\rm dw}(x_o) \equiv -dV_{\rm dw}(x_o)/dx_o$ and $V_{\rm dw}(x_o)$ is a double-well potential (thus the subscript dw), is a good example of a system where Arrhenius' law can arise. For instance, under appropriate conditions, Arrhenius' law correctly predicts the dependence of the mean first passage time $\bar{T}(x', x'')$, which is the mean time required to reach the point x'' for the first time when starting from x', on the noise amplitude and on the height of the potential barrier between the two wells. Indeed, as long as x' is located near the bottom of the left well and x'' is chosen reasonably far to the right of the potential barrier, $\bar{T}(x', x'')$ follows the Arrhenius' law $\bar{T}_A \exp(2\Delta V_A/\sigma^2)$ when $\Delta V_{\rm dw}/\sigma^2$ is large [1]. In this case, ΔV_A is simply equal to $\Delta V_{\rm dw}$, which is the height of the potential barrier that must be overcome by the particle in order to reach the right well from the bottom of the left well. On the other hand, $\bar{T}_A$ depends on the flatness around the bottom of the left well and around the top of the potential barrier. The flatter are these portions of $V_{\rm dw}(x_o)$, the larger is $\bar{T}_A$.

Using the potential (5.13) in Eqs. (5.7) and (5.8) leads to the SDDE

$$dx(t) = -\alpha \,\mathrm{sign}\big(x(t-\tau)\big)|x(t-\tau)|^n dt + \sigma dW(t), \tag{5.17}$$

which is simply the DDE (5.14) subjected to additive Gaussian white noise. In order to evaluate $\tau_{\rm meta}$ from simulations, there must be a clear criterion to determine when a particle starts to exhibit unbounded oscillatory behaviour. Although it is unclear how the onset of unbounded oscillatory trajectories could be detected, the particle can be assumed to be on such a trajectory, with a high degree of certainty, if $|x(t)|$ becomes significantly larger than the boundary $x_b(n)$ shown in Fig. 5.2. Since simulations of Eq. (5.17) have been performed only for $n \geq 1.25$ and since $x_b(1.25) \simeq 6.76$, the time scale $\tau_{\rm meta}$ has been approximated by the mean time required to reach $x = \pm 100$ for the first time when starting from a constant initial condition of $x = 0$. This quantity, known as a mean first passage time (see Sec. 5.3.3), is denoted by $\bar{T}(0, \pm 100)$. It is an accurate approximation for $\tau_{\rm meta}$, as long as the latter is much larger than the time required to reach $x = \pm 100$ from the onset of unbounded oscillatory trajectories.

Numerical simulations have shown that $\bar{T}(0, \pm 100)$ follows Arrhenius' law

$$\bar{T}(0, \pm 100) = \bar{T}_A \exp\left(\frac{2\Delta V_A}{\sigma^2}\right), \tag{5.18}$$

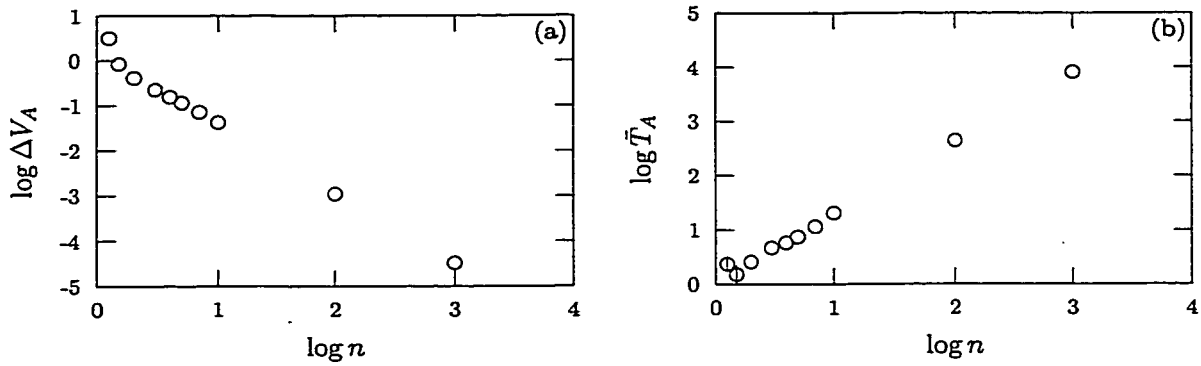

Figure 5.5: Arrhenius' law in the single-well potential. The parameters (a) ΔV_A and (b) $\bar{T}_A$ appearing in Eq. (5.18) are drawn as a function of n. They were determined using linear regressions on graphs of $\log \bar{T}(0, \pm 100)$ as a function of $1/\sigma^2$ (see Fig. 5.3) that were obtained from numerical simulations of the SDDE (5.17). Performing regressions on the linear part of these two graphs, it is found that ΔV_A and $\bar{T}_A$ are respectively proportional to $n^{-1.550 \pm 0.015}$ and $n^{1.31 \pm 0.05}$.

where the subscript A stands for Arrhenius, when σ^2 is small. This is illustrated in Fig. 5.3 for the case where $n = 10$ and $\alpha = \tau = 1$. In the context of transitions between the two wells of a nondelayed double-well potential, ΔV_A would represent the height of the potential barrier to be overcome by the particle, and $\bar{T}_A$ would depend on the flatness of the bottom of the starting well and of the top of the potential barrier (see Fig. 5.4). Both ΔV_A and $\bar{T}_A$ are plotted as a function of n in Fig. 5.5, and it is found that ΔV_A decreases and $\bar{T}_A$ increases as n becomes larger. This can easily be interpreted in terms of the boundary $x_b(n)$ and of the potential $V(x_o)$. Indeed, since the boundary $x_b(n)$ approaches 1 as n increases, smaller values of x, and thus of $V(x)$, need to be reached in order to trigger unbounded oscillatory trajectories. This is why ΔV_A decreases as n increases. Similarly, $V(x_o)$ becomes flatter around $x_o = 0$ as n increases, and it is therefore normal for $\bar{T}_A$ to increase with n (see Fig. 5.4).

5.3 Bistability

This section is devoted to rate processes between the wells of a potential. To this end, the function $V(x_o)$ appearing in Eq. (5.8) is considered here to be a symmetrical double-well potential, and the separatrix between the two wells is assumed to be located at $x = 0$. Specialising the FPE (3.14) to the case of an SDDE with additive noise, such as Eq. (5.7), yields

$$\frac{\partial}{\partial t} p(x_o, t|x', t') = -\frac{\partial}{\partial x_o}[\bar{f}(x_o, t|x', t') p(x_o, t|x', t')] + \frac{\sigma^2}{2} \frac{\partial^2}{\partial x_o^2} p(x_o, t|x', t'), \qquad (5.19)$$

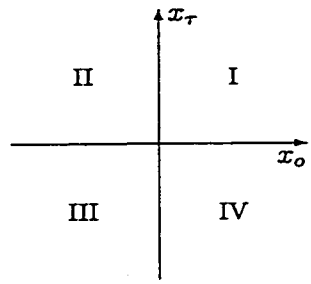

Figure 5.6: Quadrants of the $x_o x_\tau$ plane.

where the CAD $\bar{f}(x_o, t_o|x', t')$ is given by Eq. (3.12). As mentioned in Sec. 3.1, the conditional probability density $p(x_\tau, t_o - \tau|x_o, t_o; x', t')$ appearing in the definition of $\bar{f}(x_o, t_o|x', t')$ prevents Eq. (3.14), and thus Eq. (5.19), from being self-sufficient. Under the separation of time scales assumption presented in Sec. 5.3.1, however, the CAD can be approximated by its steady-state limit. As shown in Secs. 5.3.2 and 5.3.3, this allows quantities characterising the evolution of the probability density to be expressed in terms of its steady-state limit using standard techniques. Although the existence of a proper steady-state limit is assumed throughout Secs. 5.3.1 to 5.3.3, the results are still applicable in an appropriate pseudo-steady-state limit when unbounded oscillatory solutions are present. Indeed, the results of these three sections are illustrated in Sec. 5.3.4 using a potential that exhibits unbounded oscillatory trajectories.

5.3.1 Separation of Time Scales

The statistical properties of a stochastic process like $x(t)$, such as its probability densities, obviously inherit the time scales over which the process evolves. One of these is defined by the delay τ, which appears in Eq. (5.7). In the case of the bivariate probability density $p(x_o, t_o; x_\tau, t_o - \tau|x', t')$, at least two additional time scales may be relevant:

τ_{pop}: time scale over which $p(x_o, t_o; x_\tau, t_o - \tau|x', t')$ equilibrates between the four quadrants of the $x_o x_\tau$ plane (see Fig. 5.6) and

τ_{int}: time scale over which $p(x_o, t_o; x_\tau, t_o - \tau|x', t')$ relaxes within quadrants I and III, where x_o and x_τ are of the same sign.

The indices "pop" and "int" respectively stand for *population* and *internal*. The meaning of *population* in this context is explained in Sec. 5.3.2. When $\tau_{\text{pop}} \gg \tau$, the particle has a very small probability of undergoing a transition from one well to the other within τ units of time. In this case, the bivariate probability density $p(x_o, t_o; x_\tau, t_o - \tau|x', t')$ is therefore much larger

in quadrants I and III than in quadrants II and IV, and the conditional probability density $p(x_\tau, t_o - \tau | x_o, t_o; x', t')$ is much larger when x_o and x_τ are in the same well rather than in different wells. The CAD $\bar{f}(x_o, t_o | x', t')$, which is defined in terms of $p(x_\tau, t_o - \tau | x_o, t_o; x', t')$ in Eq. (3.12), can consequently be approximated by

$$\bar{f}(x_o, t_o | x', t') \simeq \int_{-\infty}^{0} dx_\tau f(x_o, x_\tau) p(x_\tau, t_o - \tau | x_o, t_o; x', t') \tag{5.20}$$

when $x_o < 0$, and by

$$\bar{f}(x_o, t_o | x', t') \simeq \int_{0}^{\infty} dx_\tau f(x_o, x_\tau) p(x_\tau, t_o - \tau | x_o, t_o; x', t') \tag{5.21}$$

when $x_o > 0$. For times much larger than τ_{int}, $p(x_o, t_o; x_\tau, t_o - \tau | x', t')$ is approximately proportional to its steady-state limit in each of quadrants I and III. Since the univariate probability density $p(x_o, t_o | x', t')$ is defined as the integral of $p(x_o, t_o; x_\tau, t_o - \tau | x', t')$ over x_τ [see Eq. (3.9)], and since $p(x_o, t_o; x_\tau, t_o - \tau | x', t')$ is much larger in quadrants I and III than in quadrants II and IV when $\tau_{\text{pop}} \gg \tau$, $p(x_o, t_o | x', t')$ is itself approximately proportional to its steady-state limit in each of the two wells. Considering that $p(x_\tau, t_o - \tau | x_o, t_o; x', t')$ is the ratio of $p(x_o, t_o; x_\tau, t_o - \tau | x', t')$ and $p(x_o, t_o | x', t')$ [see Eq. (3.10)], it is then approximately equal to its steady-state limit when x_o and x_τ are in the same well. From this, Eqs. (5.20) and (5.21) lead to

$$\bar{f}(x_o, t_o | x', t') \simeq \bar{f}^s(x_o) \tag{5.22}$$

for $t_o - t' \gg \tau_{\text{int}}$. Since the integrals in Eqs. (5.20) and (5.21) are truncated at $x_\tau = 0$, and since $p(x_o, t_o | x', t')$ and $p(x_o, t_o; x_\tau, t_o - \tau | x', t')$ cannot be proportional to their steady-state limits in the immediate neighbourhood of the x_o and x_τ-axes until complete equilibrium is reached, the difference between $\bar{f}^s(x_o)$ and $\bar{f}(x_o, t_o | x', t')$ may be somewhat greater near $x_o = 0$ than elsewhere on the x_o-axis. Still, as long as $\bar{f}^s(x_o)$ and $\bar{f}(x_o, t_o | x', t')$ are continuous around $x_o = 0$, the difference between the two should remain minimal, and Eq. (5.22) is expected to be a good approximation for all values of x_o.

Consequently, when $\tau_{\text{pop}} \gg \tau$, the FPE (3.14) reduces to

$$\frac{\partial}{\partial t} p(x_o, t | x', t') = -\frac{\partial}{\partial x_o} [\bar{f}^s(x_o) p(x_o, t | x', t')] + \frac{\sigma^2}{2} \frac{\partial^2}{\partial x_o^2} p(x_o, t | x', t') \tag{5.23}$$

for $t - t' \gg \tau_{\text{int}}$ [see Eq. (5.22)]. This approximate FPE and its equivalent backward FPE

$$\frac{\partial}{\partial t'} p(x_o, t | x', t') = -\bar{f}^s(x') \frac{\partial}{\partial x'} p(x_o, t | x', t') - \frac{\sigma^2}{2} \frac{\partial^2}{\partial x'^2} p(x_o, t | x', t') \tag{5.24}$$

can be used to study the equilibration of the probability density between the two wells of the potential when $\tau_{\text{pop}} \gg \tau$ and $\tau_{\text{pop}} \gg \tau_{\text{int}}$, regardless of the relation between τ and τ_{int}. Since $\bar{f}^s(x_o)$ is uniquely determined by the steady-state probability density $p^s(x_o)$ through Eq. (3.19), the knowledge of $p^s(x_o)$ is all that is required in order to use these two FPE's. The determination of $p^s(x_o)$ however remains a nontrivial task. Approximation schemes, like the small delay expansion presented in Chap. 4, can sometimes be used to obtain an analytical expression for $p^s(x_o)$. In other cases, numerical simulations may be the only possibility.

The steady-state CAD $\bar{f}^s(x_o)$ can be considered as arising from an effective potential $V_e(x_o)$ defined according to the equation

$$\bar{f}^s(x_o) \equiv -\frac{d}{dx_o} V_e(x_o). \tag{5.25}$$

This potential would yield the FPE (5.23) if an overdamped particle evolved in it with nondelayed coupling. This is thus an example of the correspondence, mentioned in Sec. 3.1, between delayed and nondelayed systems. The effective potential $V_e(x_o)$ can also be defined in terms of the steady-state probability density $p^s(x_o)$ when the particle is subjected to additive noise, as is the case in this chapter. Indeed, substituting Eq. (5.25) in Eq. (3.18) with $g(x_o) = 1$ results in

$$p^s(x_o) = N \exp\left(-\frac{2V_e(x_o)}{\sigma^2}\right). \tag{5.26}$$

As mentioned in Sec. 3.1, $\bar{f}(x_o, t_o|x', t') = f(x_o)$ when the delay vanishes. In this limit, Eq. (5.22) becomes an exact relation, as do Eqs. (5.23) and (5.24), and $V_e(x_o) = V(x_o)$.

5.3.2 Phenomenological Transition Rate

When experimentally studying ensembles of multistable systems, it is customary to monitor the fraction of realisations in each state as a function of time. This quantity is known as the *population number*. For a particle evolving in a double-well potential, each well is usually considered as a distinct state. Thus, the separatrix between the two wells being located at $x = 0$, the population numbers are defined as

$$N_-(t_o|x', t') \equiv \int_{-\infty}^{0} dx_o p(x_o, t_o|x', t') \tag{5.27}$$

and

$$N_+(t_o|x', t') \equiv \int_{0}^{\infty} dx_o p(x_o, t_o|x', t'). \tag{5.28}$$

Since the probability density is normalised,

$$N_-(t_o|x',t') + N_+(t_o|x',t') = 1. \tag{5.29}$$

This relation simply means that each realisation must always be within one of the two wells at any given time. In the limit where $\tau_{\text{pop}} \gg \tau$ and $\tau_{\text{pop}} \gg \tau_{\text{int}}$, introduced in Sec. 5.3.1, the univariate probability density $p(x_o,t_o|x',t')$ is expected to share the time scales τ_{pop} and τ_{int} of the bivariate probability density $p(x_o,t_o;x_\tau,t_o-\tau|x',t')$. It therefore relaxes within each well on a time scale τ_{int} and equilibrates between the two wells of the potential on a time scale τ_{pop}. Because of this, the population numbers $N_-(t_o|x',t')$ and $N_+(x_o|x',t')$ approach their steady-state limits η_- and η_+ on a time scale τ_{pop}, thus the "pop" in τ_{pop}. Mathematically, this is written as

$$N_\pm(t_o|x',t') = \eta_\pm + \left(N_\pm(t'|x',t') - \eta_\pm\right)\exp\left(-\frac{t_o-t'}{\tau_{\text{pop}}}\right). \tag{5.30}$$

Considering that the double-well potential is symmetrical, $\eta_- = \eta_+ = 1/2$.

Wu and Kapral [4] have studied the dynamics of population numbers for the nondelayed version of Eq. (5.7) with the quartic potential

$$V(x_o) = \frac{\beta}{4}x_o^4 - \frac{\alpha}{2}x_o^2,$$

where α and β are positive real constants. The corresponding FPE can be written as

$$\frac{\partial}{\partial t}p(x_o,t|x',t') = L_{\text{FP}}\,p(x_o,t|x',t'), \tag{5.31}$$

where

$$L_{\text{FP}} \equiv -\frac{\partial}{\partial x_o}f(x_o) + \frac{\sigma^2}{2}\frac{\partial^2}{\partial x_o^2}$$

is called the *Fokker-Planck operator*, $f(x_o)$ is defined by Eq. (5.8), and $x(t') = x'$ is the initial condition. The approach developed by Wu and Kapral is based on this FPE and is outlined in the following paragraph.

In order to obtain an evolution equation for the population numbers, the projection operators

$$Pq(x_o,t_o) \equiv \sum_{\pm}\eta_\pm^{-1}p^s(x_o)H(\pm x_o)\int_{-\infty}^{\infty}dx_o'H(\pm x_o')q(x_o',t_o) \tag{5.32}$$

and $Q \equiv 1 - P$ are defined. In Eq. (5.32), $q(x_o,t_o)$ is the function on which the projection

operator is applied,

$$H(x_o) \equiv \begin{cases} 0 & \text{for } x_o < 0 \\ 1/2 & \text{for } x_o = 0 \\ 1 & \text{for } x_o > 0 \end{cases}$$

is the Heaviside step function, and $p^s(x_o)$ is the steady-state probability density. The operators P and Q respectively project onto the population numbers and onto the other degrees of freedom of $q(x_o, t_o)$. Using these projection operators and the FPE (5.31), standard techniques yield

$$N_+(t_o|x', t') - N_+(0|x', t') = \sum_{\pm} \int_0^{t_o} dt'_o K_{\pm}(t'_o) N_{\pm}(t_o - t'_o), \tag{5.33}$$

where

$$K_{\pm}(t_o) \equiv \eta_{\pm}^{-1} \int_{-\infty}^{\infty} dx_o H(x_o) L_{\text{FP}} e^{QL_{\text{FP}}t_o} p^s(x_o) H(\pm x_o) \tag{5.34}$$

are called *rate kernels*. The evolution of both $N_-(t_o|x', t')$ and $N_+(t_o|x', t')$ is determined by Eq. (5.33), since these two population numbers are related by Eq. (5.29). If the rate kernels $K_{\pm}(t_o)$ approach plateau values on a time scale much smaller than the one over which the population numbers $N_{\pm}(t_o|x', t')$ decay, Eq. (5.33) leads to the phenomenological rate law

$$\frac{d}{dt} N_+(t|x', t') = -k_f N_+(t|x', t') + k_r N_-(t|x', t'), \tag{5.35}$$

where the rate constants are given by

$$k_f \equiv -\lim_{t_o \to \infty} K_+(t_o)$$

and

$$k_r \equiv \lim_{t_o \to \infty} K_-(t_o).$$

It must be noted that integrating Eq. (5.35) from $t = t'$ to $t = t_o$ and defining

$$\tau_{\text{pop}} \equiv \frac{1}{k_f + k_r} \tag{5.36}$$

allows Eq. (5.30) to be recovered in a rigorous fashion. The rate kernels $K_{\pm}(t_o)$ can be expressed in terms of the eigenvalues and eigenfunctions of the projected Fokker-Planck

operator QL_{FP}. This allows to show, among other things, that

$$k \equiv k_f = k_r = \frac{\sigma^2}{4}\left[\int_0^\infty dx p^s(x) \int_0^x \frac{dy}{p^s(y)}\left(1 - 2\int_0^y dz p^s(z)\right)\right]^{-1} \tag{5.37}$$

in the small σ^2 limit. The forward and reverse rate constants are in this case equal because of the symmetry of the potential.

Although this theory has been developed by Wu and Kapral in the context of a particular system, the derivation is rather general and the results seem to apply to all symmetrical double-well potentials. It should thus be applicable to systems described by the SDDE (5.7) as long as the effective potential $V_e(x_o)$ is composed of two symmetrical wells. This conclusion is supported by the example presented in Sec. 5.3.4.

5.3.3 Mean First Passage Time

The time required to reach a given point from another one for the first time is known as the *first passage time*. This quantity obviously depends on the initial condition and varies from one realisation to another. In the particular case of a time homogeneous process $x(t)$, the first passage time is independent of the initial time and can be denoted as $T(x', x'')$, where x' is the initial point and x'' is the end point. The mean $\bar{T}(x', x'')$ of this quantity, the mean first passage time (MFPT), can be calculated for a homogeneous process using the procedure described in the following paragraphs [1]. It must be noted that the details of the calculation depend on whether $x' \leq x''$ or $x' \geq x''$.

Assuming that $x' \leq x''$, the point $x = x''$ must be specified as an absorbing boundary and $x = -\infty$ as a reflecting boundary. With this choice of boundary conditions, a given particle can reach x'' only once and obviously remains in the interval $(-\infty, x'')$ until this happens. The probability $F_T(x'', t''|x', t')$ that the particle reach $x = x''$ at $t = t''$ or at an earlier time, given that it starts from $x = x'$ at $t = t'$, is therefore equal to the probability that the particle be missing from the interval $(-\infty, x'')$ at time t''. In other words,

$$F_T(x'', t''|x', t') = 1 - \int_{-\infty}^{x''} dx_o p(x_o, t''|x', t'), \tag{5.38}$$

where the end point x'' is excluded from the integral. The function $F_T(x'', t''|x', t')$ is the probability distribution function of $T(x', x'')$, and the MFPT can thus be written as (see

Sec. 2.1.3)

$$\begin{aligned}\bar{T}(x',x'') &= \int_{t'}^{\infty} dt''(t''-t')\frac{\partial}{\partial t''}F_T(x'',t''|x',t') \\ &= -\int_{t'}^{\infty} dt''(t''-t')\frac{\partial}{\partial t''}[1-F_T(x'',t''|x',t')] \\ &= \int_{t'}^{\infty} dt''[1-F_T(x'',t''|x',t')]. \end{aligned} \tag{5.39}$$

Between the second and third lines of Eq. (5.39), an integration by parts has been performed under the assumption that

$$\lim_{t''\to\infty}(t''-t')[1-F_T(x'',t''|x',t')] = 0,$$

which simply states that the probability of not having reached $x = x''$ at $t = t''$ or at an earlier time must decrease sufficiently rapidly as t'' increases. Since $x(t)$ is a time homogeneous process, $p(x_o,t_o|x',t')$ is time-shift invariant and so is $F_T(x'',t''|x',t')$. This allows Eq. (5.39) to be written as

$$\bar{T}(x',x'') = \int_0^{\infty} ds[1-F_T(x'',s|x',0)],$$

where $s \equiv t''-t'$, which shows that $\bar{T}(x',x'')$ is also time-shift invariant. This supports the idea, mentioned at the beginning of this section, that $T(x',x'')$ is independent of the initial time t' for homogeneous processes.

The time-shift invariance of $p(x_o,t_o|x',t')$ implies that

$$\frac{\partial}{\partial t'}p(x_o,t_o|x',t') = -\frac{\partial}{\partial t_o}p(x_o,t_o|x',t'),$$

and with this result, the backward FPE (5.24) becomes

$$\frac{\partial}{\partial t_o}p(x_o,t_o|x',t') = \bar{f}^s(x')\frac{\partial}{\partial x'}p(x_o,t_o|x',t') + \frac{\sigma^2}{2}\frac{\partial^2}{\partial x'^2}p(x_o,t_o|x',t'). \tag{5.40}$$

Integrating Eq. (5.40) from $x_o = -\infty$ to $x_o = x''$ and from $t_o = t'$ to $t_o = \infty$, and using Eqs. (5.38) and (5.39), leads to the differential equation

$$\bar{f}^s(x')\frac{\partial}{\partial x'}\bar{T}(x',x'') + \frac{\sigma^2}{2}\frac{\partial^2}{\partial x'^2}\bar{T}(x',x'') = -1. \tag{5.41}$$

In order to solve this equation, appropriate boundary conditions must first be specified. Since the particle is immediately absorbed if $x' = x''$, then

$$\bar{T}(x', x'')\big|_{x'=x''} = 0.$$

For $x' = -\infty$, the reflecting boundary condition is obtained by enforcing [see part (c) of Sec. 2.1.5]

$$\lim_{x' \to -\infty} \frac{\partial}{\partial x'} p(x_o, t_o | x', t') = 0,$$

which implies that

$$\lim_{x' \to -\infty} \frac{\partial}{\partial x'} \bar{T}(x', x'') = 0.$$

With these boundary conditions, Eq. (5.41) yields

$$\bar{T}(x', x'') = \frac{2}{\sigma^2} \int_{x'}^{x''} \frac{dy}{p^s(y)} \int_{-\infty}^{y} dz p^s(z), \tag{5.42a}$$

which is valid when $x' \leq x''$. A similar procedure leads to

$$\bar{T}(x', x'') = \frac{2}{\sigma^2} \int_{x''}^{x'} \frac{dy}{p^s(y)} \int_{y}^{\infty} dz p^s(z) \tag{5.42b}$$

when $x' \geq x''$.

5.3.4 Example: Quartic Potential

The quartic potential

$$V(x_o) = \frac{\beta}{4} x_o^4 - \frac{\alpha}{2} x_o^2, \tag{5.43}$$

where α and β are positive coefficients, is an archetypal example of double-well potentials and is therefore an appropriate test-bed for the methods presented in this section. Substituting $V(x_o)$ in Eqs. (5.7) and (5.8) leads to the SDDE

$$dx(t) = [\alpha x(t-\tau) - \beta x^3(t-\tau)]dt + \sigma dW(t), \tag{5.44}$$

the deterministic part of which is

$$dx(t) = [\alpha x(t-\tau) - \beta x^3(t-\tau)]dt. \tag{5.45}$$

Range of delays	Asymptotic limit
$\tau \leq 0.785$	Trajectories approach a fixed point located at $x = -1$.
$0.786 \leq \tau \leq 1.538$	Trajectories approach a limit cycle. Particles are confined to the left well for $\tau \leq 1.260$. Around $\tau = 1.260$, they start to cross the boundary between the two wells, but they do not reach the bottom of the right well until approximately $\tau = 1.325$. For delays larger than 1.325, the limit cycle spans beyond both local minima. It is symmetrical for $1.325 \leq \tau \leq 1.522$, and becomes asymmetrical around $\tau = 1.523$. In addition, it undergoes a sequence of period doubling bifurcations between approximately $\tau = 1.534$ and $\tau = 1.538$.
$1.539 \leq \tau \leq 1.725$	Trajectories are aperiodic, except for some windows of τ where they approach a limit cycle.
$1.726 \leq \tau$	Trajectories diverge.

Table 5.1: Bounded asymptotic limits of the deterministic trajectories in the quartic potential with delayed coupling, $\alpha = \beta = 1$ (see App. A.1), and the particle initially located in the left well ($x < 0$). The range of delays for which the various behaviours are observed have been determined through numerical integration of the DDE (5.45) with constant initial conditions over $t \in [-\tau, 0]$.

The DDE (5.45) has three fixed points: $x_1 = -\sqrt{\alpha/\beta}$, $x_2 = 0$, and $x_3 = \sqrt{\alpha/\beta}$. Linearising it around x_1 or x_3 yields

$$dy(t) = -2\alpha y(t-\tau)dt, \tag{5.46}$$

where $y(t) \equiv x(t) - x_{1,3}$. The results of the stability analysis performed in Sec. 2.2.3 are easily adapted to Eq. (5.46). In particular, x_1 and x_3 are stable when $\alpha\tau < \pi/4$ and unstable when $\alpha\tau > \pi/4$. On the other hand, the fixed point x_2 is always unstable, as can be shown by linearising the DDE around it. This analysis indicates that a particle evolving in accordance with Eq. (5.45) should relax to either x_1 or x_3 when $\alpha\tau < \pi/4$ and exhibit other types of asymptotic behaviour when $\alpha\tau > \pi/4$. The asymptotic limits of its trajectories can be studied in more detail with numerical simulations. Using these, it was found that the DDE (5.45) exhibits both bounded and unbounded trajectories (see Table 5.1 and Fig. 5.7). The presence of unbounded trajectories clearly prevents the existence of a steady-state probability density for the SDDE (5.44). As mentioned in Sec. 5.2, however, a pseudo-steady-state probability density $p^m(x_o)$ can nevertheless be defined when the transition rate τ_{meta}^{-1} from bounded to unbounded trajectories is sufficiently small. It can then be used as a substitute for $p^s(x_o)$ in Eqs. (5.37) and (5.42).

As the delay decreases, the values of x required to reach deterministically unbounded trajectories become arbitrarily large (see Fig. 5.7) and τ_{meta}^{-1} therefore approaches zero. The pseudo-steady-state probability density $p^m(x_o)$ is thus well-defined in this limit and can be approximated using the small delay expansion presented in Chap. 4. Setting the integration

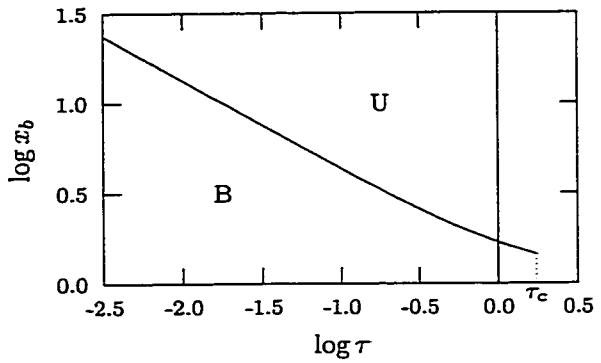

Figure 5.7: Boundedness of the deterministic trajectories in the quartic potential with delayed coupling, $\alpha = \beta = 1$ (see App. A.1), and constant initial conditions. The boundary x_b, which separates the initial conditions leading to bounded (B) and unbounded (U) solutions of Eq. (5.45), has been determined using numerical simulations. It must be noted that all constant initial conditions lead to unbounded trajectories when the delay is larger than $\tau_c \simeq 1.725$. For small delays, x_b seems proportional to $1/\sqrt{\tau}$.

constant c to zero in Eq. (4.5) leads to

$$p_a^m(x_o) = N_a \exp\left[-\frac{x_o^2}{3\tau\sigma^2} - \frac{1+2\alpha\tau-18\beta\tau^2\sigma^2}{9\beta\tau^2\sigma^2}\ln\left(\frac{1-\alpha\tau}{1-\alpha\tau+3\beta\tau x_o^2}\right)\right], \tag{5.47}$$

which is formally valid for $\tau < 1$. Similarly,

$$\bar{f}_a^m(x_o) = \frac{(\alpha - 6\beta\tau\sigma^2)x_o - \beta x_o^3}{1-\tau(\alpha-3\beta x_o^2)} \tag{5.48}$$

follows from Eq. (4.6). These approximate expressions for $p^m(x_o)$ and $\bar{f}^m(x_o)$ are quite accurate when $\alpha = \tau = 1$ and $\tau = \sigma^2 = 0.1$, as shown in Fig. 5.8. In addition, Eqs. (5.47) and (5.48) qualitatively agree with numerical simulation results up to roughly $\sigma^2 = 1$ when $\alpha = \tau = 1$ and $\tau = 0.1$, and up to about $\tau = 0.4$ when $\alpha = \tau = 1$ and $\sigma^2 = 0.1$.

Before Eqs (5.37) and (5.42) can be used, the separation of time scales assumption that led to the FPE (5.23) must first be verified. To do so, τ_{pop} and τ_{int} must obviously be determined. As mentioned in Sec. 5.3.2, $p(x_o, t_o|x', t')$ and $p(x_o, t_o; x_\tau, t_o - \tau|x', t')$ are expected to relax on similar time scales when $\tau_{\text{pop}} \gg \tau$ and $\tau_{\text{pop}} \gg \tau_{\text{int}}$. This allows τ_{pop} and τ_{int} to be determined from the transients of $p(x_o, t_o|x', t')$, which is somewhat simpler than considering $p(x_o, t_o; x_\tau, t_o - \tau|x', t')$ directly. For $\tau = \sigma^2 = 0.1$, it was found through numerical simulations that τ_{int} is of order one and that $\tau_{\text{pop}} = 341 \pm 22$. The separation of time scales is thus valid for this set of parameter values, and Eqs. (5.37) and (5.42) can be used to determine τ_{pop} and $\bar{T}(x', x'')$. In fact, as shown in Figs. 5.9(a,b) and 5.10(c,d), these equations yield values that are of the right order of magnitude for a significant range

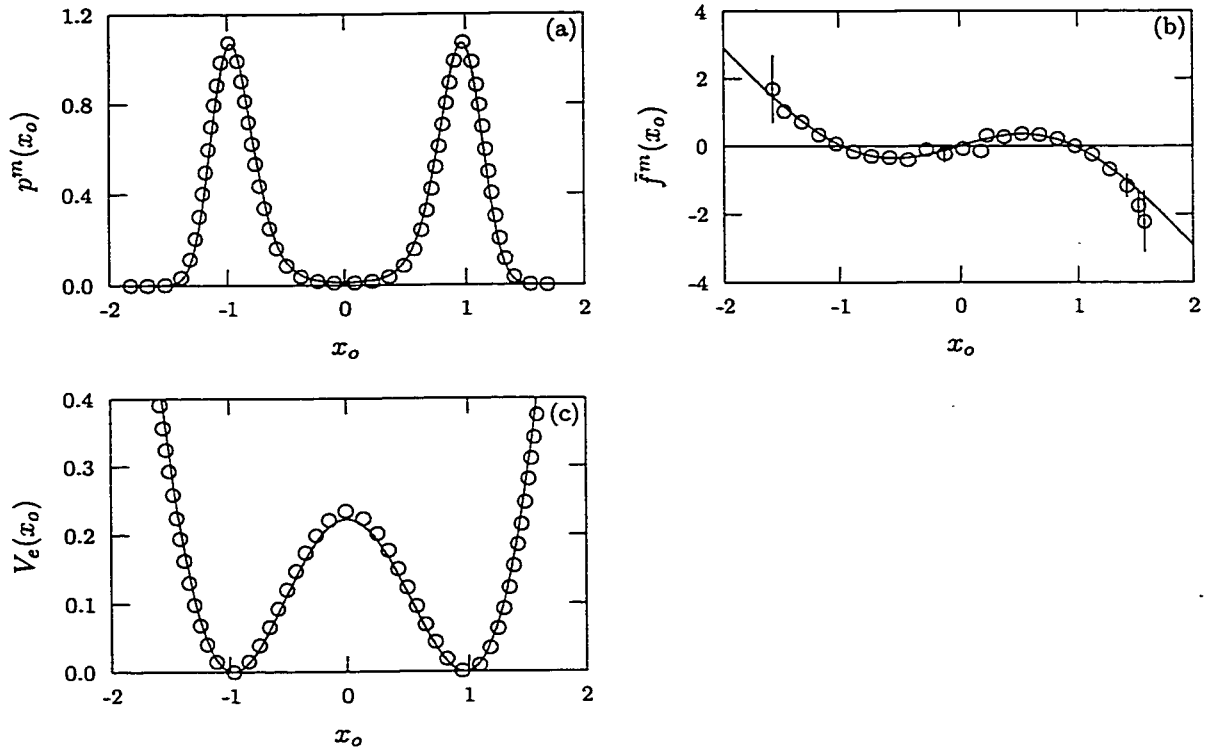

Figure 5.8: Pseudo-steady-state (a) probability density and (b) CAD in the quartic potential with delayed coupling, $\alpha = \beta = 1$ (see App. A.1), and $\tau = \sigma^2 = 0.1$. In (a) and (b), the circles represent simulation results for the SDDE (5.44), and the continuous lines stand for the approximate functions $p_a^m(x_o)$ and $\bar{f}_a^m(x_o)$ [Eqs. (5.47) and (5.48)]. The effective potentials in (c) correspond to the probability densities of (a) and were obtained using Eq. (5.26) with values of N such that their global minima are zero. The barrier between the two wells of the potential determined from numerical simulations has a height of 0.235 ± 0.002.

of τ and σ^2. It is important to note, however, that they lead to significantly more accurate results when $p^m(x_o)$ is determined through numerical simulations rather than approximated by $p_a^m(x_o)$ [Eq. (5.47)]. Indeed, Eqs. (5.37) and (5.42) seem very sensitive to discrepancies in the (pseudo-)steady-state probability density, even in regions where its magnitude is small. The key in understanding this sensitivity lies in the effective potential $V_e(x_o)$. For instance, Eq. (5.47) seems to perfectly predict the shape of the pseudo-steady-state probability density when $\tau = \sigma^2 = 0.1$ [see Fig. 5.8(a)]. However, some subtle differences are present and lead to significant discrepancies in $V_e(x_o)$ [see Fig. 5.8(c)]. In particular, the effective potential barrier between the two wells is smaller when $p_a^m(x_o)$ is considered instead of $p^m(x_o)$, and it is thus more easily overcome by the particle. This is why $p_a^m(x_o)$ leads in this case to values of τ_{pop} and $\bar{T}(-1, 1)$ that are significantly smaller than those obtained with $p^m(x_o)$ [see Figs. 5.9(b) and 5.10(a)].

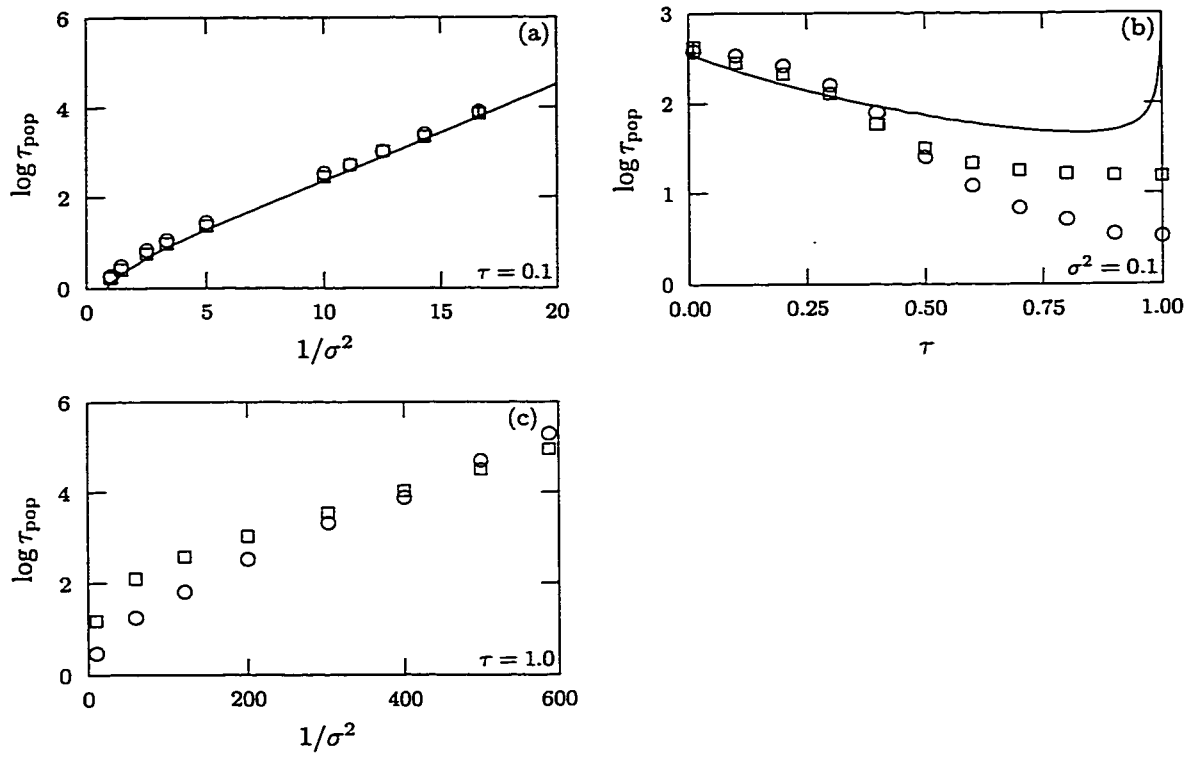

Figure 5.9: Time scale τ_{pop} in the quartic potential with delayed coupling and $\alpha = \beta = 1$ (see App. A.1). Results are given for (a) $\tau = 0.1$, (b) $\sigma^2 = 0.1$, and (c) $\tau = 1.0$. The circles represent data obtained from phenomenological simulations of Eq. (5.44). On the other hand, the squares and the solid line both result from Eqs. (5.36) and (5.37). For the squares, $p^m(x_o)$ was determined using numerical simulations of Eq. (5.44); for the solid line, it was approximated by $p^m_a(x_o)$ [Eq. (5.47)]. The solid line is omitted from graph (c) because Eq. (5.47) is not valid for $\tau = 1.0$.

It is therefore essential to use the most accurate representation of the pseudo-steady-state probability density in Eqs. (5.37) and (5.42) in order to obtain proper values for τ_{pop} and $\bar{T}(x', x'')$. It must however be stressed that even an exact expression for $p^m(x_o)$ would not yield exact values for τ_{pop} and $\bar{T}(x', x'')$, since approximations have been used in deriving Eqs. (5.37) and (5.42). In particular, only when $\tau = 0$ does Eq. (5.22), and thus Eqs. (5.23) and (5.24), reduce to an exact relation. In all other cases, the FPE (5.23) and the backward FPE (5.24), on which Eqs. (5.37) and (5.42) are based, are only approximate. Furthermore, as discussed in Sec. 5.3.1, the $\bar{f}(x_o, t_o|x', t') \simeq \bar{f}^s(x_o)$ approximation may be somewhat less appropriate around $x_o = 0$ than elsewhere on the x_o-axis. Since Eqs. (5.37) and (5.42) are fairly sensitive to discrepancies in $p^m(x_o)$ around $x_o = 0$, this may lead to some inaccuracy in the values obtained for τ_{pop} and $\bar{T}(x', x'')$. Once again, this can be illustrated using the $\tau = \sigma^2 = 0.1$ example. For these values of τ and σ^2, Eq. (5.37)

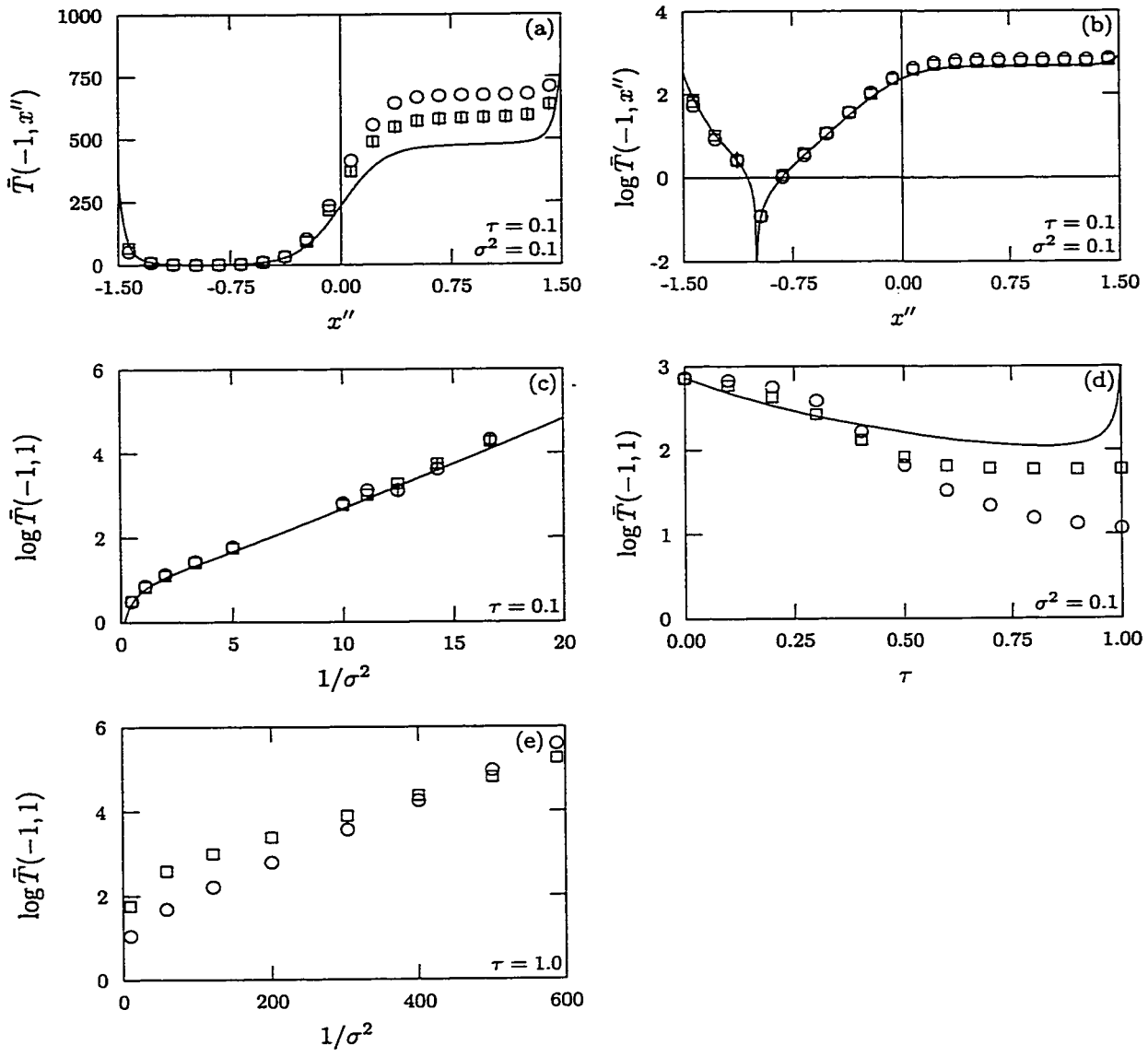

Figure 5.10: Mean first passage time $\bar{T}(x', x'')$ in the quartic potential with delayed coupling and $\alpha = \beta = 1$ (see App. A.1). For $\tau = \sigma^2 = 0.1$, the MFPT from $x' = -1$ to a whole range of end points is given on (a) a linear scale and (b) a semilogarithmic scale. In addition, the MFPT from $x' = -1$ to $x'' = 1$ is given for (c) $\tau = 0.1$, (d) $\sigma^2 = 0.1$, and (e) $\tau = 1.0$. The circles represent data obtained from simulations of Eq. (5.44). On the other hand, the squares and the solid line both result from Eq. (5.42). For the squares, $p^m(x_o)$ was determined using numerical simulations of Eq. (5.44); for the solid line, it was approximated by $p_a^m(x_o)$ [Eq. (5.47)]. The solid line is omitted from graph (e) because Eq. (5.47) is not valid for $\tau = 1.0$.

Delay	Barrier height	
	τ_{pop}	$\bar{T}(-1,1)$
0.1	0.243 ± 0.006	0.24 ± 0.04
1.0	0.0082 ± 0.0005	0.0083 ± 0.0001

Table 5.2: Arrhenius' law in the quartic potential with delayed coupling and $\alpha = \beta = 1$ (see App. A.1). The effective barrier height ΔV_A appearing in Eq. (5.18) is given for both τ_{pop} and $\bar{T}(x', x'')$. It was obtained using regressions on the linear part of the numerical simulation results (circles) in Figs. 5.9(a,c) and 5.10(c,e).

with a numerically determined $p^m(x_o)$, believed to be accurate, led to $\tau_{\text{pop}} = 283 \pm 8$. On the other hand, phenomenological simulations yielded $\tau_{\text{pop}} = 341 \pm 22$. Even though these two values are of the same order of magnitude, they are nevertheless significantly different. This discrepancy is also observed for $\bar{T}(-1, x'')$, but is larger for $x'' \in [0, 1]$ than for $x'' \in [-1, 0]$ (see Fig. 5.10). This last observation indicates that the accuracy of the $\bar{f}(x_o, t_o|x', t') \simeq \bar{f}^s(x_o)$ approximation may be inadequate around $x_o = 0$. Overall, although Eqs. (5.37) and (5.42) can be used to determine the order of magnitude of τ_{pop} and $\bar{T}(x', x'')$ when τ and σ^2 are sufficiently small, they should not be relied on in the context of SDDE's when accurate values are required.

As is clear from Figs. 5.9(a,c) and 5.10(c,e), τ_{pop} and $\bar{T}(-1, 1)$ follow Arrhenius' law [Eq. (5.18)] when σ^2 is small, whether $\tau = 0.1$ or $\tau = 1.0$. The latter case is particularly interesting, since the deterministic attractors consist of limit cycles (see Table 5.1). It is another example of a transition where Arrhenius' law applies without both attractors being fixed points, the first one being the transition to unbounded oscillatory trajectories in the single-well potential presented in Sec. 5.2.2. As expected, the effective barrier height ΔV_A appearing in Arrhenius' law varies with the delay and, for a given value of τ, is the same for both τ_{pop} and $\bar{T}(-1, 1)$ (see Table 5.2). The value of ΔV_A corresponds to the height of the potential barrier between the two wells of $V_e(x_o)$ when $\tau = 0.1$ [see Fig. 5.8(c)], but not when $\tau = 1.0$. In fact, when limit cycles are present, a bivariate probability density and a bivariate potential would probably characterise more appropriately the system than univariate ones. This could explain, along with the breakdown of the $\bar{f}(x_o, t_o|x', t') \simeq \bar{f}^s(x_o)$ approximation, why Eqs. (5.37) and (5.42) do not predict the right values for τ_{pop} and $\bar{T}(x', x'')$ when the delay is large [see Figs. 5.9(b,c) and 5.10(d,e)].

Chapter 6

Conclusion

The well-known Fokker-Planck equation plays a very important role in the analysis of systems described by nondelayed stochastic differential equations. Unfortunately, the presence of delayed feedback in a differential equation implicitly entails the existence of an infinite-dimensional phase space. Because of this, the FPE associated with a stochastic delay differential equation has to be formulated in terms of an infinite number of independent variables in order to take into account all the available degrees of freedom. Although this can be formally done in a number of ways (see Secs. 3.1 and 3.3.2), some kind of projection or truncation is required if the FPE is to be used in any practical application. In this respect, the derivation in Sec. 3.1 of the exact FPE (3.14) corresponds to a particularly simple projection scheme. However, important information is improperly discarded by this approach, and Eq. (3.14) cannot independently yield the univariate probability density function.

Even though the phase space in which evolves a system described by a delay differential equation is effectively infinite-dimensional, the various degrees of freedom are in general partially slaved to one another by the integration process. Consequently, it may be possible to approximate the long term behaviour of an SDDE by using a set of differential equations defined over a finite-dimensional phase space. For instance, the Taylor expansion presented in Chap. 4 leads from a univariate SDDE with nondelayed diffusion to a univariate nondelayed SDE [Eq. (4.2)] on which the usual Fokker-Planck approach can be applied [see Eq. (4.4)]. This approximation is expected to be valid for short delays, provided that the possible oscillatory modes of the original SDDE be strongly damped. It must be noted that although the FPE (3.14) does not initially intervene in this approximation scheme, substituting the results of the Taylor expansion in this equation leads to an alternative and complementary approximation of the original SDDE [see Eq. (4.7)]. Thus, despite its limitations, this FPE

can still be helpful when used in association with appropriate approximation schemes.

This is particularly true when dealing with bistable delay differential equations driven by additive noise. Under the separation of time scales assumption presented in Sec. 5.3, Eq. (3.14) reduces in this case to an FPE [Eq. (5.23)] that is uniquely determined by the steady-state probability density. This FPE can then be used to characterise noise-induced rate processes in such systems. For instance, in the context of an overdamped particle with delayed coupling to a symmetrical and stochastically driven double-well potential, it can be used with standard techniques to express the transition rate between the two wells of the potential in terms of the noise amplitude and of the steady-state probability density (see Sec. 5.3.2). The same can also be done for the mean first passage time, which is the mean time required to go from one point to another for the first time (see Sec. 5.3.3).

However, there exists no steady-state probability density for the quartic potential considered in Sec. 5.3.4. For this system, as for a large number of SDDE's with no instantaneous feedback, all realisations eventually stabilise on an attractor that is best described as an unbounded oscillatory trajectory (see Sec. 5.2). Since on this trajectory the dynamical variable oscillates with an amplitude that increases indefinitely with time, there exists no steady-state limit and thus no steady-state probability density. Still, in regimes where the transition rate to this globally stable attractor is sufficiently small, the transitions between the basins of attraction of the remaining attractors may be studied in a pseudo-steady-state limit. This allows the transition rate and the mean first passage time mentioned in the previous paragraph to be calculated using a pseudo-steady-state probability density instead of the non-existent steady-state one.

For this quartic potential, the transition rate between the two wells and the mean first passage time from the bottom of one well to the bottom of the other both follow Arrhenius' law when the noise amplitude is small. It is particularly interesting to note that this is true even when the delay is so large that the attractor in each well is a limit cycle instead of a fixed point. Similarly, the transition rate to unbounded oscillatory trajectories in the single-well potential presented in Sec. 5.2.2 also follows Arrhenius' law when the noise amplitude is sufficiently small. These two examples clearly show that Arrhenius' law can be valid even when the attractors involved are not all fixed points. However, the dynamics that leads to Arrhenius' law in these two cases is not yet fully understood. The use of probability densities and effective potentials defined over higher-dimensional phase spaces could play a crucial role in this respect. On a different note, it would be important to verify if the existence of unbounded oscillatory trajectories depends on the fact that a particle is overdamped and if they exist in inertial systems.

The separation of time scales approach introduced in Sec. 5.3 can be adapted to a wide range of systems. Indeed, the derivation of the approximate FPE (5.23) in Sec. 5.3.1 does not depend on the symmetry of the potential or on the number of wells. It can thus be used with potentials that are asymmetrical or possess more than two wells. Similarly, the expressions obtained in Sec. 5.3.3 for the mean first passage time can also be applied to these cases without any modification. On the other hand, the formula presented in Sec. 5.3.2 for the transition rate between wells needs to be generalised before it can be used with these potentials. This separation of time scales approach can also be employed with SDDE's involving multiplicative noise. If the diffusion term is delayed, however, the resulting FPE includes steady-state averages of both the drift and the diffusion terms of the SDDE [see Eqs. (3.16) and (3.17)] and cannot be expressed solely in terms of the steady-state probability density.

With regard to the short delay approximation of Chap. 4, higher-order expansions could be achieved by using the integral form of the Taylor expansion formula [47]. Such a technique would also allow an SDDE with delayed diffusion to be approximated by a nondelayed SDE. Unfortunately, this approximation would still be limited to short delays, and the presence of multiple stochastic integrals would prevent the usual FPE from being used. On the other hand, approximate and self-sufficient FPE's for SDDE's with delayed diffusion and relatively large delays could possibly be obtained by projecting or truncating the infinite-dimensional FPE's discussed in Secs. 3.1 and 3.3.2. In Sec. 3.1, for instance, a closure scheme in which a given multivariate probability density is written in terms of lower-order ones may prove to be a viable approach.

Throughout this thesis, the focus has been on delay differential equations driven by Gaussian white noise. This is an appropriate choice when the correlation time of the fluctuations is negligible compared to the deterministic time scales of the system, but when this condition is not verified, the fluctuations need to be modelled using a stochastic process that has a non-zero correlation time. The Ornstein-Uhlenbeck and dichotomous processes are often used for this purpose. Consequently, it would be important to adapt the results of this research to SDDE's involving these stochastic processes. This should be particularly easy for the small delay approximation of Chap. 4, since it is merely based on a Taylor expansion.

Overall, it was found that the Fokker-Planck approach can play a significant role in the analysis of stochastic delay differential equations. Considering that these equations are now recognised as an important modelling tool, it is essential that the development of this methodology continue to be actively pursued.

Appendix A

Numerical Simulations

A.1 Units

When performing numerical analysis, each parameter characterising the system under study must obviously be set to some numerical value. Because of this, the analysis must be repeated for several sets of parameter values in order to appropriately sample parameter space. However, the number of sets that are required can often be reduced by properly choosing the units in which the various quantities are expressed. This can be illustrated using Eq. (2.58),

$$\frac{d}{dt}x(t) = -\alpha x(t-\tau). \tag{A.1}$$

If t and τ are scaled in such a way as to be expressed in units of α^{-1}, Eq. (A.1) becomes

$$\frac{d}{dt}x(t) = -x(t-\tau) \tag{A.2}$$

and only τ needs to be varied in order to completely sample parameter space. On the other hand, if t and α are respectively measured in units of τ and τ^{-1}, the equation

$$\frac{d}{dt}x(t) = -\alpha x(t-1) \tag{A.3}$$

is obtained and only α needs to be varied. There is no universal rule for choosing the most appropriate units. The optimal choice depends on the particular application.

Instead of writing two versions of the same equation, it is often possible to specify parameter assignments that allow the scaled equation to be obtained from the original one. For instance, Eq. (A.2) is simply Eq. (A.1) with $\alpha = 1$. The units used in this thesis,

Equations	Units					Assignments			
	t	x	τ	W	σ	α	β	τ	σ
(2.49)	$1/\alpha$	α/β	—	$1/\sqrt{\alpha}$	$\sqrt{\alpha}$	1	1	—	—
(2.57)	$1/\alpha$	$\sigma/\sqrt{\alpha}$	$1/\alpha$	$1/\sqrt{\alpha}$	—	1	—	—	1
(2.58)	$1/\alpha$	—	$1/\alpha$	—	—	1	—	—	—
(3.44), (3.45)	$1/\alpha$	α/β	$1/\alpha$	$1/\sqrt{\alpha}$	$\beta/\sqrt{\alpha}$	1	1	—	—
(4.15)	$1/\alpha$	α/β	$1/\alpha$	$1/\sqrt{\alpha}$	$\sqrt{\alpha}$	1	1	—	—
(5.14) with $n \neq 1$	τ	$(\alpha\tau)^{1\ n}$	—	—	—	1	—	1	—
(5.17) with $n \neq 1$	τ	$(\alpha\tau)^{1\ n}$	—	$\sqrt{\tau}$	$\alpha^{1\ n}\tau^{1/2\ n}$	1	—	1	—
(5.44)	$1/\alpha$	$\sqrt{\alpha/\beta}$	$1/\alpha$	$1/\sqrt{\alpha}$	$\alpha/\sqrt{\beta}$	1	1	—	—
(5.45)	$1/\alpha$	$\sqrt{\alpha/\beta}$	$1/\alpha$	—	—	1	1	—	—

Table A.1: Units used for the numerical analysis of the various differential equations. When $n = 1$, Eqs. (5.14) and (5.17) reduce to Eqs. (2.58) and (2.57) respectively.

and the corresponding assignments, are listed in Table A.1 for each differential equation on which numerical analysis has been performed.

A.2 Algorithms

A.2.1 Integration Schemes

Throughout this research project, differential equations have been numerically integrated using either the Euler, the stochastic Euler, or the stochastic midpoint integration scheme. These three methods follow more or less directly from the definitions of the Riemann, the Ito, and the Stratonovich integrals [Eqs (2.34), (2.37), and (3.22)].

a) Euler

The deterministic equation

$$x(t+\Delta t) = x(t) + \int_t^{t+\Delta t} f\big(x(t), x(t-\tau)\big)dt \tag{A.4}$$

involves only a Riemann integral. Specifying $n = 1$ and $t_1{}' = t_1$ in Eq. (2.34) yields the approximate iterative equation

$$x(t+\Delta t) \simeq x(t) + f\big(x(t), x(t-\tau)\big)\Delta t, \tag{A.5}$$

which is the well-known Euler integration scheme. This method was used for numerically integrating all deterministic DDE's.

b) Stochastic Euler

The stochastic Euler integration scheme, which is a generalisation of the previous method, was used for Ito SDDE's. In this case, the equation

$$x(t+\Delta t) = x(t) + \int_t^{t+\Delta t} f\big(x(t), x(t-\tau)\big)dt + \mathcal{I}\int_t^{t+\Delta t} \sigma g\big(x(t), x(t-\tau)\big)dW(t)$$

involves both a Riemann and an Ito integral. Treating the Riemann integral in the same way as in the Euler integration scheme and setting $n = 1$ in Eq. (2.37) leads to

$$x(t+\Delta t) \simeq x(t) + f\big(x(t), x(t-\tau)\big)\Delta t + \sigma g\big(x(t), x(t-\tau)\big)\Delta W, \tag{A.6}$$

where $\Delta W \equiv W(t+\Delta t) - W(t)$. As can be seen from Eq. (2.28), ΔW is a Gaussian distributed random variable with a zero mean and a Δt variance. Furthermore, since $W(t)$ is Markovian and since the integration steps do not overlap, the values assumed by ΔW for any two steps are independent of one another.

c) Stochastic Midpoint

In the classical midpoint integration scheme, the Riemann integral appearing in Eq. (A.4) is approximated by

$$\int_t^{t+\Delta t} f\big(x(t), x(t-\tau)\big)dt \simeq f\left(\frac{x(t)+x(t+\Delta t)}{2}, \frac{x(t-\tau)+x(t+\Delta t-\tau)}{2}\right)\Delta t,$$

where the value of $x(t+\Delta t)$ appearing on the right-hand side is approximated using the Euler integration scheme. It is interesting to note that setting $n = 1$ in Eq. (3.22) leads to a similar equation for Stratonovich integrals. Indeed, this yields

$$\mathcal{S}\int_t^{t+\Delta t} g\big(x(t), x(t-\tau)\big)dW(t) \simeq g\left(\frac{x(t)+x(t+\Delta t)}{2}, \frac{x(t-\tau)+x(t+\Delta t-\tau)}{2}\right)\Delta W,$$

where ΔW is defined in the same way as in part (b). Using these approximate expressions for Riemann and Stratonovich integrals, the equation

$$x(t+\Delta t) = x(t) + \int_t^{t+\Delta t} f\big(x(t), x(t-\tau)\big)dt + \mathcal{S}\int_t^{t+\Delta t} \sigma g\big(x(t), x(t-\tau)\big)dW(t)$$

becomes

$$x(t+\Delta t) \simeq x(t) + f\left(\frac{x(t)+x(t+\Delta t)}{2}, \frac{x(t-\tau)+x(t+\Delta t-\tau)}{2}\right)\Delta t + \sigma g\left(\frac{x(t)+x(t+\Delta t)}{2}, \frac{x(t-\tau)+x(t+\Delta t-\tau)}{2}\right)\Delta W, \qquad \text{(A.7)}$$

where the value of $x(t+\Delta t)$ appearing on the right-hand side can now be approximated using the stochastic Euler integration scheme. Since Eq. (A.7) is a straightforward generalisation of the midpoint integration scheme, it seems natural to call it the *stochastic midpoint integration scheme.* This method was used for integrating the Stratonovich SDDE (3.45) in Sec. 3.4.2.

A.2.2 Sampling

In a stochastic simulation, all quantities involving the value of the state variable are in fact random variables. This is true even for statistical properties, such as the probability of being in a certain region of phase space, since a simulation cannot yield the infinite number of sample values that would be required for an exact determination. It is therefore important to evaluate, at the very least, both the mean and the variance of each quantity resulting from a stochastic simulation. This can be done, in general, by using sample ensemble averages. If a given quantity X is calculated for each of n distinct realisations, thus leading to the sample set $\{X_i | i \in N, i \leq n\}$, its mean and variance can be respectively approximated by the sample mean

$$\langle X \rangle \simeq \frac{1}{n}\sum_{i=1}^{n} X_i \equiv \bar{X}_e$$

and the sample variance

$$\langle X^2 \rangle - \langle X \rangle^2 \simeq \frac{n}{n-1}\left[\frac{1}{n}\sum_{i=1}^{n} X_i^2 - \left(\frac{1}{n}\sum_{i=1}^{n} X_i\right)^2\right],$$

where the subscript e stands for *ensemble average*. Another quantity that must often be calculated is the variance of the sample mean $\bar{X}_e$. It is given by

$$\begin{aligned}\langle \bar{X}_e^2 \rangle - \langle \bar{X}_e \rangle^2 &= \frac{\langle X^2 \rangle - \langle X \rangle^2}{n} \\ &\simeq \frac{1}{n-1}\left[\frac{1}{n}\sum_{i=1}^{n} X_i^2 - \left(\frac{1}{n}\sum_{i=1}^{n} X_i\right)^2\right]. \end{aligned} \tag{A.8}$$

A stationary process for which ensemble and time averages are equivalent is termed *ergodic*. For such a system, the sample mean and the sample variance of a quantity $X(t)$ can be determined from a single realisation. For instance, they can be calculated using

$$\begin{aligned}\langle X \rangle &\simeq \frac{1}{n}\sum_{i=1}^{n} X(i\Delta t) \\ &\equiv \bar{X}_t\end{aligned}$$

and

$$\langle X^2 \rangle - \langle X \rangle^2 \simeq \frac{n}{n-1}\left[\frac{1}{n}\sum_{i=1}^{n} X^2(i\Delta t) - \left(\frac{1}{n}\sum_{i=1}^{n} X(i\Delta t)\right)^2\right],$$

where n represents the number of times at which $X(t)$ is being sampled, Δt is the time interval between successive samplings, and the subscript t stands for *time average*. Since the various values of $X(t)$ may be correlated, the correlation time τ_{cor} of $\bar{X}_t$ (see Sec. 2.1.4) must be taken into account when calculating its variance. It can be shown that

$$\begin{aligned}\langle \bar{X}_t^2 \rangle - \langle \bar{X}_t \rangle^2 &\simeq \left(1 + \frac{2\tau_{\text{cor}}}{\Delta t}\right)\frac{\langle X^2 \rangle - \langle X \rangle^2}{n} \\ &\simeq \frac{1}{n-1}\left(1 + \frac{2\tau_{\text{cor}}}{\Delta t}\right)\left[\frac{1}{n}\sum_{i=1}^{n} X^2(i\Delta t) - \left(\frac{1}{n}\sum_{i=1}^{n} X(i\Delta t)\right)^2\right] \end{aligned} \tag{A.9}$$

when $\Delta t \ll \tau_{\text{cor}} \ll n\Delta t$ [46]. On the other hand, correlations can be neglected when $\Delta t \gg \tau_{\text{cor}}$. In this large Δt limit, τ_{cor} can be set to zero in Eq. (A.9) and there are no restrictions on the value of n.

In this research project, all stochastic simulations involved the calculation of a mean value, whether through an ensemble or a time average, as the last step of the computation. Throughout the thesis, the numerical results arising from stochastic simulations are thus of the form "mean $\pm$ standard deviation of the mean", where the standard deviation is defined as the square root of the variance. In graphs, the standard deviation is represented by an

error bar. It is however omitted for points where it would be smaller than the symbol.

A.2.3 Steady-State Measurements

a) Mean and Variance

In Sec. 4.2.1, for the linear SDDE, the variance of $x(t)$ was determined by successively performing ensemble and time averages. Indeed:

1. The variance of $x(t)$ was determined as a function of time from a set of sample realisations.
2. The transients were dropped from the values of the variance obtained in step 1.
3. The mean of the variance resulting from step 2 was calculated using a time average. The standard deviation of this mean was given by Eq. (A.9). The correlation time appearing in this equation was also determined from the results of step 2.

In Sec. 4.2.2, for the logistic SDDE, the order of these calculations was modified in order to avoid the necessity of calculating correlation times. In this case:

1. The time required by the mean and the variance to reach steady-state was determined through preliminary simulations.
2. For each of several realisations:
   (a) The system was allowed to relax for the amount of time determined in step 1.
   (b) Once at steady-state, the mean and the variance of $x(t)$ were determined through time averages.
3. Ensemble averages were performed on the values of the mean and the variance obtained in step 2. The standard deviations of these quantities were given by Eq. (A.8), where no correlation time comes into play.

Because of its advantage in the determination of the standard deviations, this second framework was also used for the steady-state probability density and the steady-state CAD.

b) Probability Density

The steady-state probability density $p^s(x_o)$ was obtained from simulations by periodically sampling and binning sample paths after transients had relaxed. More precisely:

1. The time required by the mean and the variance to reach steady-state was determined through preliminary simulations. All other quantities of interest were then assumed to relax on similar time scales.

2. The x-axis was divided in bins of equal width.

3. For each of several realisations:

   (a) The system was allowed to relax for the amount of time determined in step 1.

   (b) Once at steady-state, the residence time in each bin was evaluated by periodically sampling $x(t)$. This step basically corresponds to a time average.

4. The mean of the residence times obtained in step 3(b) was calculated for each bin.

5. The average residence times of step 4 were divided by the time span of step 3(b) and by the width of the bins to yield the steady-state probability density at the centre of each bin.

In Sec. 5.3.4, the pseudo-steady-state probability density $p^m(x_o)$ in the quartic potential was determined using the same approach, but with step 3(b) slightly modified. When an unbounded oscillatory trajectory was spawned, sample points on it were discarded. A new realisation was then initiated and allowed to relax, and sampling was resumed. This continued until the required number of samples was attained.

c) Conditional Average Drift

The approach used to obtain the steady-state CAD $\bar{f}^s(x_o)$ was similar to the one presented in part (b). Steps 3 to 5 were simply replaced by these two:

3. For each of several realisations:

   (a) The system was allowed to relax for the amount of time determined in step 1.

   (b) Once at steady-state, $f\big(x(t), x(t-\tau)\big)$ was periodically sampled and binned according to the value of $x(t)$.

4. The mean of $f\big(x(t), x(t-\tau)\big)$ was calculated for each bin. This yielded $\bar{f}^s(x_o)$.

In the case of the delayed linear equation in Sec. 4.2.1, only one realisation was used. The sampling time was however chosen large enough to allow the determination of the standard deviation without having to worry about the correlation time.

A.2.4 Dynamical Measurements

a) Phenomenological Time Scale

In Sec. 5.3, the time scale τ_{pop} was obtained from simulations in two different ways: through Eq. (5.37) and the steady-state probability density $p^s(x_o)$, and directly through phenomenological simulations. The algorithm used in conjunction with Eq. (5.37) was based on the one described in part (b) of Sec. A.2.3. In this case, steps 3 to 5 were replaced by:

3. For each of several realisations:
   (a) The system was allowed to relax for the amount of time determined in step 1.
   (b) Once at steady-state, the residence time in each bin was evaluated by periodically sampling $x(t)$.
   (c) The steady-state probability density was normalised [see step 5 in part (b) of Sec. A.2.3].
   (d) The time scale τ_{pop} was determined using Eqs. (5.36) and (5.37).
4. An ensemble average was performed on the values of τ_{pop} obtained in step 3.

For phenomenological simulations, all realisations were initiated from a point in the left well and the population numbers $N_{\pm}(t_o|x',t')$ were evaluated by monitoring the fraction of samples located in each well as a function of time. When a phenomenological rate law was valid, graphs of $\ln(N_{\pm}(t_o|x',t') - \eta_{\pm})$ as functions of t_o were then linear [see Eq. (5.30)] and τ_{pop} was easily extracted from their slope. In Sec. 5.3.4, the order of magnitude of τ_{int} was similarly determined, but by considering the variance of the state variable in the left well instead of the population numbers.

b) Mean First Passage Time

Throughout Chap. 5, the mean first passage time was determined from simulations by averaging the first passage time over realisations. In Sec. 5.3, however, it was also calculated from the steady-state probability density. This was done by using the first approach presented in part (a), except that Eqs. (5.36) and (5.37) were replaced by Eq. (5.42).

Appendix B

Publications and Conferences

B.1 Refereed Publications

- S. Guillouzic, I. L'Heureux, and A. Longtin. Small delay approximation of stochastic delay differential equations. *Phys. Rev. E*, 59:3970-3982, 1999.

  Erratum: A term arising from the use of Ito calculus is missing from the definition of the approximate drift $f_a(x_o)$ [Eq. (15a)]. The expression for $f_a(x_o)$ is however correct if Stratonovich calculus is used in Eqs. (1) and (14). The analysis of the linear SDDE is unaffected by the omission, but the one of the logistic SDDE would need to be revised according to the approach presented in this thesis. On a different note, the dashed line appearing in Fig. 8 represents the drift function of Eq. (37) instead of the one of Eq. (A8). Finally, the noise amplitude σ is missing from the diffusion term of the latter equation.

- S. Guillouzic, I. L'Heureux, and A. Longtin. Transition rates for stochastic delay differential equations. In D. S. Broomhead, E. A. Luchinskaya, P. V. E. McClintock, and T. Mullin (eds.), *Stochastic and Chaotic Dynamics in the Lakes*, vol. 502 of *AIP Conference Proceedings*, American Institute of Physics, Melville, NY, 2000, pp. 456–461.

- S. Guillouzic, I. L'Heureux, and A. Longtin. Rate processes in a delayed, stochastically driven, and overdamped system. *Phys. Rev. E*, 61:4906–4914, 2000.

  Erratum: The base 10 logarithm was used instead of the natural logarithm in the calculation of the effective barrier height for the captions of Figs. 5, 6, and 8. Consequently, the values of ΔU listed in these captions should be multiplied by $\ln 10$.

B.2 Conference Presentations

- Approximation des petits délais pour les équations différentielles stochastiques à délai. Congrès de l'Association canadienne-française pour l'avancement des sciences, Ottawa, Canada, May 1999.
- Transition Rates for Stochastic Delay Differential Equations. International Conference on Stochastic and Chaotic Dynamics, Ambleside, United Kingdom, August 1999.

Bibliography

[1] C. W. Gardiner. *Handbook of Stochastic Methods for Physics, Chemistry and the Natural Sciences*, 2nd ed. Springer-Verlag, New York, 1997.

[2] W. Horsthemke and R. Lefever. *Noise-Induced Transitions: Theory and Applications in Physics, Chemistry, and Biology.* Springer-Verlag, New York, 1984.

[3] I. L'Heureux and R. Kapral. White noise induced transitions between a limit cycle and a fixed point. *Phys. Lett. A*, 136:472–476, 1989.

[4] X.-G. Wu and R. Kapral. Projected dynamics: Analysis of a chemical reaction model. *J. Chem. Phys.*, 91:5528–5543, 1989.

[5] V. I. Mel'nikov. The Kramers problem: Fifty years of development. *Phys. Rep.*, 209:1–71, 1991.

[6] P. Hanggi, T. J. Mroczkowski, F. Moss, and P. V. E. McClintock. Bistability driven by colored noise: Theory and experiment. *Phys. Rev. A*, 32:695–698, 1985.

[7] J. Masoliver, B. J. West, and K. Lindenberg. Bistability driven by Gaussian colored noise: First-passage times. *Phys. Rev. A*, 35:3086–3094, 1987.

[8] I. L'Heureux and R. Kapral. Transition rates in a bistable system driven by external dichotomous noise. *J. Chem. Phys.*, 88:7468–7477, 1988.

[9] I. L'Heureux and R. Kapral. Direct simulation of dichotomous noise-induced transitions in a bistable system. *J. Chem. Phys.*, 90:2453–2459, 1989.

[10] I. L'Heureux, R. Kapral, and K. Bar-Eli. Noise-induced transitions in an excitable system. *J. Chem. Phys.*, 91:4285–4298, 1989.

[11] J. M. Porrà, J. Masoliver, K. Lindenberg, I. L'Heureux, and R. Kapral. Bistability driven by dichotomous noise: A comment. *Phys. Rev. A*, 45:6092–6094, 1992.

[12] I. L'Heureux. Reaction rate kernel for dichotomous noise-induced transitions in bistable systems. *Phys. Rev. E*, 51:2787–2798, 1995.

[13] S. Guillouzic and I. L'Heureux. Kinetics of dichotomous noise-induced transitions in a multistable multivariate system. *Phys. Rev. E*, 55:5060–5072, 1997.

[14] M. C. Mackey and L. Glass. Oscillation and chaos in physiological control systems. *Science*, 197:287–289, 1977.

[15] T. L. Saaty. *Modern Nonlinear Equations.* Dover, New York, 1981.

[16] V. B. Kolmanovskiĭ and A. D. Myshkis. *Applied Theory of Functional Differential Equations.* Kluwer, Boston, 1992.

[17] K. Ikeda, H. Daido, and O. Akimoto. Optical turbulence: Chaotic behavior of transmitted light from a ring cavity. *Phys. Rev. Lett.*, 45:709–712, 1980.

[18] F. A. Hopf, D. L. Kaplan, H. M. Gibbs, and R. L. Shoemaker. Bifurcations to chaos in optical bistability. *Phys. Rev. A*, 25:2172–2182, 1982.

[19] P. Nardone, P. Mandel, and R. Kapral. Analysis of a delay-differential equation in optical bistability. *Phys. Rev. A*, 33:2465–2471, 1986.

[20] K. Ikeda and K. Matsumoto. High-dimensional chaotic behavior in systems with time-delayed feedback. *Physica D*, 29:223–235, 1987.

[21] P. J. Wangersky and W. J. Cunningham. Time lag in prey-predator population models. *Ecology*, 38:136–139, 1957.

[22] A. Beuter, J. Bélair, and C. Labrie. Feedback and delays in neurological diseases: A modeling study using dynamical systems. *Bull. Math. Biol.*, 55:525–541, 1993.

[23] J. G. Milton, A. Longtin, A. Beuter, M. C. Mackey, and L. Glass. Complex dynamics and bifurcations in neurology. *J. Theor. Biol.*, 138:129–147, 1989.

[24] C. M. Marcus and R. M. Westervelt. Stability of analog neural networks with delay. *Phys. Rev. A*, 39:347–359, 1989.

[25] M. C. Mackey. Commodity price fluctuations: Price dependent delays and nonlinearities as explanatory factors. *J. Econ. Theory*, 48:497–509, 1989.

[26] M. R. Roussel. The use of delay differential equations in chemical kinetics. *J. Phys. Chem.*, 100:8323–8330, 1996.

[27] M. J. Suarez and P. S. Schopf. A delayed action oscillator for ENSO. *J. Atmos. Sci.*, 45:3283–3287, 1988.

[28] K. Bar-Eli and R. J. Field. Earth-average temperature: A time delay approach. *J. Geophys. Res.*, 103:25949–25956, 1998.

[29] A. Longtin, J. G. Milton, J. E. Bos, and M. C. Mackey. Noise and critical behavior of the pupil light reflex at oscillation onset. *Phys. Rev. A*, 41:6992–7005, 1990.

[30] K. Vasilakos and A. Beuter. Effects of noise on a delayed visual feedback system. *J. Theor. Biol.*, 165:389–407, 1993.

[31] Y. Chen, M. Ding, and J. A. S. Kelso. Long memory processes ($1/f^{\alpha}$ type) in human coordination. *Phys. Rev. Lett.*, 79:4501–4504, 1997.

[32] J. García-Ojalvo and R. Roy. Noise amplification in a stochastic Ikeda model. *Phys. Lett. A*, 224:51–56, 1996.

[33] R. Kapral, E. Celarier, P. Mandel, and P. Nardone. Noisy delay-differential equations in optical bistability. In N. B. Abraham and J. Chrostowski (eds.), *Optical Chaos*, vol. 667 of *Proceedings of SPIE*, International Society for Optical Engineering, Bellingham, WA, 1986, pp. 175–182.

[34] L. Stone, P. I. Saparin, A. Huppert, and C. Price. El Niño chaos: The role of noise and stochastic resonance on the ENSO cycle. *Geophys. Res. Lett.*, 25:175–178, 1998.

[35] S. Kim, S. H. Park, and H.-B. Pyo. Stochastic resonance in coupled oscillator systems with time delay. *Phys. Rev. Lett.*, 82:1620–1623, 1999.

[36] M. K. S. Yeung and S. H. Strogatz. Time delay in the Kuramoto model of coupled oscillators. *Phys. Rev. Lett.*, 82:648–651, 1999.

[37] J. Foss, F. Moss, and J. Milton. Noise, multistability, and delayed recurrent loops. *Phys. Rev. E*, 55:4536–4543, 1997.

[38] H. Grabert and S. Linkwitz. Effect of time-delayed friction on the escape from a metastable well. *Phys. Rev. A*, 37:963–972, 1988.

[39] D. Kohen and D. J. Tannor. Phase space distribution function formulation of the method of reactive flux: Memory friction. *J. Chem. Phys.*, 103:6013–6020, 1995.

[40] K. Lindenberg, A. H. Romero, and J. M. Sancho. On the generalized Kramers problem with exponential memory friction. *Physica D*, 133:348–361, 1999.

[41] R. Reigada, A. H. Romero, K. Lindenberg, and J. M. Sancho. On the generalized Kramers problem with oscillatory memory friction. *J. Chem. Phys.*, 111:676–688, 1999.

[42] T. Ohira and Y. Sato. Resonance with noise and delay. *Phys. Rev. Lett.*, 82:2811–2815, 1999.

[43] T. Ohira. A Fokker-Planck equation for delayed stochastic dynamics. In *Proceedings of the 3rd Workshop on Orders and Structures in Complex Systems*, International Institute for Advanced Studies, Kyoto, 1996, pp. 74–78.

[44] T. Ohira and T. Yamane. Delayed stochastic systems. *Phys. Rev. E*, 61:1247–1257, 2000.

[45] A. Papoulis. *Probability, Random Variables, and Stochastic Processes.* McGraw-Hill, New York, third edition, 1991.

[46] K. Binder and D. W. Heermann. *Monte Carlo Simulation in Statistical Physics: An Introduction.* Springer-Verlag, New York, 1988.

[47] P. E. Kloeden and E. Platen. *Numerical Solution of Stochastic Differential Equations.* Springer-Verlag, New York, 1992.

[48] L. E. El'sgol'ts and S. B. Norkin. Translated by J. L. Casti. *Introduction to the Theory and Application of Differential Equations with Deviating Arguments.* Academic Press, New York, 1973.

[49] G. J. Nazaroff. Stability of linear stochastic differential delay systems. *IEEE Trans. Automat. Contr.*, 18:672–673, 1973.

[50] S.-E. A. Mohammed. *Stochastic Functional Differential Equations.* Pitman, Boston, 1984.

[51] S.-E. A. Mohammed and M. K. R. Scheutzow. Lyapunov exponents and stationary solutions for affine stochastic delay equations. *Stochastics Stochastics Rep.*, 29:259–283, 1990.

[52] X. Mao. Razumikhin-type theorems on exponential stability of stochastic functional differential equations. *Stochastic Process. Appl.*, 65:233–250, 1996.

[53] D. R. Bell and S.-E. A. Mohammed. Smooth densities for degenerate stochastic delay equations with hereditary drift. *Annals Prob.*, 23:1875–1894, 1995.

[54] J. Losson and M. C. Mackey. Coupled map lattices as models of deterministic and stochastic differential delay equations. *Phys. Rev. E*, 52:115–128, 1995.

[55] U. Küchler and B. Mensch. Langevins stochastic differential equation extended by a time-delayed term. *Stochastics Stochastics Rep.*, 40:23–42, 1992.

[56] M. C. Mackey and I. G. Nechaeva. Solution moment stability in stochastic differential delay equations. *Phys. Rev. E*, 52:3366–3376, 1995.

[57] J. Hunter and J. G. Milton. Stability of ensemble moments of stochastic delay equations: Additive and parametric white noise. Private communication, 1996.

[58] J. Hunter and J. G. Milton. Statistical characteristics of the solution of a stochastic linear differential delay equation with a colored noise input. Private communication, 1996.

[59] T. Ohira. Oscillatory correlation of delayed random walks. *Phys. Rev. E*, 55:R1255–R1258, 1997.

[60] E. M. Wright. A non-linear difference-differential equation. *J. Reine Angew. Math*, 194:66–87, 1955.

[61] H. T. Banks. Delay systems in biological models: Approximation techniques. In V. Lakshmikantham (ed.), *Nonlinear Systems and Applications: An International Conference*, Academic Press, New York, 1977, pp. 21–38.

[62] B. Mensour. *Dynamical Invariants, Multistability, Controllability and Synchronization in Delay-Differential and Difference Equations.* PhD thesis, University of Ottawa, 1997.

[63] H. Haken. *Advanced Synergetics: Instability Hierarchies of Self-Organizing Systems and Devices.* Springer-Verlag, New York, 1983.

[64] J. M. Cushing. *Integrodifferential Equations and Delay Models in Population Dynamics.* Springer-Verlag, New York, 1977.